

# Sorption Experiments in Brine Solutions with Sedimentary Rock and Bentonite

NWMO TR-2011-11

December 2011

**Peter Vilks, Neil H. Miller and Kent Felushko**

Atomic Energy of Canada Limited

**nwmo**

NUCLEAR WASTE  
MANAGEMENT  
ORGANIZATION

SOCIÉTÉ DE GESTION  
DES DÉCHETS  
NUCLÉAIRES



**Nuclear Waste Management Organization**  
22 St. Clair Avenue East, 6<sup>th</sup> Floor  
Toronto, Ontario  
M4T 2S3  
Canada

Tel: 416-934-9814  
Web: [www.nwmo.ca](http://www.nwmo.ca)

**Sorption Experiments in Brine Solutions with Sedimentary Rock and Bentonite**

**NWMO TR-2011-11**

December 2011

**Peter Vilks, Neil H. Miller and Kent Felushko**  
Atomic Energy of Canada Limited

---

Disclaimer:

This report does not necessarily reflect the views or position of the Nuclear Waste Management Organization, its directors, officers, employees and agents (the "NWMO") and unless otherwise specifically stated, is made available to the public by the NWMO for information only. The contents of this report reflect the views of the author(s) who are solely responsible for the text and its conclusions as well as the accuracy of any data used in its creation. The NWMO does not make any warranty, express or implied, or assume any legal liability or responsibility for the accuracy, completeness, or usefulness of any information disclosed, or represent that the use of any information would not infringe privately owned rights. Any reference to a specific commercial product, process or service by trade name, trademark, manufacturer, or otherwise, does not constitute or imply its endorsement, recommendation, or preference by NWMO.

---



## ABSTRACT

**Title:** Sorption Experiments in Brine Solutions with Sedimentary Rock and Bentonite  
**Report No.:** NWMO TR-2011-11  
**Author(s):** Peter Vilks, Neil H. Miller and Kent Felushko  
**Company:** Atomic Energy of Canada Limited  
**Date:** December 2011

### Abstract

This report summarizes the results of an experimental program investigating sorption processes in Na-Ca-Cl brine solutions with Canadian sedimentary rocks and bentonite. Protocols for batch sorption tests with Na-Ca-Cl brine solutions were first developed. These included guidelines for experimental configurations, solid/liquid ratios, phase separation methods and sorption time scales. The sorption of Sr(II), Ni(II), Cu(II), Eu(III) and U(VI) was then characterized on bentonite, shale and limestone in Na-Ca-Cl brine solutions with total dissolved solid (TDS) values as high as 300 g/L.

Strontium did not sorb in brine solutions, indicating that sorption coefficients for group 1 and group 2 elements, such as Ra(II), should be assigned values of 0. In contrast, transition metals, such as Ni and Cu, and the trivalent Eu and hexavalent U sorb by surface complexation mechanisms to bentonite, shale and limestone in brine solutions. The sorption of Ni and Cu increased with pH increases from 6 to 8, while the effect of pH on Eu and U sorption was not clear. The high concentrations of Ca in the brine competed with Ni for sorption sites. The formation of complexes with carbonate reduced the sorption of Eu and U. Although Ni sorption was 70 to 90 percent complete after 1 week, Ni continued to sorb at a slow rate and probably did not reach steady-state until after 4 weeks. The sorption of Eu and U appeared to reach a steady-state after 1 to 2 weeks, although Eu sorption on limestone may have continued for longer than 4 weeks in some cases. The sorption of U appeared to be reversible over a several week period, but the sorption of Ni and Eu was not reversible within a two week period.

On the basis of these experiments, preliminary recommendations for sorption coefficients applicable to sedimentary rocks are suggested.



**TABLE OF CONTENTS**

	<b><u>Page</u></b>
<b>ABSTRACT .....</b>	<b>v</b>
<b>1. INTRODUCTION .....</b>	<b>1</b>
<b>2. ROCK SAMPLE CHARACTERIZATION .....</b>	<b>3</b>
<b>2.1 X-RAY DIFFRACTION .....</b>	<b>5</b>
<b>2.2 THERMAL ANALYSES.....</b>	<b>7</b>
<b>2.3 LEACHABLE ELEMENTS .....</b>	<b>11</b>
<b>2.4 SURFACE AREA ANALYSES .....</b>	<b>13</b>
<b>3. AQUEOUS SPECIATION .....</b>	<b>13</b>
<b>4. BATCH SORPTION EXPERIMENTS .....</b>	<b>14</b>
<b>4.1 GENERAL METHODS .....</b>	<b>14</b>
<b>4.2 RESULTS.....</b>	<b>18</b>
4.2.1 Strontium .....	19
4.2.2 Nickel.....	20
4.2.3 Copper.....	39
4.2.4 Uranium .....	44
4.2.5 Europium .....	55
<b>5. MASS TRANSPORT EXPERIMENT .....</b>	<b>67</b>
<b>5.1 METHODS .....</b>	<b>67</b>
<b>5.2 RESULTS.....</b>	<b>68</b>
<b>6. DISCUSSION .....</b>	<b>72</b>
<b>6.1 DEVELOPMENT OF EXPERIMENTAL PROTOCOLS .....</b>	<b>72</b>
<b>6.2 SORPTION RESULTS .....</b>	<b>75</b>
<b>7. CONCLUSIONS .....</b>	<b>80</b>
<b>ACKNOWLEDGEMENTS.....</b>	<b>81</b>
<b>REFERENCES .....</b>	<b>82</b>
<b>APPENDIX A: PROTOCOLS USED IN SORPTION EXPERIMENTS .....</b>	<b>87</b>

## LIST OF TABLES

	<u>Page</u>
Table 1: Solids Used in Sorption Experiments.....	4
Table 2: Mineralogical Composition Identified by X-Ray Diffraction.....	6
Table 3: TGA Data Corresponding to DTA Peaks in Queenston Shale .....	10
Table 4: Selected Trace Elements in Rock Samples.....	12
Table 5: B.E.T. Surface Areas of Rock Samples Used in Sorption Studies .....	13
Table 6: Solutions Used in Batch Sorption Experiments.....	15
Table 7: Ranges of Sorbing Element Concentrations for Sorption Tests .....	15
Table 8: The pH of Test Solutions in Contact with Solids .....	17
Table 9: Initial Nickel Sorption Results .....	21
Table 10: Nickel Sorption on Bentonite in 300 g/L TDS Brine as a Function of Time.....	23
Table 11: Nickel Sorption as a Function of TDS .....	25
Table 12: Kinetic Study of Ni Sorption in 200 mL Volume with no Sample Preconditioning .....	28
Table 13: Kinetic Study of Ni Sorption in 200 mL Volume with Conditioned Solids.....	32
Table 14: Effect of Sample Preconditioning on Nickel Sorption .....	34
Table 15: Nickel Desorption Experiment in 100 g/L TDS Na-Ca-Cl Brine .....	37
Table 16: Average Ni Sorption $K_d$ Values ( $\text{cm}^3/\text{g}$ ) for Brine Solutions.....	38
Table 17: Copper Sorption Results with the 300 g/L TDS Na-Ca-Cl Brine.....	40
Table 18: Copper Sorption as a Function of TDS .....	41
Table 19: Average Cu Sorption $K_d$ Values ( $\text{cm}^3/\text{g}$ ) for Brine Solutions.....	44
Table 20: Uranium Sorption as a Function of TDS .....	45
Table 21: Uranium Sorption in 10 g/L TDS as a Function of Total Carbonate in Solution .....	48
Table 22: Kinetic Study of U Sorption in 200 mL Volume with Conditioned Solids.....	49
Table 23: Uranium Desorption Experiment in 100 g/L TDS Na-Ca-Cl Brine .....	53
Table 24: Average U Sorption $K_d$ Values ( $\text{cm}^3/\text{g}$ ) for Brine Solutions.....	55
Table 25: Europium Sorption as a Function of Time in 300 g/L TDS Na-Ca-Cl Brine .....	56
Table 26: Europium Sorption Variation with Solid/Liquid Ratio in 300 g/L TDS Brine .....	58
Table 27: Kinetic Study of Eu Sorption in 200 mL Volume with Conditioned Solids.....	60
Table 28: Europium Desorption Experiment in 100 g/L TDS Na-Ca-Cl Brine .....	65
Table 29: Average Eu Sorption $K_d$ Values ( $\text{cm}^3/\text{g}$ ) for Brine Solutions.....	67
Table 30: Summary of Element Sorption Coefficients ( $\text{cm}^3/\text{g}$ ) .....	79

## LIST OF FIGURES

	<u>Page</u>
Figure 1: X-Ray Diffraction Spectra of Wyoming Sodium Bentonite .....	5
Figure 2: X-Ray Diffraction Spectra of Queenston Shale.....	6
Figure 3: X-Ray Diffraction Spectra of Cobourg Limestone .....	7
Figure 4: Differential Thermal Analyses and Thermogravimetric Analyses Plots of Wyoming Sodium Bentonite.....	8
Figure 5: Differential Thermal Analyses and Thermogravimetric Analyses Plots of Queenston Shale.....	9
Figure 6: Differential Thermal Analyses and Thermogravimetric Analyses Plots of Limestone .10	
Figure 7: Nickel Sorption versus Total Nickel in System Expressed as (A) Total Nickel Sorbed, (B) Mass-Based Sorption Coefficient and (C) Surface-Based Sorption Coefficient.....	22
Figure 8: Nickel Sorption on Bentonite as a Function of Time Expressed as (A) Percent Sorbed, (B) Moles Ni Sorbed, and (C) $K_d$ Values. Analytical Uncertainties Are Smaller than the Symbols. ....	24

Figure 9: Nickel Sorption as a Function of TDS Shown for Total Ni Concentrations of $1 \times 10^{-4}$ and $1 \times 10^{-5}$ mol/L.....	26
Figure 10: Nickel Sorption Expressed as a Function of pH.....	27
Figure 11: Average Nickel Sorption Coefficients as a Function of Time for 200 mL Volume Tests .....	29
Figure 12: Nickel Sorption as a Function of Time and Solution Composition Using Conditioned Solid Phases. ....	34
Figure 13: Ni Sorption Coefficients as a Function of (A) TDS, (B) pH, and (C) $[\text{CO}_3]$ .....	36
Figure 14: Nickel Desorption Test .....	37
Figure 15: Copper Sorption Coefficient Versus Total Copper in the 300 g/L Brine System.....	40
Figure 16: Copper Sorption as a Function of TDS.....	42
Figure 17: Copper Sorption Variation with pH .....	43
Figure 18: Uranium Sorption as a Function of TDS .....	46
Figure 19: Uranium Sorption in 10 g/L Brine as a Function of Carbonate Concentration .....	47
Figure 20: Uranium Sorption as a Function of Time and Solution Composition using Conditioned Solids; the Solid/Liquid Ratios are 0.5, 1 and 2.5 g/100 mL for Bentonite, Shale and Limestone.....	51
Figure 21: Seven Day Uranium $K_d$ Values as a Function of (A) TDS, (B) pH, and (C) $[\text{CO}_3]$ , the Solid/Liquid Ratios are 0.5, 1 and 2.5 g/100 mL for Bentonite, Shale and Limestone .....	52
Figure 22: Uranium Desorption Experiment .....	54
Figure 23: Europium Sorption with Time Shown as Percent Sorbed, $K_d$ Values and $K_a$ Values. Data are from the Tests with a Total Eu Concentration of $4.39 \times 10^{-4}$ mol/L .....	57
Figure 24: Europium Sorption $K_d$ Values as a Function of Solid/Liquid Ratio.....	59
Figure 25: Kinetic Study of Eu Sorption in 200 mL Volume with Conditioned Solids, the Solid/Liquid Ratios are 0.5, 1 and 2.5 g/100 mL for Bentonite, Shale and Limestone .....	63
Figure 26: Seven Day Europium Sorption Coefficients as a Function of (A) TDS, (B) pH, and (C) $[\text{CO}_3]$ , the Solid/Liquid Ratios are 0.5, 1 and 2.5 g/100 mL for Bentonite, Shale and Limestone .....	64
Figure 27: Europium Desorption Experiment.....	66
Figure 28: Estimated Permeability as a Function of Eluted water .....	69
Figure 29: Chloride Concentration as a Function of Water Mass Eluted from Shale Matrix .....	70
Figure 30: Concentration of Uranine in Water Eluted from Shale Matrix.....	71
Figure 31: The pH Dependence of Metal Sorption on Fe Oxide (After Stumm, 1992).....	77



## 1. INTRODUCTION

The sorption of radionuclides onto mineral surfaces within the geosphere, and on the materials making up the engineered barriers of a deep geologic repository, is a potential mechanism for slowing the transport of radionuclides to the surface environment. The transport of radionuclides by diffusive or advective processes can be retarded, or slowed down, by physical restraints such as low permeability, low transport porosity and/or high storage capacity, and by chemical processes that include sorption and precipitation. Some highly soluble elements, such as iodine and technetium (VII), are poorly sorbed and will likely be transported with close to the same velocity as groundwater. However, a number of elements, such as the actinides, have low solubilities and are sorbed by rock surfaces. The transport of these elements may be significantly retarded by chemical processes, reducing the total radionuclide dose that is transported to the surface environment. Sorption is of particular interest as a chemical retardation process because it reduces transport even when the concentration of a given radionuclide is below its solubility limit.

With the Canadian Government's selection of the Adaptive Phased Management approach for the long-term management of Canada's used nuclear fuel in 2007, both crystalline and sedimentary rock formations are under consideration as potential host formations (NWMO, 2005). Sedimentary rocks in Canada, for example in the Michigan Basin, have been observed to contain Na-Ca-Cl and Ca-Na-Cl brine solutions with total dissolved solids (TDS) concentrations exceeding 300 g/L. Therefore, there is a need to establish an understanding of how brine solutions affect sorption on sedimentary rocks.

Vilks (2009) performed a state of the science review of sorption literature with a focus on defining current knowledge on sorption in highly saline solutions. The international literature contains data for radionuclide sorption on sedimentary formations at the Gorleben site, Germany, for a range of groundwaters that include NaCl brines with TDS as high as 159 g/L. Actinide sorption on dolomite in the presence of NaCl brines with TDS up to 338 g/L has been described for the WIPP site in New Mexico, USA. Information from these programs, combined with current understanding of sorption mechanisms, indicates that in brine solutions, the mass action effects of  $\text{Na}^+$  and  $\text{Ca}^{2+}$  will significantly reduce or eliminate the sorption of elements such as  $\text{Cs}^+$ ,  $\text{Sr}^{2+}$  and  $\text{Ra}^{2+}$  that are sorbed by coulombic attraction. In contrast, elements with a strong tendency to hydrolyse at pH values above 6 will be sorbed by surface complexation with minimal effects from TDS. Although this information provides valuable background knowledge, an experimental program is required to further develop the understanding of sorption processes in Na-Ca-Cl and Ca-Na-Cl brine solutions with sedimentary rocks.

To improve the understanding of sorption processes, the following questions were addressed as part of this work program:

- Is the mass action effect of Na and Ca in brine solutions able to diminish the sorption of alkali and alkali earth elements?
- Does the ionic strength of brine solutions have a significant influence on sorption?
- How does the likely change in dominant sorption mechanism affect sorption kinetics and reversibility?
- Will sorption be less reversible with dominance of specific chemical sorption?

With an understanding of sorption processes, it is possible to move toward developing a sorption database based on existing data and any new data obtained from sorption experiments of program-specific relevant rock types. The development of every international sorption database has included “in-house” experiments with rock types and water compositions typical of conditions for a proposed host rock. These experiments have included both batch and dynamic transport experiments. The “in-house” studies provide a measure of site specific sorption properties for selected elements that build an understanding of sorption process in the host rock. The “in-house” data is supplemented with information from the NEA sorption database (Rüegger and Ticknor, 1992) and the literature, using reasoned arguments to justify the selection of data. More recently, mechanistic sorption models are being applied to help justify data selection and to improve the process of extrapolating sorption data to in-situ conditions not readily accessible to experimentation (Davis et al., 2005, and Ochs et al., 2006).

International programs that have addressed sorption on sediments in the presence of highly saline groundwater have focused on the Gorleben salt deposit in Germany and the Waste Isolation Pilot Plant (WIPP) in New Mexico, USA. A significant amount of work was performed on understanding sorption process in sediments at the Gorleben site that were contacted by groundwaters with a variety of U.S. salinities. This work has been summarized by Warnecke et al. (1994). The WIPP site is situated in bedded salt in contact with Na-Cl groundwater with TDS values up to 338 g/L. The WIPP site is currently an operating repository for low and intermediate level transuranic waste. The sorption database developed for this site is documented by the USEPA (1998). As with the Gorleben site, sorption research related to the WIPP site has been completed. Other countries, including Belgium, France and Switzerland, are considering clay formations as potential hosts for a deep geologic repository. Bradbury and Baeyens (2003, 2010) and Bradbury et al. (2010) describe the ongoing derivation of sorption values for compacted MX-80 bentonite, Opalinus Clay and generic Swiss argillaceous rocks. Although the sorption values apply to ionic strengths of only 0.1 to 0.4 mol/L, the data from the Swiss program provide a useful reference to assist in understanding sorption phenomenon in Canadian sedimentary rocks.

To develop an understanding of sorption processes in brine solutions, NWMO initiated a two stage sorption experimental program. Following the approach used to establish international sorption databases, the NWMO program involves “in-house” experiments using Canadian rocks, and a range of brine compositions. The first stage experimental program includes batch experiments to address sorption specific issues, and dynamic transport experiments designed to relate sorption processes to mass transport. These experiments will develop experimental protocols and collect initial data. The second stage will build on the understanding gained in the first stage. In addition, more emphasis may be placed on using mechanistic surface complexation models to improve the understanding of sorption processes and to develop predictive abilities.

With the long-term aim of establishing a sorption database, the objectives of the first stage experimental program was to define sorption in Canadian brine solutions in sedimentary rock and included:

- Performance of batch sorption experiments with limestone, shale and bentonite, using variable brine concentrations to determine site-specific sorption coefficients and evaluate the effect of TDS. Elements used in the sorption tests should be selected to characterize sorption mechanisms affecting radionuclides relevant to performance assessment;



- Performance of kinetic studies to determine appropriate sorption times and the reversibility of sorption reactions;
- Performance of a set of batch experiments to evaluate the effect of the Na(I)/Ca(II) ratio;
- Performing transport experiments in rock cores to demonstrate our ability to quantify sorption in mass transport; and
- Characterization of the properties of shale, limestone and bentonite samples that may be required for mechanistic sorption modelling and optimization of datasets for eventual application in sorption modelling.

This report summarizes progress in the first stage experimental program to explore sorption in brine solutions. The objectives of this work were to:

- Characterize the rock samples to be used in sorption experiments;
- Develop experimental protocols for performing batch sorption experiments with Na-Ca-Cl brine solutions (issues to be addressed include analytical capabilities, reasonable concentration ranges, experimental time scales, solid/liquid ratios, and phase separation methods);
- Characterize sorption of Sr, Ni, Cu, Eu and U on bentonite, shale and limestone in Na-Ca-Cl brine solutions with TDS values as high as 300 g/L, which includes providing preliminary recommendations for sorption coefficients applicable to sedimentary rocks; and
- Initiate laboratory-based mass transport experiments.

The rationale for the selected elements (Sr, Ni, Cu, Eu and U) is:

- Strontium (Sr) is a chemical analog to radium and other group 1 and 2 elements;
- Nickel is a chemical analog for transition elements and lead;
- Copper is a component of one of the reference designs container for used nuclear fuel;
- Europium is a chemical analog for trivalent actinides; and
- Uranium is the primary component of used nuclear fuel.

## 2. ROCK SAMPLE CHARACTERIZATION

The rock samples used in sorption tests were Wyoming sodium bentonite, Cobourg limestone and Queenston shale. The bentonite was a granular Wyoming high quality sodium bentonite supplied by Bentonite Performance Minerals LLC ([www.bentonite.com](http://www.bentonite.com)). This material is similar to the commonly referenced MX-80, which is a Wyoming sodium bentonite. The Queenston shale and Cobourg limestone sample was taken from cored borehole samples (DGR1-459.27 mBGS and DGR3-689.02 mBGS) at the Bruce nuclear site in southwestern Ontario.

The mineral compositions reported for Wyoming sodium bentonite and Ordovician limestone and shale are summarized in Table 1. The table also reports expected rock properties, such as cation exchange capacity (CEC) and likely surface sites, that would influence sorption. While the CEC and surface complexation properties of Wyoming sodium bentonite have been reported in the literature, the properties of Queenston shale and Cobourg limestone are less well known. The properties of these samples were characterized to confirm their consistency with published data and to determine properties that are useful for understanding sorption properties. The rock properties that were characterized included mineralogical composition by XRD and thermal analyses, water leachable element content, and surface area analyses.

**Table 1: Solids Used in Sorption Experiments**

<b>Geologic Material</b>	<b>Reference</b>	<b>Major Minerals</b>	<b>Expected Properties</b>
Average Cobourg argillaceous limestone	- NWMO, 2011	calcite (81 wt%) dolomite (8 wt%) sheet silicate (6 wt%) quartz (3 wt%)	low CEC surface sites <ul style="list-style-type: none"> <li>• CO<sub>3</sub> major</li> <li>• Si-O minor</li> <li>• Al-O minor</li> </ul>
Queenston Shale	- Barone et al., 1990	Illite (40 wt%) chlorite (10 wt%) quartz (26 wt%) calcite (13 wt%) dolomite (5 wt%) feldspar (4 wt%) hematite (trace)	CEC = 12.5 meq/100 g surface sites <ul style="list-style-type: none"> <li>• Si-O major</li> <li>• Al-O major</li> <li>• Fe-O minor</li> <li>• CO<sub>3</sub> minor</li> </ul>
Queenston Shale from Bruce Nuclear Site	- NWMO, 2011	sheet silicate (40 wt%) quartz (17 wt%) calcite (24 wt%) dolomite (14 wt%) gypsum (trace) anhydrite (trace) halite (trace) hematite (trace) goethite (trace)	surface sites <ul style="list-style-type: none"> <li>• Si-O major</li> <li>• Al-O major</li> <li>• Fe-O minor</li> <li>• CO<sub>3</sub> minor</li> </ul>
Wyoming Sodium Bentonite	- Lajudie et al., 1995 - Liu and Neretnieks, 2006	montmorillonite (75 wt%) quartz (15.2 wt%) feldspar (5 to 8 wt%) calcite (1.4 wt%) kaolinite < 1 wt%) illite (< 1 wt%)	CEC = 79 to 85 meq/100 g edge sites (OH)=2.8 meq/100g surface sites <ul style="list-style-type: none"> <li>• Si-O major</li> <li>• Al-O major</li> <li>• CO<sub>3</sub> minor</li> </ul>

## 2.1 X-RAY DIFFRACTION

X-Ray diffraction (XRD) analyses were performed on powdered samples of the Wyoming sodium bentonite, Queenston shale and Cobourg limestone to further characterize the materials used in sorption experiments. X-Ray diffraction analyses were performed at Whiteshell and the University of Manitoba.

Table 2 summarizes the minerals identified by XRD for each rock sample. The XRD spectra are presented in Figures 1 through 3.

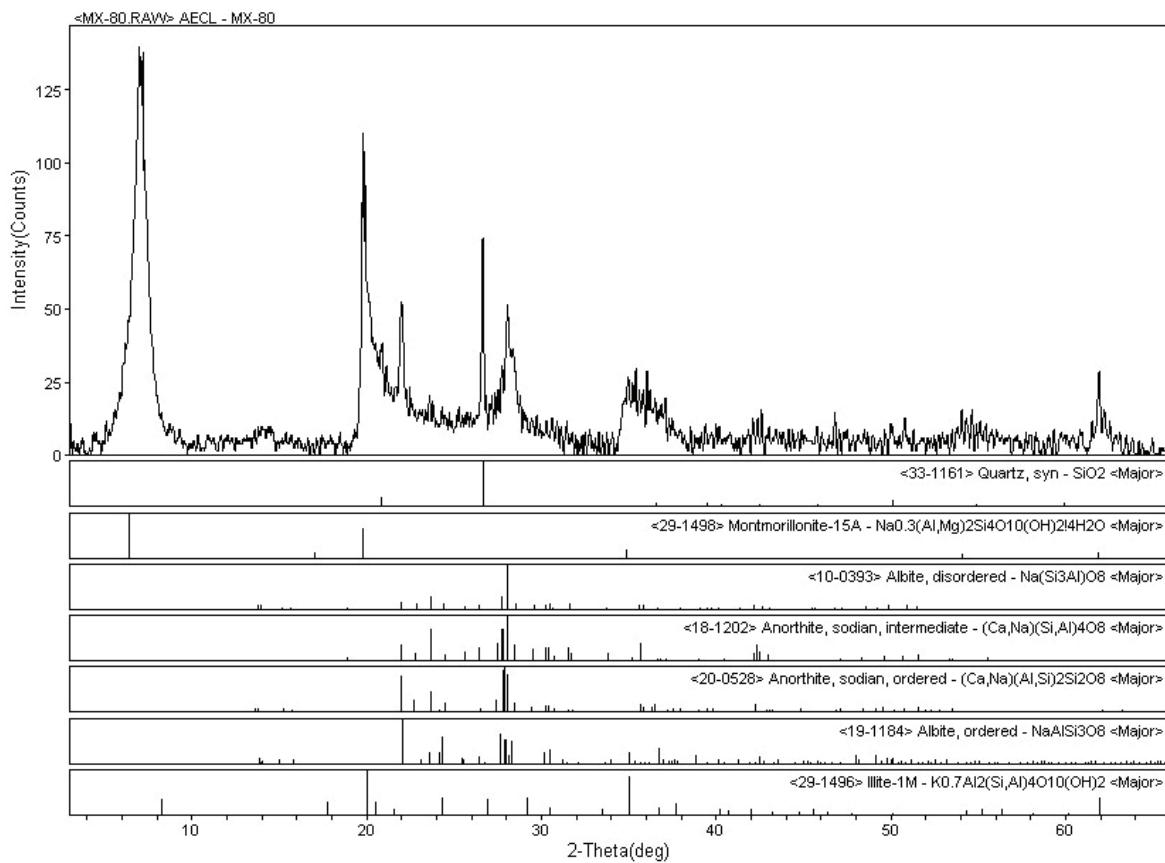
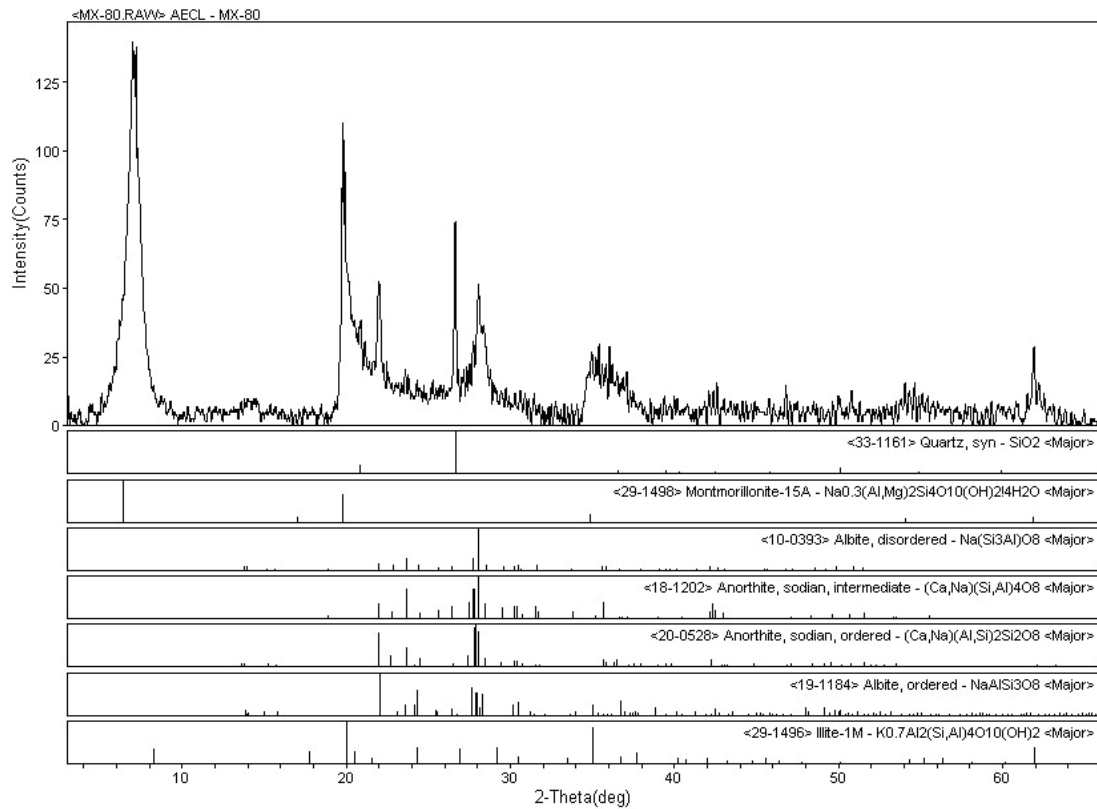


Figure 1: X-Ray Diffraction Spectra of Wyoming Sodium Bentonite

**Table 2: Mineralogical Composition Identified by X-Ray Diffraction**

Wyoming Sodium Bentonite	Queenston Shale	Cobourg Limestone
Montmorillonite	Illite	Calcite
Quartz	Quartz	Quartz
Illite	Chorite (clinocllore)	Dolomite
Feldspar (albite, anorthite)	Calcite	
	Ankerite (Ca(Fe, Mg) (CO <sub>3</sub> ) <sub>2</sub> )	



**Figure 2: X-Ray Diffraction Spectra of Queenston Shale**

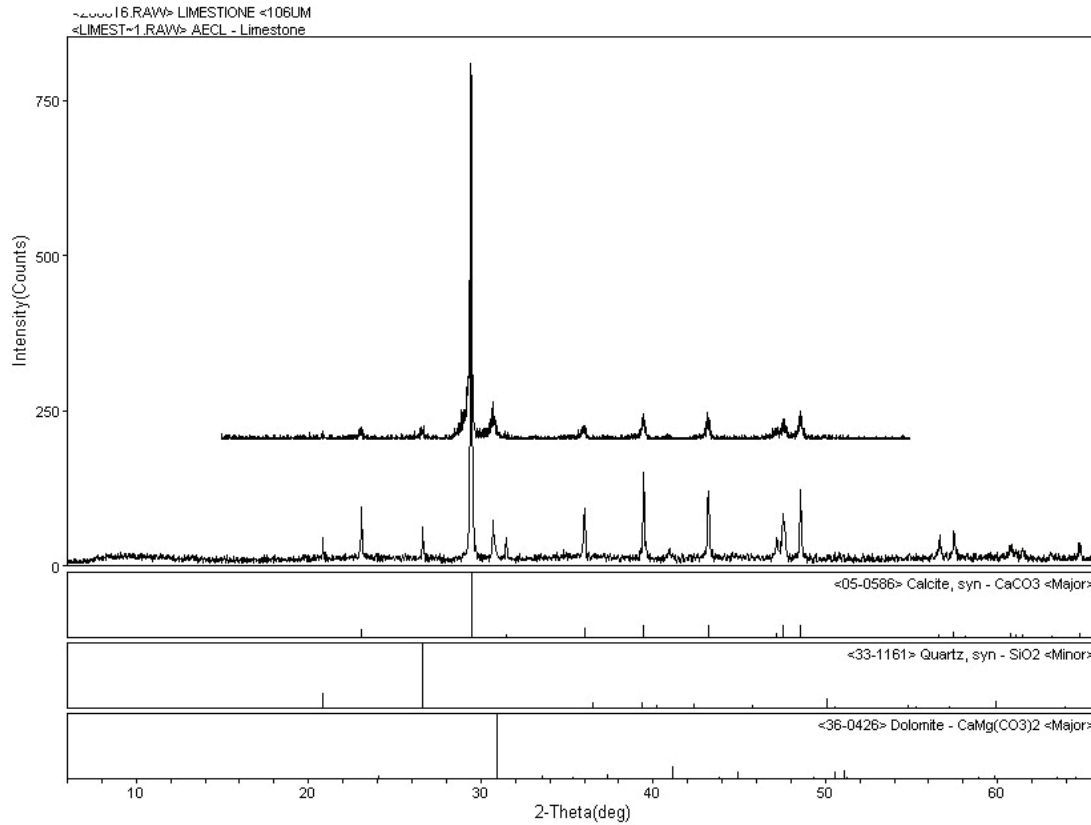


**Figure 3: X-Ray Diffraction Spectra of Cobourg Limestone**

## 2.2 THERMAL ANALYSES

Thermal analyses of Wyoming sodium bentonite, Queenston shale, and Cobourg limestone were performed using Differential Thermal Analysis (DTA) and Thermogravimetric Analysis (TGA) on powdered rock samples between 106 and 212  $\mu\text{m}$ , to correspond the size used in sorption experiments. For DTA, the sample of interest and an inert reference material are heated together and the temperature difference between the sample and the reference are recorded as a function of temperature. A plot of the temperature differential, as microvolts, versus temperature produces a DTA curve, also known as a thermogram. Any exothermic or endothermic changes in the sample can be detected relative to the inert reference. The DTA curve can provide data on transformations, such as glass transitions, crystallization, melting and sublimation that may have occurred at different temperatures. These types of transitions may be specific to certain minerals, and may provide additional evidence regarding the mineral content of rock samples.

TGA was performed by heating samples and measuring changes in weight as a function of temperature. TGA is usually used together with DTA to characterize the loss of adsorbed and structural water, and other degradation temperatures that may be specific to certain minerals.

The thermal analyses were conducted on samples with no prior drying using a Rheomatics STA 1500 simultaneous thermal analysis (DTA + TGA) instrument. The analyses were performed using calcined alumina as the reference standard and an atmosphere of static air. The samples were heated up to 950°C using a heating rate of 10°C/min. Initial sample weights ranged from 52 to 67 mg.

The DTA and TGA results for Wyoming sodium bentonite are presented in Figure 4. DTA endothermic peaks are located at 111°C and 704°C, which correspond to the loss of uncombined water and dehydroxylation, respectively. The TGA curve displays weight losses corresponding to these endothermic peaks. As shown by the TGA curve, the weight loss between 25°C and 160°C, corresponding to the loss of free water, was 6.13%. The weight loss from 505°C to 800°C was 5%, corresponding to water loss from dehydroxylation. The total weight loss after 950°C was 11.3%. The DTA and TGA curves are typical of “Wyoming” type bentonite (Earnest, 1991).

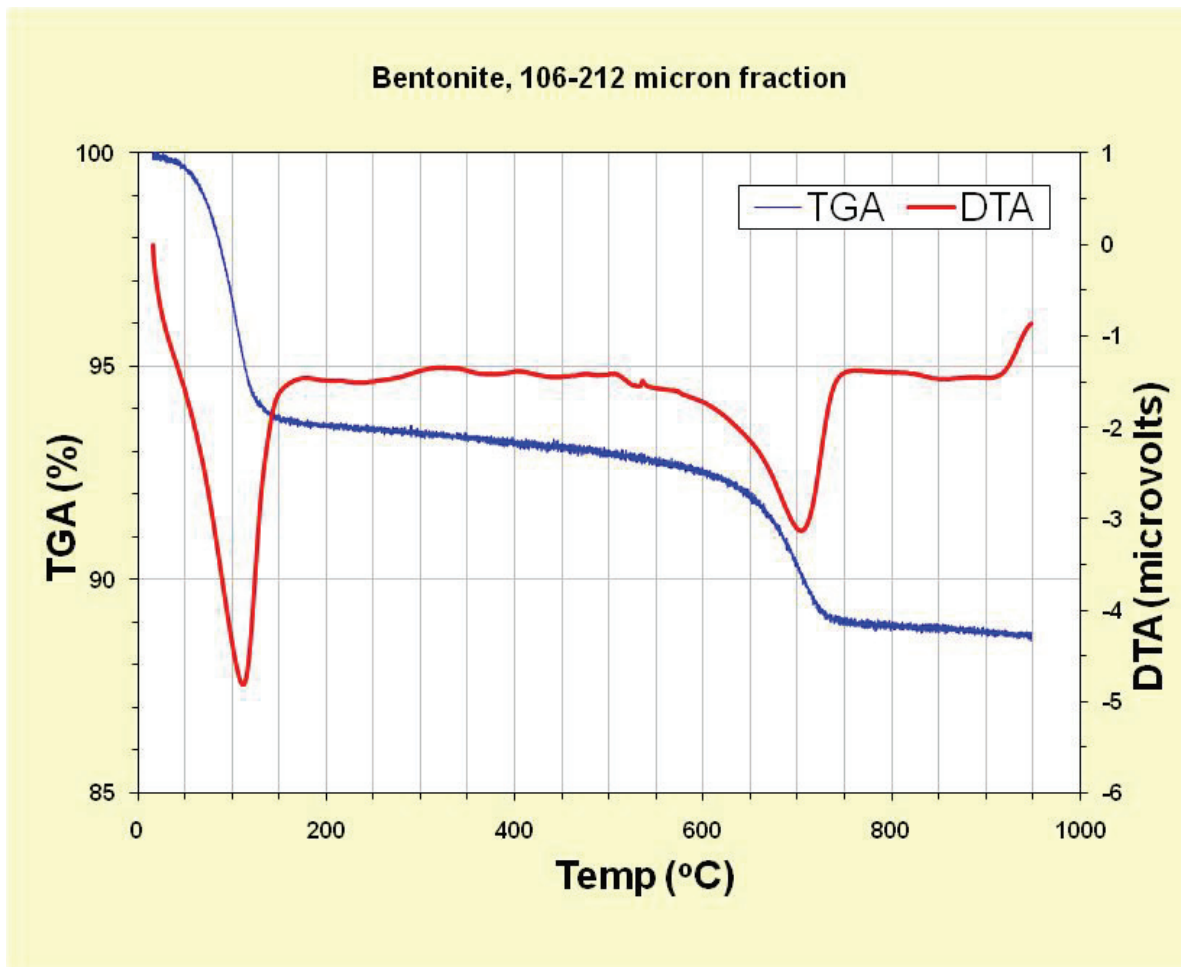


Figure 4: Differential Thermal Analyses and Thermogravimetric Analyses Plots of Wyoming Sodium Bentonite

The TGA and DTA results for Queenston shale are summarized in Figure 5 and Table 3. DTA endothermic peaks are located at 82.5°C, ~574°C (weak trough), 748°C and 788°C. The peak at 82.5°C corresponds to uncombined water loss, and the peak at 574°C is typical of the dehydroxylation of the clay lattice in illite (Earnest, 1991). Typically a quartz transition will occur at 573°C, but in this case it is masked by the presence of illite. The peak at 788°C may correspond to carbonate decomposition. The DTA exothermic peaks are found at 687°C, 767°C, 826°C and 900°C. The uncombined water loss up to a temperature of 128°C was 1.35%. The TGA residue at 950°C corresponded to 19.06% weight loss.

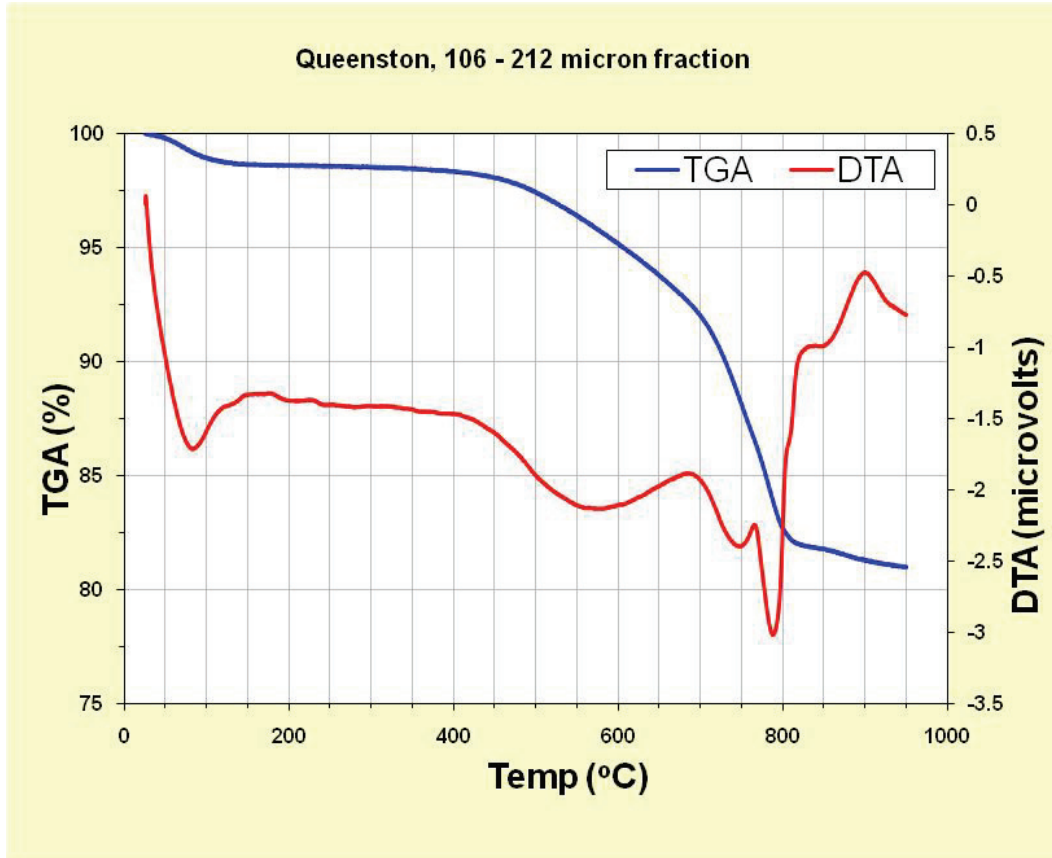
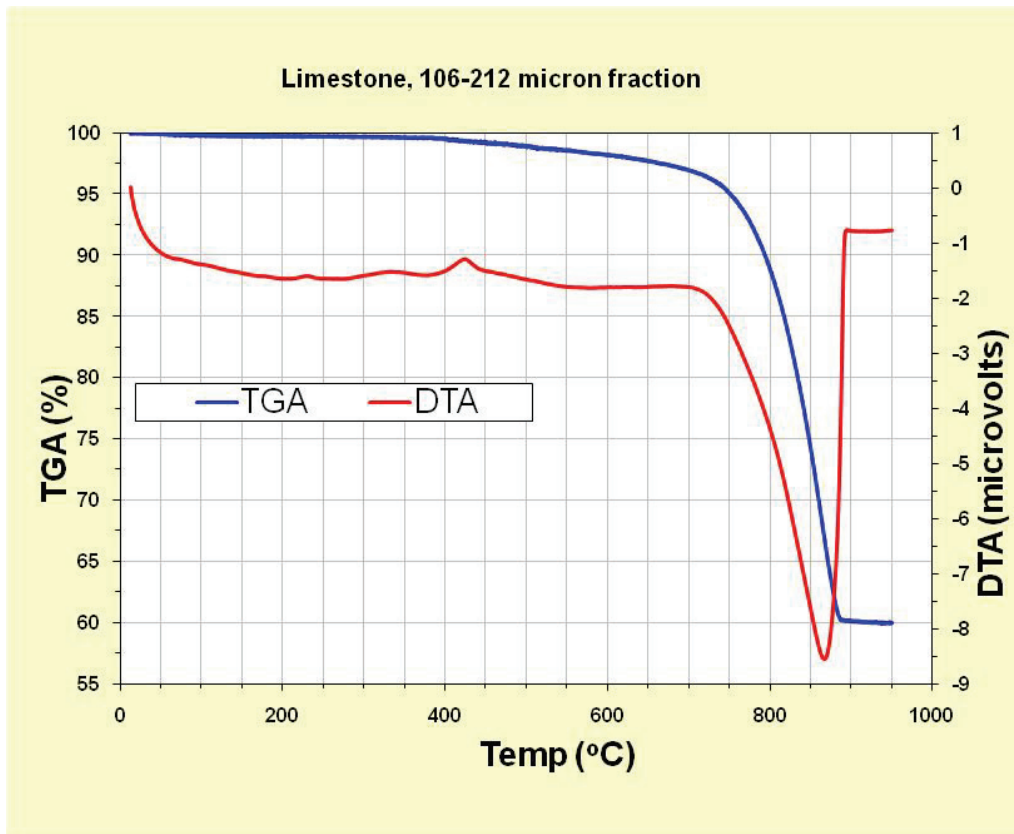


Figure 5: Differential Thermal Analyses and Thermogravimetric Analyses Plots of Queenston Shale

**Table 3: TGA Data Corresponding to DTA Peaks in Queenston Shale**

Type of DTA Peak	Temperature (°C)	% Cumulative Weight Loss
endothermic	82.5	0.84
endothermic	574	4.25
exothermic	687	7.46
endothermic	748	11.75
exothermic	767	13.61
endothermic	788	16.19
exothermic	826	18.09
exothermic	900	18.72

The TGA and DTA data for Cobourg limestone are presented in Figure 6. A DTA exothermic event was noted at 424°C. The onset of carbonate decomposition was extrapolated to 708°C, based on the DTA curve. The DTA carbonate decomposition minimum was at 867°C, and the carbonate decomposition peak was completed at 893°C. The total TGA weight loss to 950°C was 40.06%. The TGA weight loss associated with CO<sub>3</sub> decomposition was 36.60%. Since the theoretical weight loss for pure CaCO<sub>3</sub> is 43.96%, the sample was estimated to have 91% CaCO<sub>3</sub>.



**Figure 6: Differential Thermal Analyses and Thermogravimetric Analyses Plots of Limestone**



In summary, the thermal analyses supplement the results of XRD analyses. The results of the thermal analyses indicate that the Wyoming sodium bentonite is composed mainly of montmorillonite, with insignificant thermal contributions from other elements, which were identified as quartz, illite and feldspar by XRD analyses. The Queenston shale has a very high illite content and significant carbonate content, which could be calcite or ankerite. The thermal properties of quartz in Queenston shale samples were masked by illite. The Cobourg limestone was estimated to be 91% calcite, with no evidence of quartz or illite which was observed by XRD analyses. Apparently the concentrations of quartz and illite were too low to be detected with thermal analyses.

### 2.3 LEACHABLE ELEMENTS

In order to determine whether elements of interest in sorption experiments could be leached from solids used and complicate the interpretation of sorption tests, the concentrations of selected elements (Ba, Sr, Cs, Li, Rb, Cu, Ni, U) were determined for Wyoming sodium bentonite, Queenston shale and Cobourg limestone. The total element concentration and fraction leached by distilled water were analyzed. Distilled water was selected as a mild solvent to leach elements trapped as salts or loosely held by coulombic attraction. A benefit of distilled water is that it would not cause interference that could be associated with high salt concentrations.

To dissolve rock samples (0.25 g) for total elemental analyses, 50 mL of 7% HF and 55% HNO<sub>3</sub> was added and shaken at 90°C overnight. Samples were then evaporated to dryness at 120°C. Two mL of 50% H<sub>2</sub>SO<sub>4</sub> were then added, and the sample was evaporated overnight at 180°C to convert any fluorides of Ca, Ba and Sr to sulphates. Finally, 50 mL of 1% HNO<sub>3</sub> was added and the sample was allowed to dissolve overnight at 90°C. The samples were analysed using ICP-MS by the Manitoba Technology Centre Ltd. (ALS Laboratory Group), in Winnipeg, Manitoba.

A second set of rock samples was leached with distilled water using Soxhlet extraction. During Soxhlet extraction, distilled water was vaporized and allowed to condense and drip into the body of the extractor that contains the rock sample. Once the extractor fills with fluid, the fluid siphons back into the reservoir of distilled water. With repeated cycles, elements leached from the rock sample are concentrated in the reservoir of distilled water. Rock sample weights ranged from 0.25 to 1.3 g, and the volume of extracting fluid was 250 mL. After the Soxhlet extraction was complete, the fluid containing extracted elements was acidified to pH ~ 2 with HNO<sub>3</sub>, and submitted for ICP-MS analysis. Results were corrected for reagent blanks.

Table 4 summarizes the contents of measured trace elements in bentonite, shale and limestone. The “total mg/kg” corresponds to the total elemental concentration in the solid, based on the complete digestion of the rock sample. The “leached mg/kg” is the concentration of the element leached by Soxhlet extraction, normalized to the mass of the rock sample. The leached fraction corresponds to the element concentration that can be extracted by deionized water, without the presence of other cations that could drive cation exchange reactions. Leachable elements may be weakly sorbed or are associated with soluble salts contained within the rock samples. The percent leached values in Table 4 suggest that bentonite has the highest percentages of leachable elements, followed by shale and then limestone.

**Table 4: Selected Trace Elements in Rock Samples**

	Li	Rb	Cs	Ba	Sr	Ni	Cu	U
<b>Bentonite</b>								
Total (mg/kg)	17	12	182	266	236	13	7.1	12
Leached (mg/kg)	0	2.7	0	39	137	5	-	4.5
% Leached	0	22	0	15	58	38		38
<b>Shale</b>								
Total (mg/kg)	47	126	95	132	191	44	21	1.8
Leached (mg/kg)	1.7	7.9	59	7.3	60	0.9	4.1	0
% Leached	3.6	6.3	62	5.5	31	2.1	20	0
<b>Limestone</b>								
Total (mg/kg)	0	22	44	48	324	10	7.7	0.7
Leached (mg/kg)	0	1.1	0	4.7	32	0.7	-	0.1
% Leached	0	5.1	0	10	10	6.6		8.5

Li, Rb and Cs are monovalent Group I cations that are likely to sorb by non-specific coulombic attraction. Li was present in the bentonite and shale, but its very small leachable fraction indicates that it was fixed in mineral structures. Rb was present in higher concentrations and was 5 to 22 percent leachable. Cs was present in relatively high concentrations in all rock types. It was strongly fixed in bentonite and limestone, but was very leachable from shale. Cs is often fixed in the interlayer structures of clay minerals, so perhaps the leachable fraction from shale was from a soluble salt located in the rock matrix. Ba and Sr are divalent Group 2 cations that are also likely to sorb by non-specific coulombic attraction. The leachability of Ba varied from 5 to 15 percent. Sr was significantly more leachable (10 to 58%) than Ba. The most Sr was leached from bentonite. Although limestone had the highest Sr concentration, most of the Sr appears to be fixed within the carbonate minerals. As expected, bentonite has more leachable Sr than limestone due to the bigger surface area and cation exchange capacities in bentonite compared to limestone. Desorption tests with Sr indicate that Sr was leached from bentonite in brine solutions (Section 3.2.1).

Ni and Cu are divalent transition elements that are expected to sorb by both coulombic forces and specific surface complexation reactions. The total concentrations of both elements in the solids are too low to affect sorption experiments carried out as part of this research, even if all of the Cu and Ni were leached into solution. A relatively high proportion of the Ni on bentonite was leachable, while most of the Ni was fixed on shale and limestone. This suggests that bentonite has a high concentration of exchangeable sorption sites that sorb Ni, while Ni is fixed in mineral structures within shale and limestone. Leachate Cu concentrations are not available for bentonite and limestone because the leachates appear to have been contaminated with Cu. U is a hexavalent (under these redox conditions) actinide that is expected to sorb by surface complexation. The total U concentrations on the solids were too low to affect sorption experiments carried out in this research. As with Ni, a relatively high proportion of U was leachable from bentonite, but was not leachable from the shale and limestone. This suggests that the U contained in shale and limestone was held in mineral structures and is not likely to be in equilibrium with solutions contacting these rocks.

## 2.4 SURFACE AREA ANALYSES

The surface area of a solid influences the total sorption capacity of the solid. The surface areas of the Wyoming sodium bentonite, Queenston shale and Cobourg limestone were estimated using gas absorption, following the B.E.T. (Brunauer, Emmett and Teller, 1938) method. Rock samples (2 g) with the same particle size (100 to 200  $\mu\text{m}$ ) as used in the sorption experiments were submitted to Exova (Mississauga, Ontario, [www.exova.com](http://www.exova.com)) for surface area analyses. Exova performed the analyses as per USP32/NF27/S2, <846>, Method 2. A portion of the sample was outgassed at 40° C for two hours to remove residual gas. The surface area analyses were performed using a Coulter SA3100 instrument (M11B03579). Nitrogen gas was used as the adsorbate in the  $P/P_0$  range of 0.05 to 0.30. The results of the surface area analyses are summarized in Table 5.

**Table 5: B.E.T. Surface Areas of Rock Samples Used in Sorption Studies**

Rock	Surface area ( $\text{m}^2/\text{g}$ )
Wyoming sodium bentonite	24.981
Queenston shale	11.516
Cobourg limestone	2.894

## 3. AQUEOUS SPECIATION

Aqueous chemistry of brine solutions and the elements used in sorption tests was estimated using PHREEQC (Parkhurst and Appelo, 1999), a geochemical modeling program for speciation, batch-reaction, one-dimensional transport and inverse geochemical calculations that can be downloaded from the US Geological Survey website. The version of this program used in these calculations was PHREEQC Interactive 2.17.4137.

Chemical speciation calculations are complicated for high ionic strength solutions, since they are dependent on ion activity corrections. PHREEQC implements both Pitzer and SIT (specific ion interaction theory) ion interaction approaches for activity coefficient corrections for high ionic strength solutions. The best estimate of ion activities at high ionic strength brines is given by the Pitzer equations. The Pitzer database "data0.ypf.R2" produced by the Yucca Mountain Project includes Pitzer ion interaction coefficients. This database was converted from EQ3/6 format to PHREEQC format (Benbow et al. 2008). In addition, this database contains thermodynamic data for a number of elements that are of interest to radionuclide transport, including Am, Cm, Cs, Co, Cu, Ni, Nd, Np, Pu, Sr, Tc, Th and U. Unfortunately no data for europium are included in this database. Additional data for many other elements of interest in radionuclide migration are included in the SIT.dat database that is available with the downloaded PHREEQC package. Single ion activity coefficients in this database are estimated with the Specific Ion Interaction Theory (SIT). While SIT theory has proved to be simple and adequate to apply to ionic strengths from 0.5 to 3 mol/L, Pitzer theory is outstanding for precision and accuracy in reproducing experimental behaviour with ionic strengths up to 20 mol/L (Elizalde and Aparicio, 1995). The SIT.dat database is the PHREEQC version of the ThermoChimie v.7.b

thermodynamic database developed for ANDRA, the French National Radioactive Waste Management Agency. The database includes SIT parameters when data are available. If the SIT parameters are not available (such as for As, Bi, Nb, and Tc), then the Debye-Huckel approach was used for calculation of activity corrections included in the database.

#### 4. BATCH SORPTION EXPERIMENTS

The purpose of the initial batch sorption experiments was to establish the experimental protocols that would be used to characterize the sorption characteristics of limestone, shale and bentonite for key elements, including  $\text{Sr}^{+2}$ ,  $\text{Cu}^{+2}$ ,  $\text{Ni}^{+2}$ ,  $\text{Eu}^{+3}$ , and U(VI) ( $\text{UO}_2^{2+}$ ). Initial experiments were performed to identify workable element concentration ranges and pH ranges, test analytical methods, and establish workable solid/liquid ratios and phase separation methods.

##### 4.1 GENERAL METHODS

The rock types characterized in Section 2 were used in the sorption studies (Wyoming sodium bentonite, Queenston shale and Cobourg limestone). The shale and limestone samples were first crushed and powdered in the laboratory. Because the bentonite was received in a granular form its grain size was reduced by gentle grinding with a mortar and pestle. The shale, limestone and bentonite were dry sieved to collect a size fraction between 100 and 200  $\mu\text{m}$  for use in the sorption experiments.

The solutions used in the sorption tests are summarized in Table 6. The brine solution used in the initial batch sorption experiments was a Na-Ca-Cl brine with a TDS of 300 g/L. This brine was chosen because it was likely to provide the greatest experimental challenges, and would show the maximum effect of TDS concentration on measured sorption properties. The brine solutions were made from reagent grade  $\text{CaCl}_2$  and  $\text{NaCl}$ . The concentrations of the main components were 2.11 mol/L  $\text{Na}^+$ , 1.59 mol/L  $\text{Ca}^{+2}$ , and 5.29 mol/L  $\text{Cl}^-$ . The pH of the brine exposed to the atmosphere varied between 5.9 and 6.2. When contacted with solids the pH of 300 g/L Na-Ca-Cl brine solution varied between 5.9 and 6.8. In subsequent tests to study the effect of salinity on sorption, additional brine solutions with TDS values of 10, 25, 100 and 200 g/L were produced by diluting the 300 g/L Na-Ca-Cl brine with distilled water. A final 100 g/L Na-Cl brine solution was used to determine to what extent sorption is affected by competition with  $\text{Ca}^{+2}$ .

Sorption experiments were performed with Sr, Ni, Cu, U and Eu in order to test experimental methodologies, analytical capabilities, and practical concentration ranges. Strontium was obtained as  $\text{SrCl}_2 \cdot 6\text{H}_2\text{O}$  (Canada Wide Scientific, reagent grade). Copper was obtained as  $\text{CuCl}_2 \cdot 2\text{H}_2\text{O}$  (J.T. Baker, Baker analysed reagent grade). Nickel was added as  $\text{NiCl}_2 \cdot 6\text{H}_2\text{O}$  (J.T. Baker, Baker analysed reagent grade). Uranium solutions were prepared from uranyl nitrate hexahydrate ( $\text{N}_2\text{O}_8\text{U} \cdot 6\text{H}_2\text{O}$ ), supplied by Fluka Chemie AG. Europium was obtained as  $\text{EuCl}_3 \cdot 6\text{H}_2\text{O}$  (Aldrich 212881, 99.9% pure).

**Table 6: Solutions Used in Batch Sorption Experiments**

TDS (g/L)	[Na] (mol/L)	[Ca] (mol/L)	[Cl] (mol/L)	*[CO <sub>3</sub> ] <sub>total</sub> (mol/L)	**Ionic Strength (mol/kg)	***pH Range
300 Na-Ca-Cl	2.11	1.59	5.29	5 x 10 <sup>-5</sup>	7.53	5.9 to 6.8
200 Na-Ca-Cl	1.41	1.06	3.53	1 x 10 <sup>-4</sup>	4.87	6.4 to 7.1
100 Na-Ca-Cl	0.700	0.530	1.76	2 x 10 <sup>-4</sup>	2.36	6.7 to 7.6
25 Na-Ca-Cl	0.180	0.180	0.44	4 x 10 <sup>-4</sup>	0.59	6.9 to 7.8
10 Na-Ca-Cl	0.070	0.053	0.18	4 x 10 <sup>-4</sup>	0.23	7.3 to 7.9
100 Na-Cl	1.71	0.008	1.71	8 x 10 <sup>-3</sup>	1.78	7.0 to 7.3

\* Predicted to be in equilibrium with calcite using PHREEQC with the NWMO thermodynamic database which was derived from data0.ypf.R2 (includes Pitzer ion interaction coefficients) (Benbow et al., 2008)

\*\* Ionic strength calculated with PHREEQC using the NWMO database

\*\*\* Measured pH values in contact with solids

Analyses of Sr, Cu and Ni were performed by the Analytical Science Branch (Whiteshell) of the Atomic Energy of Canada Limited (AECL), using inductively-coupled plasma (ICP). The presence of 300 g/L salt interfered with ICP analyses, generating a relatively large amount of uncertainty. Therefore, a colorimetric method was adopted for nickel analysis, which was based on the formation of a Ni ion complex with bromo-PADAP. The method for Ni analysis described by Marczenko and Balcerzak (2000) was modified to minimize the interference of Ca. The Ni-bromo-PADAP complex was determined at a wavelength of 558 nm while buffered at pH 7.85 with triethanolamine buffer. The Ni detection limit was approximately 3 x 10<sup>-6</sup> mol/L. Uranium was determined colorimetrically as its bromo-PADAP complex at pH 7.85 (Johnson and Florence, 1971; Marczenko and Balcerzak, 2000). The uranium detection limit was approximately 7 x 10<sup>-7</sup> mol/L. Europium was determined on acidified samples using time resolved fluorescence (phosphorescence) by a method developed at Whiteshell of AECL. The excitation wavelength for europium was 340 nm and the emission wavelength for detection of europium was 595 nm. The europium detection limit was 1 x 10<sup>-6</sup> mol/L. The ranges of sorbing element concentrations used to initiate sorption tests were determined by both the element analytical detection limits and solubility considerations (Table 7).

**Table 7: Ranges of Sorbing Element Concentrations for Sorption Tests**

	Sr	Cu	Ni	U	Eu
Concentration (mol/L)	1x10 <sup>-4</sup> to 5x10 <sup>-3</sup>	1x10 <sup>-5</sup> to 1x10 <sup>-4</sup>	1x10 <sup>-5</sup> to 3x10 <sup>-3</sup>	1x10 <sup>-5</sup> to 1x10 <sup>-4</sup>	1x10 <sup>-5</sup> to 5x10 <sup>-4</sup>

The pH of sample solutions was determined with a Radiometer Analytical SAS combined pH electrode (pH C2401-8). The pH electrode was calibrated with NBS reference buffer solutions with an ionic strength of 0.1 mol/L (Wu et al., 1988). It is recognized that pH measurements in brine solutions (in neutral pH ranges) may be affected by changes in liquid junction potentials as a result of higher salt concentrations (Hinds et al., 2009; Baumann, 1973). A standard procedure of measuring pH was adopted that consisted of determining pH in unstirred samples after the majority of solids had settled out of suspension. Additional analyses of Ba, Cs, Cu, Li,

Ni, Rb, Sr, and U extracted from rock samples were performed by the ALS Laboratory Group in Winnipeg using inductively-coupled plasma mass spectrometry (ICPMS).

Sorption tests were performed using two different approaches. The first approach involved using a relatively small sample volume (10 or 20 mL) for each test to produce a single sorption measurement. In the second approach the solution volume was increased to 200 mL. This provided the ability to take multiple samples from the same sorption test at various time intervals and to have better control over pH.

The reaction vessels used in the small volume tests were polycarbonate, 30 mL volume Oak Ridge type centrifuge tubes. The experimental solid/liquid ratios were varied by using solid weights of either 0.1 or 1.0 g, and solution volumes of either 10 or 20 mL. Mineral solids were first weighed into each centrifuge tube. Then the brine solutions with different element concentrations were added to each tube. Centrifuge tubes with no minerals were used as blanks to check for sorption on centrifuge tube walls and to serve as a measure of the amount of each element that was available for sorption. All sorption tests were performed with single elements to avoid complications with analytical interferences and competition for sorption sites by different elements.

Sorption experiments were performed in contact with the atmosphere, which has a partial CO<sub>2</sub> pressure of  $3.3 \times 10^{-4}$  atm. and a partial O<sub>2</sub> pressure of 0.21 atm. (Stumm and Morgan, 1981). The experimental time frame varied from 3 h to 28 d. Samples were shaken once a day for 15 seconds. At the end of the reaction period, the solids were separated from solution by centrifuging for 15 minutes at 20000 rpm. The supernatant solutions were decanted into clean plastic vials. After measuring pH, the water samples were acidified to pH 2 with 1 mol/L HCl to ensure that elements remained in solution. This procedure was also performed for the blank solutions.

The larger volume tests were performed using 250 mL, polypropylene Nalgene wide mouth bottles. The starting solution volume was 200 mL. Depending upon the element and the type of rock, the mass of solids was varied from 1 g to 16 g to optimize the change in element solution concentration produced by the sorption process. The target was to have 40 to 60 percent of the total element sorbed to ensure optimum accuracy in measuring the amount sorbed and the amount left in solution. If the amount of sorption approaches 100 percent, the concentration of the sorbing element in solution approaches and likely falls below the detection limit. The resulting uncertainty in the "equilibrium" element concentration in solution will result in a very high uncertainty in the derived sorption coefficient. Furthermore, if sorption is slow to reach equilibrium, and if there is a very large drop in solution concentration, it could be that the amount of element sorbed is the product of a higher dissolved element concentration. This would produce a sorption coefficient that is too high. After weighing out mineral samples into the reaction vessel, brine solutions (without the element used for sorption tests) were added and the minerals were conditioned in the brine solution for at least one week. During this period the pH was periodically checked. After the conditioning period, one half of the brine solution (by volume) was removed and replaced with an equal volume of brine containing the element of interest in the sorption test. This step initiated the sorption test. The sorption test was sampled at selected times by removing 10 mL of solution just after shaking to ensure that the sample contained rock sample and that the solid/liquid ratio would not be altered by sampling. The pH of the remaining samples in the reaction vessel was determined at the time of sampling. The samples were centrifuged and acidified as described above. Blank tests were performed with identical solution volumes and element concentrations, except that they contained no solids. The blank tests were sampled immediately after the sorption test was initiated to confirm the

initial concentration of the element being studied. These samples were acidified without centrifuging. Afterwards, the blank tests were sampled every time that samples were taken for sorption measurements. These samples were centrifuged and acidified in the same way as samples from the sorption experiments. The pH values of blank tests were adjusted to bracket the pH values observed in the reaction vessels with mineral solids.

When test solutions contact solids, they tend to reach an equilibrium pH value within 1 to 3 days. As shown in Table 8, the equilibrium pH value depends mainly upon the type of solution. The decrease in pH with increasing salt concentration may be explained to some degree by the increase in  $H^+$  ion activity coefficient with higher ionic strength (Wiesner et al., 2006). In most cases the equilibrium pH values of bentonite are slightly higher than those of shale and limestone, which are identical. The exception is the 100 g/L Na-Cl brine containing a significantly larger concentration of  $CO_3^{2-}$ , which will be discussed later. Attempts to manipulate experimental pH by the addition of acid or base failed to produce steady-state pH values that were significantly different from the equilibrium values. Since carbonate is present in all solid samples, it is reasonable to assume that  $CO_3^{2-}$  will be released to solution, as determined by equilibrium with calcite and by the Ca content of the experimental solution. Calculations using geochemical modelling with PHREEQC suggest that the pH values of rock suspensions can be explained by equilibrium with calcite, whose solubility decreases significantly with higher Ca concentrations in the more concentrated brines. PHREEQC simulations also predicted that the acid-base properties of montmorillonite were not able to account for the high pH in the bentonite suspended in the 10 g/L solution. Attempts to reduce high pH values in sorption experiments included the reduction of solid/liquid ratios, conditioning solids at lower pH and increasing total dissolved carbonate concentration to reduce calcite dissolution. The problem with adding concentrated acid to maintain pH is the acid will keep dissolving carbonate, thereby changing the solid and solution composition. The use of pH buffers is a possibility, but their use was avoided in this study due to potential effects on sorption reactions. To minimize the change in solution composition created by the release of  $CO_3^{2-}$ , in later tests  $CO_3^{2-}$  was added to the starting solutions in amounts that were in equilibrium with calcite as determined by the amount of Ca in solution (Table 6). The use of  $CO_3^{2-}$  as a pH buffer only had potential at higher  $CO_3^{2-}$  concentration Na-Cl brines, and was not practical for Na-Ca-Cl brines due to the precipitation of calcite.

**Table 8: The pH of Test Solutions in Contact with Solids**

Solution	Average Equilibrium pH values			N	$H^+$ Activity Coefficient
	Bentonite	Shale	Limestone		
10 g/L Na-Ca-Cl	7.7 ± 0.4	7.5 ± 0.2	7.5 ± 0.2	34	0.79
25 g/L Na-Ca-Cl	7.7 ± 0.1	7.3 ± 0.4	7.3 ± 0.4	6	0.82
100 g/L Na-Ca-Cl	7.2 ± 0.4	6.9 ± 0.2	6.9 ± 0.2	30	1.35
200 g/L Na-Ca-Cl	7.0 ± 0.1	6.5 ± 0.1	6.6 ± 0.2	6	3.31
300 g/L Na-Ca-Cl	6.5 ± 0.2	6.2 ± 0.3	6.2 ± 0.3	52	9.57
100 g/L Na-Cl	7.1 ± 0.1	7.2 ± 0.1	7.1 ± 0.1	12	1.26

Note:  $H^+$  activity coefficient is the MacInnes coefficient estimated by PHREEQC using the data0.ypf.R2 database. The number of values used to calculate average pH is n.

Sorption results were expressed as sorption coefficients ( $K_d$ ) and as percent sorbed. Sorption coefficients were calculated as follows:

$$K_d = \frac{S}{C} = \frac{(C_0 - C) \times vol}{C \times m} \times 1000 \quad (\text{cm}^3/\text{g}) \quad (1)$$

Where:  $C_0$  = initial concentration of sorbate (mol/L) determined from blank solutions.

$C$  = equilibrium concentration of sorbate measured in solution (mol/L)

$S$  = concentration of sorbate on the solid (mol/g)

Vol = total volume of solution (L)

$m$  = mass of sorbing solid in the system (g)

Conversion factor: 1000  $\text{cm}^3/\text{L}$

The percent sorbed is defined as:

$$\text{percent sorbed} = \frac{\text{mass sorbate removed from solution} \times 100\%}{\text{total sorbate available for sorption}} \quad (2)$$

If sorption measurements are being performed on rock coupons in which the sorbate does not significantly penetrate into the mass of the coupon and sorption occurs mainly on the surface, it is better to report sorption in terms of sorbed mass per specific surface area ( $A_{sp}$ ). The specific surface area has units of area per mass solid ( $\text{cm}^2/\text{g}$ ), and may be estimated by BET measurements. In this case the concentration of sorbate on the solid ( $S_A$ ) has unit of  $\text{mol}/\text{cm}^2$ , and the sorption coefficient is defined as  $K_a$  where

$$K_a = \frac{S_A}{C} \times 1000 \quad (\text{cm}) \quad (3)$$

The value of  $K_a$  is related to  $K_d$  by the following

$$K_a = \frac{K_d}{A_{sp}} \quad (4)$$

## 4.2 RESULTS

This section presents the results of batch sorption tests performed to characterize the sorption of Sr, Ni, Cu, U and Eu onto bentonite, shale and limestone in brine solutions. The sorption experiments studied the effect of solution composition and changes in sorption as a function of time for periods up to 4 weeks. The effect of preconditioning crushed rock samples with test solutions before sorption experiments was tested. The reversibility of Ni, Eu and U sorption with respect to changes in sorbate solution concentration was investigated. Finally, the results of the sorption tests were used to propose preliminary estimates of sorption coefficient values that could be used in predicting radionuclide transport in sedimentary rocks under saline conditions.

Each element is discussed under its own subsection. The results of initial tests are presented first and each section concludes with recommended values for sorption coefficients. Note that



since the experimental volumes in this report ranged from 10 to 200 mL, for comparison purposes the solid/liquid ratio is reported as g per 100 mL.

#### 4.2.1 Strontium

The main strontium species in brine solutions used in the experiments (Table 6) was predicted using PHREEQC and SIT.dat thermodynamic database. The results suggest that  $\text{Sr}^{2+}$  and  $\text{SrCl}^+$  are the dominant species, with a very small fraction of  $\text{SrHCO}_3^+$  appearing if the carbonate concentration is as high as  $1 \times 10^{-3}$  mol/L. The lack of hydroxyl species suggests that Sr will not sorb significantly by surface complexation. Since Sr may also interact with carbonate to form strontianite, there is a possibility that it could form surface complexes with any carbonate minerals. The main sorption mechanism for Sr is by coulombic attraction in low ionic strength solutions. The only radioisotope of interest is  $^{90}\text{Sr}$ , with a half-life of 29 a. Although  $^{90}\text{Sr}$  is not of significant interest to the safety case for a deep geologic repository due to its short half-life, Sr sorption may be a good marker for sorption by cation exchange and as such, can be used as a chemical analog for  $\text{Ra}^{2+}$ .

Strontium sorption experiments were performed using the 300 g/L TDS Na-Ca-Cl brine. The experimental time was one week. At this time the pH values of the bentonite, shale and limestone suspensions were identical to the values shown in Table 8. Strontium sorption was not observed on any of the solids in the brine solution. The  $\text{Sr}^{2+}$  concentration of brine solutions in contact with solids actually increased due to the release of  $\text{Sr}^{2+}$  from the solids. This observation suggests that  $\text{Ca}^{2+}$  in the brine caused the desorption of  $\text{Sr}^{2+}$  by a cation exchange reaction. About 180 to 200 mg/kg (ppm)  $\text{Sr}^{2+}$  was desorbed from bentonite, while the amount of  $\text{Sr}^{2+}$  desorbed per mass of shale varied between 0 and 60 mg/kg, and that desorbed from limestone was 0 to 20 mg/kg. As discussed in Section 2.3, leaching experiments determined that the Sr desorbed from the solids was part of their original composition. These results indicate that  $\text{Sr}^{2+}$  sorbs mainly by nonspecific cation exchange, and is not able to compete with the high concentration of  $\text{Ca}^{2+}$  in the brine. Consequently no further measurements of  $\text{Sr}^{2+}$  sorption were undertaken.

*Summary:* As a chemical analog of group 1 and 2 elements, the results of sorption tests with  $\text{Sr}^{2+}$  indicate that group 1 and 2 elements will not be sorbed by sedimentary rocks in concentrated brine solutions. Therefore, it should be assumed that group 1 and group 2 elements, such as  $\text{Ra}^{2+}$ , have a sorption coefficient of 0 in brine solutions.

#### 4.2.2 Nickel

In brine solutions, the dominant soluble nickel species are predicted to be  $\text{NiCl}^+$  and  $\text{Ni}^{2+}$ . Solubility limiting solids for Ni in brine solutions are  $\text{Ni}(\text{OH})_2$  and  $\text{NiCO}_3$ , suggesting that Ni has an affinity for carbonate and oxygen sites coordinated with Si, Al or another metal. Nickel is expected to sorb by a combination of surface complexation and cation exchange, although the latter is probably limited in brine solutions due to the mass action of salts. Since  $\text{Ni}^{2+}$  has a relatively simple chemistry and a higher solubility than other elements such as Cu, it is relatively simple to use experimentally. Although Ni sorption values may be lower than Pb sorption values, Ni is a useful conservative analog element for Pb when Pb data are lacking (Vilks, 2011).

*Initial Sorption Tests With Ni:* The initial Ni sorption tests were performed in the 300 g/L brine solution using 10 mL sample volumes, a solid/liquid ratio of 10 g/100 mL (i.e. 1 g/10 mL), and total Ni concentrations ranging from  $7.5 \times 10^{-5}$  to  $9.0 \times 10^{-3}$  mol/L. The purpose of these tests was to evaluate experimental methodology and to identify an ideal range of Ni concentrations to use for measuring sorption on bentonite, shale and limestone. Results for a 10 day reaction time are presented in Table 9. The table includes the total Ni concentration that was available for sorption onto the solid. Any effects of sorption onto container walls have been accounted for in these values. The pH values correspond to measurements at the end of the experiment. Sorption is described in the form of sorption coefficients ( $K_d$ ) values calculated with Equation 1, as well as the percent of the total Ni that was sorbed (calculated with Equation 2). From an experimental point of view the percent sorbed values were reasonable, not being zero and not reaching the upper 90%. Table 9 includes sorption values ( $K_a$ ) which represent sorption as a function of surface area. These were calculated from  $K_d$  values and BET surface areas of bentonite, shale and limestone, as described in Section 2.4 and presented in Table 5

Figure 7 illustrates Ni sorption as a function of the Ni concentration in solution. Figure 7A shows that the amount of sorbed Ni increased with the amount of Ni in solution, but not in a linear fashion. Sorption coefficients, being a ratio of sorbed to dissolved Ni, decreased with increasing Ni in solution (Figure 7B). This indicates that sorption sites were being filled with increasing Ni concentrations. The sorption values for the lowest concentrations are probably more representative of the trace radionuclide concentrations in groundwater. Bentonite had the highest sorption capacity for Ni, followed by shale. Sorption on limestone was comparatively low. This could imply that Ni has an affinity for clays and not for carbonate. However, differences in surface area could also play a role. Figure 7C illustrates the variation of  $K_a$  values, referenced to surface areas estimated by BET (Table 5), with Ni concentration. Except for at trace Ni concentrations ( $7.48 \times 10^{-5}$  mol/L), the limestone  $K_a$  values are the highest, implying that surface area played an important role in determining the difference of sorption between limestone and the other solids.

**Table 9: Initial Nickel Sorption Results**

<b>Solid</b>	<b>TDS (g/L)</b>	<b>Time (h)</b>	<b>Total [Ni] (mol/L)</b>	<b>pH</b>	<b>K<sub>d</sub> (cm<sup>3</sup>/g)</b>	<b>K<sub>a</sub> (cm)</b>	<b>% sorbed</b>
bentonite	300	240	9.06 x 10 <sup>-3</sup>	6.04	2.1	8.5 x 10 <sup>-6</sup>	17
			4.48 x 10 <sup>-3</sup>	6.14	3.4	1.4 x 10 <sup>-6</sup>	25
			9.40 x 10 <sup>-4</sup>	6.28	19	7.8 x 10 <sup>-5</sup>	66
			4.70 x 10 <sup>-4</sup>	6.39	28	1.1 x 10 <sup>-4</sup>	74
			7.48 x 10 <sup>-5</sup>	6.56	71	2.9 x 10 <sup>-4</sup>	88
shale	300	240	9.06 x 10 <sup>-3</sup>	5.91	1.2	1.0 x 10 <sup>-5</sup>	10
			4.48 x 10 <sup>-3</sup>	5.94	2.0	1.7 x 10 <sup>-5</sup>	16
			9.40 x 10 <sup>-4</sup>	6.03	4.4	3.8 x 10 <sup>-5</sup>	31
			4.70 x 10 <sup>-4</sup>	6.07	6.1	5.3 x 10 <sup>-5</sup>	38
			7.48 x 10 <sup>-5</sup>	6.11	10	9.0 x 10 <sup>-5</sup>	51
limestone	300	240	9.06 x 10 <sup>-3</sup>	5.95	0.5	1.8 x 10 <sup>-5</sup>	5
			4.48 x 10 <sup>-3</sup>	5.92	0.6	2.1 x 10 <sup>-5</sup>	6
			9.40 x 10 <sup>-4</sup>	5.98	1.5	5.1 x 10 <sup>-5</sup>	13
			4.70 x 10 <sup>-4</sup>	5.98	2.2	7.5 x 10 <sup>-5</sup>	18
			7.48 x 10 <sup>-5</sup>	6.01	1.4	4.8 x 10 <sup>-5</sup>	12

- Solid/liquid ratio = 10 g/100 mL
- Sample volume = 10 mL

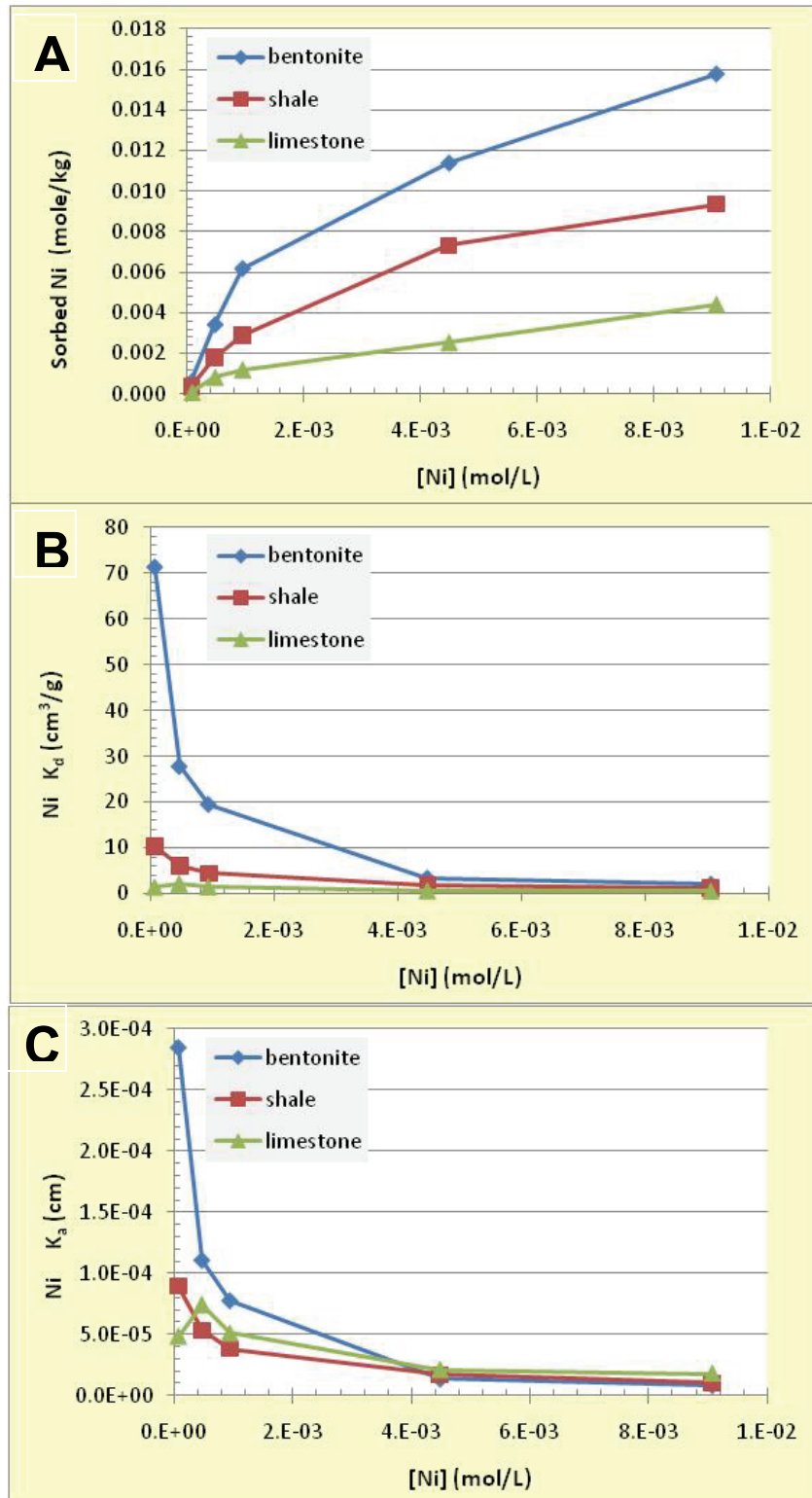


Figure 7: Nickel Sorption versus Total Nickel in System Expressed as (A) Total Nickel Sorbed, (B) Mass-Based Sorption Coefficient and (C) Surface-Based Sorption Coefficient

*Initial Test to Evaluate Ni Sorption Kinetics:* Nickel sorption on bentonite in the 300 g/L TDS brine, using 3 different Ni concentrations, was studied as a function of time for up to 28 days, using 1g of solid in 10 mL of solution. The sorption results are summarized in Table 10, and illustrated in Figure 8. The pH values remained relatively constant for the duration of the experiment. Figure 8 shows the same Ni sorption results in the forms of (A) percent sorbed, (B) moles sorbed per kg bentonite, and (C)  $K_d$  values. Although a significant portion of the Ni sorbed within the first 24 hours, sorption continued to increase with time. Even though the sorption process appeared to be close to being complete by 14 days, a slow sorption reaction appeared to continue up to and probably beyond 28 days. The solution with the highest Ni concentration had the most moles of Ni sorbed. However, the highest percent sorbed and the highest sorption coefficients were observed with the lowest Ni concentrations, in which case the reservoir of dissolved Ni was depleted more rapidly. The high percent sorbed values, reaching 90 percent for the lower Ni concentrations, are of concern because the reduced concentrations of dissolved Ni increase the uncertainty of the sorption coefficients. Since it is beneficial to use the lower Ni concentrations, the high percent sorbed values at lower Ni concentrations indicate that the solid/liquid ratio needs to be reduced in future experiments.

**Table 10: Nickel Sorption on Bentonite in 300 g/L TDS Brine as a Function of Time**

Total [Ni] (mol/L)	Time (d)	pH	$K_d$ (cm <sup>3</sup> /g)	$K_a$ (cm)	% sorbed
$2 \times 10^{-3}$	0.125	6.3	3.7	$1.5 \times 10^{-5}$	27
	0.23	6.3	1.8	$7.4 \times 10^{-5}$	16
	1	6.2	3.5	$1.4 \times 10^{-5}$	26
	3	6.0	5.8	$2.3 \times 10^{-5}$	37
	14	6.1	9.8	$3.9 \times 10^{-5}$	50
	28	6.1	12	$4.8 \times 10^{-5}$	55
$5 \times 10^{-4}$	0.125	6.4	4.3	$1.7 \times 10^{-5}$	30
	0.23	6.4	3.1	$1.2 \times 10^{-5}$	23
	1	6.4	8.3	$3.3 \times 10^{-5}$	45
	3	6.3	13	$5.3 \times 10^{-5}$	57
	14	6.4	44	$1.8 \times 10^{-4}$	82
	28	6.5	104	$4.1 \times 10^{-4}$	91
$1 \times 10^{-4}$	0.125	6.5	6.2	$2.5 \times 10^{-5}$	38
	0.23	6.5	3.9	$1.6 \times 10^{-5}$	28
	1	6.5	15	$5.9 \times 10^{-5}$	60
	3	6.5	21	$8.3 \times 10^{-5}$	68
	14	6.7	93	$3.7 \times 10^{-4}$	90
	28	6.7	225	$9.0 \times 10^{-4}$	96

- Solid/liquid ratio = 10 g/100 mL
- Sample volume = 10 mL
- 300 g/L TDS Na-Ca-Cl brine
- Sorption on bentonite

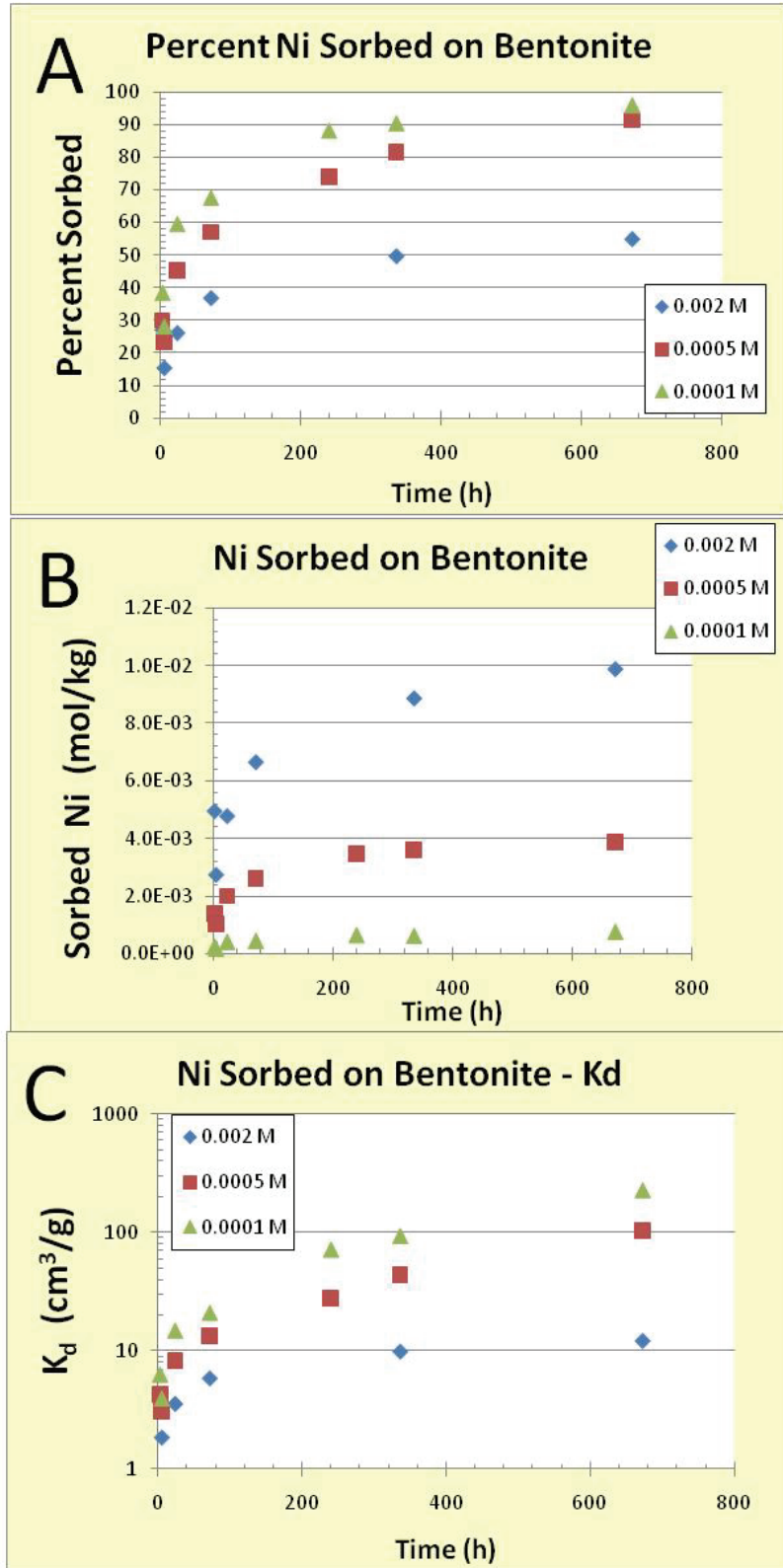


Figure 8: Nickel Sorption on Bentonite as a Function of Time Expressed as (A) Percent Sorbed, (B) Moles Ni Sorbed, and (C)  $K_d$  Values. Analytical Uncertainties Are Smaller than the Symbols

*Sorption as a Function of Brine Solution:* The sorption of Ni on bentonite, shale and limestone was evaluated as a function of brine concentration for TDS values of 10, 25, 100, 200 and 300 g/L. The reaction time was 7 days. These tests used 1 g of solid in a 10 mL volume, and the initial Ni concentrations were  $1 \times 10^{-5}$  and  $1 \times 10^{-4}$  mol/L. The experimental results are summarized in Table 11 and Figure 9.

**Table 11: Nickel Sorption as a Function of TDS**

Solid	Total [Ni] (mol/L)	TDS (g/L)	pH	$K_d$ (cm <sup>3</sup> /g)	$K_a$ (cm)	% sorbed
bentonite	$1.0 \times 10^{-4}$	300	6.5	71	$2.8 \times 10^{-4}$	88
		200	6.8	102	$4.1 \times 10^{-4}$	91
		100	7.2	191	$7.6 \times 10^{-4}$	95
		25	7.5	295	$1.2 \times 10^{-3}$	97
		10	7.8	371	$1.5 \times 10^{-3}$	97
shale	$1.0 \times 10^{-4}$	300	6.0	11	$9.1 \times 10^{-5}$	51
		200	6.4	13	$1.1 \times 10^{-4}$	56
		100	6.7	20	$1.7 \times 10^{-4}$	66
		25	7.1	54	$4.7 \times 10^{-4}$	84
		10	7.4	119	$1.0 \times 10^{-3}$	92
limestone	$1.0 \times 10^{-4}$	300	6.0	2.3	$8.0 \times 10^{-4}$	19
		200	6.4	2.4	$8.2 \times 10^{-4}$	19
		100	6.8	3.2	$1.1 \times 10^{-4}$	24
		25	7.2	7.6	$2.6 \times 10^{-4}$	43
		10	7.3	19	$6.5 \times 10^{-4}$	65
bentonite	$1.0 \times 10^{-5}$	300	6.4	63	$2.5 \times 10^{-4}$	86
		200	6.7	94	$3.7 \times 10^{-4}$	90
		100	7.1	196	$7.8 \times 10^{-4}$	95
		25	7.5	66	$2.6 \times 10^{-4}$	87
		10	7.8	181	$7.2 \times 10^{-4}$	95
shale	$1.0 \times 10^{-5}$	300	5.9	55	$4.8 \times 10^{-4}$	85
		200	6.2	68	$5.9 \times 10^{-4}$	87
		100	6.5	93	$8.1 \times 10^{-4}$	90
		25	7.0	37	$3.2 \times 10^{-4}$	79
		10	7.2	133	$1.2 \times 10^{-3}$	93
limestone	$1.0 \times 10^{-5}$	300	5.9	10	$3.4 \times 10^{-4}$	50
		200	6.2	6.8	$2.4 \times 10^{-4}$	41
		100	6.5	10	$3.4 \times 10^{-4}$	50
		25	6.9	13	$4.6 \times 10^{-4}$	57
		10	7.2	28	$9.7 \times 10^{-4}$	74

- Sorption time = 7 day
- Solid/liquid ratio = 10 g/100 mL

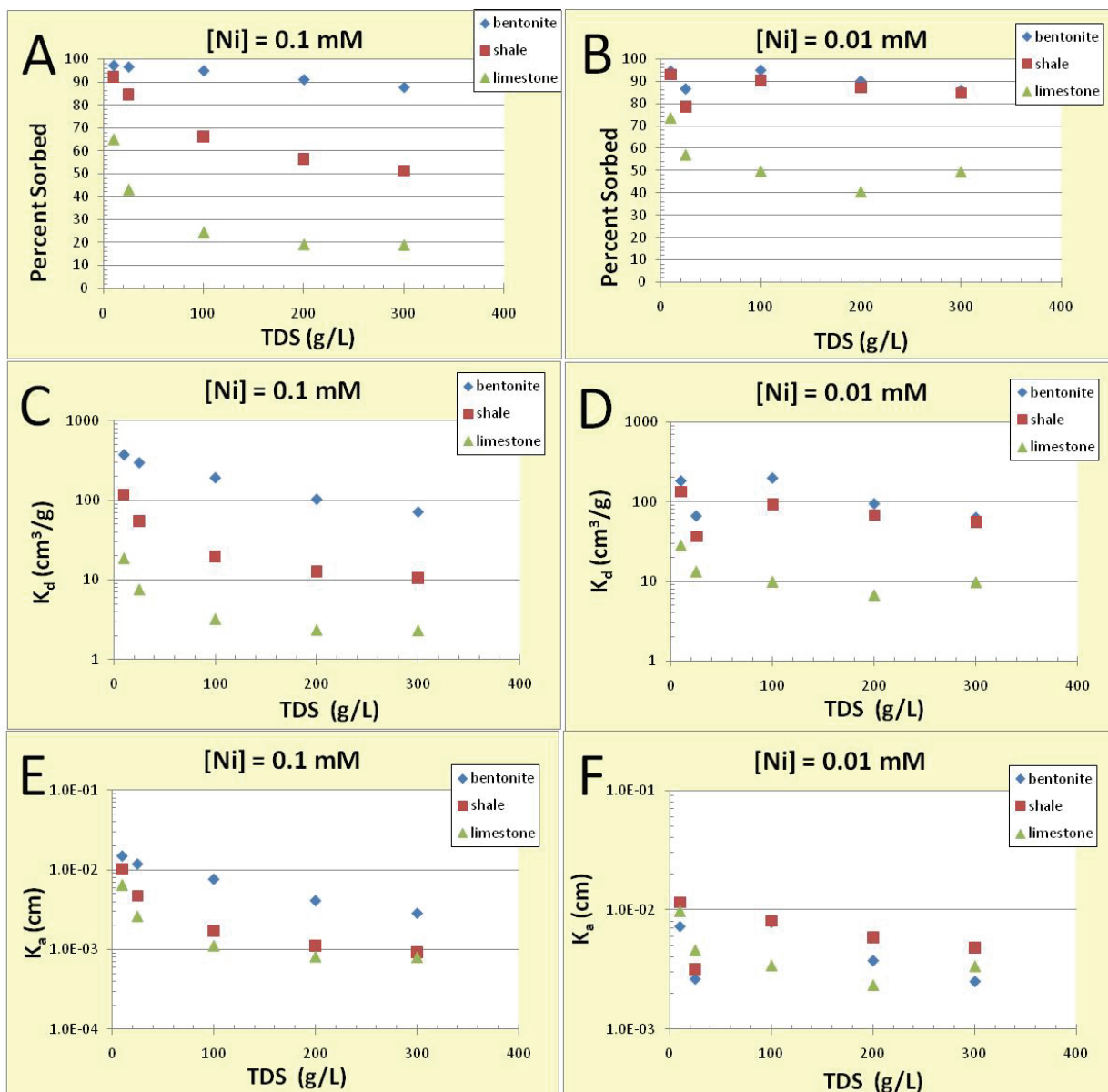


**Figure 9: Nickel Sorption as a Function of TDS Shown for Total Ni Concentrations of  $1 \times 10^{-4}$  and  $1 \times 10^{-5}$  mol/L**

In these tests the percent Ni sorbed was too high for bentonite for both Ni concentrations (86-97%). Not only was the accuracy of the  $K_d$  values compromised, but also with most of the Ni sorbed in all tests the variations with solution composition become masked. The percent sorbed on shale was too high for the lower Ni concentration ( $1 \times 10^{-5}$  mol/L), but reasonable for the higher Ni concentration ( $1 \times 10^{-4}$  mol/L). The percent sorbed on limestone was in a good range for most cases (40-70%).

The experimental results show that Ni sorption decreased with increasing TDS, particularly from 10 to 100 g/L. This could be from the mass action effect of the increasing concentrations of Na



and Ca. However, as shown in Table 11, the pH values in the rock suspensions increased with lower TDS values. Figure 10 shows that Ni sorption on all solids increases with pH in the pH range of 6 to 7.8. This is similar to the trend of increasing Ni sorption with pH reported for sorption on Fe oxide (Stumm, 1992) and on chlorite (Zazzi, 2009). This suggests that the pH effect on surface complexation reactions might be more important than the mass action of salts in determining the magnitude of Ni sorption in brine solutions. This question needs to be addressed with sorption tests that use a single TDS solution under different pH values and that have better pH control for the duration of the test and cover a broader pH range. The results of these tests again confirmed the need to reduce solid/liquid ratios, particularly at lower TDS values. Since sorption on limestone is lower than on shale and bentonite, the solid/liquid ratios for tests with limestone could be higher. When sorption is expressed per surface area (Figure 9E, F), Ni sorption values were still significantly higher for bentonite than the other solids at the higher Ni concentration, but not when the Ni concentration was reduced to  $1 \times 10^{-5}$  mol/L.

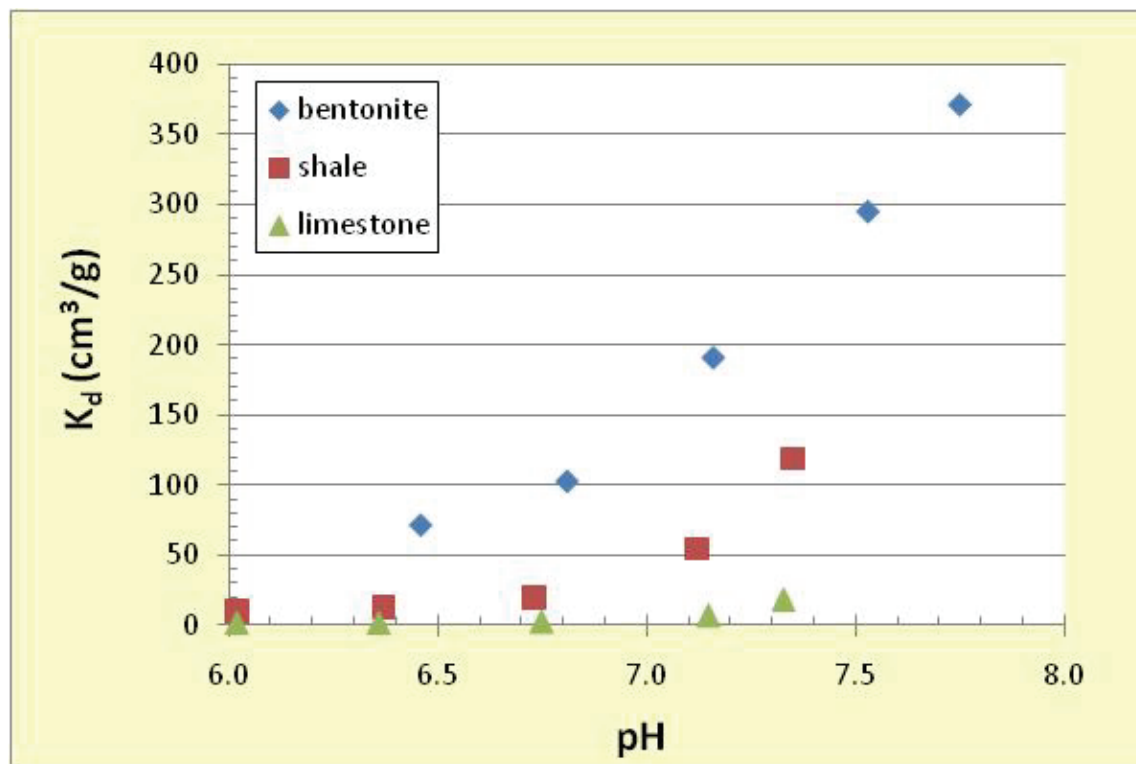


**Figure 10: Nickel Sorption Expressed as a Function of pH**

*Nickel Sorption Kinetics Using a 200 mL Sample Volume:* The purpose of these experiments was to study Ni sorption on bentonite, shale and limestone as a function of time in solutions with TDS values of 10 and 300 g/L. The experimental approach was changed to using a 200 mL solution volume that was sampled at times ranging from 0.04 to 28 days. The total Ni concentration used in these tests was  $1 \times 10^{-4}$  mol/L. Two samples were taken at each interval to estimate experimental uncertainty associated with sampling and analysis. The experimental solid/liquid ratio was reduced for bentonite and shale, and increased for limestone in an attempt to achieve percent sorbed values in the range of 40 to 60 percent. The experimental results are summarized in Table 12 and Figure 11.

**Table 12: Kinetic Study of Ni Sorption in 200 mL Volume with no Sample Preconditioning**

Solid	TDS (g/L)	Solids (g/100 mL)	Time (d)	pH	$K_d$ (cm <sup>3</sup> /g)	$K_a$ (cm)	% sorbed
bentonite	10	0.5	0.042	7.3	58 ± 8	2.3 × 10 <sup>-4</sup>	23 ± 3
			0.125	7.4	82 ± 3	3.3 × 10 <sup>-4</sup>	29 ± 1
			1	7.4	112 ± 4	4.5 × 10 <sup>-4</sup>	36 ± 1
			3	7.4	138 ± 5	5.5 × 10 <sup>-4</sup>	41 ± 1
			7	7.3	169 ± 6	6.8 × 10 <sup>-4</sup>	46 ± 1
			14	7.6	194 ± 19	7.8 × 10 <sup>-4</sup>	49 ± 3
			28	7.6	207 ± 7	8.3 × 10 <sup>-4</sup>	51 ± 1
shale	10	0.5	0.042	7.3	29 ± 2	2.5 × 10 <sup>-4</sup>	13 ± 1
			0.125	7.4	35 ± 5	3.1 × 10 <sup>-4</sup>	15 ± 2
			1	7.3	86 ± 7	7.5 × 10 <sup>-4</sup>	30 ± 2
			3	7.4	153 ± 0	1.3 × 10 <sup>-3</sup>	43 ± 0
			7	7.5	214 ± 0	1.9 × 10 <sup>-3</sup>	52 ± 0
			14	7.6	222 ± 22	1.9 × 10 <sup>-3</sup>	53 ± 3
			28	7.6	262 ± 18	2.3 × 10 <sup>-3</sup>	57 ± 2
limestone	10	7.5	0.042	7.5	3.7 ± 0	1.3 × 10 <sup>-4</sup>	22 ± 0
			0.125	7.6	5.3 ± 0	1.8 × 10 <sup>-4</sup>	28 ± 0
			1	7.5	8.6 ± 0.3	3.0 × 10 <sup>-4</sup>	39 ± 1
			3	7.5	13 ± 1	4.3 × 10 <sup>-4</sup>	48 ± 2
			7	7.4	15 ± 1	5.1 × 10 <sup>-4</sup>	53 ± 1
			14	7.5	19 ± 1	6.5 × 10 <sup>-4</sup>	58 ± 2
			28	7.5	25 ± 3	8.5 × 10 <sup>-4</sup>	65 ± 3
bentonite	300	0.5	0.042	6.3	13 ± 17	5.2 × 10 <sup>-5</sup>	6 ± 8
			0.125	6.3	43 ± 3	1.7 × 10 <sup>-4</sup>	18 ± 1
			1	6.4	44 ± 8	1.7 × 10 <sup>-4</sup>	18 ± 3
			3	6.4	43 ± 3	1.7 × 10 <sup>-4</sup>	18 ± 1
			7	6.4	53 ± 18	2.1 × 10 <sup>-4</sup>	21 ± 6
			14	6.4	66 ± 20	2.6 × 10 <sup>-4</sup>	24 ± 6
			28	6.4	82 ± 4	3.3 × 10 <sup>-4</sup>	29 ± 1
shale	300	0.5	0.042	6.3	21 ± 0	1.8 × 10 <sup>-4</sup>	9 ± 0
			0.125	6.3	21 ± 5	1.8 × 10 <sup>-4</sup>	9 ± 2
			1	6.3	44 ± 8	3.8 × 10 <sup>-4</sup>	18 ± 3
			3	6.3	23 ± 7	2.0 × 10 <sup>-4</sup>	10 ± 3
			7	6.3	16 ± 0	7.0 × 10 <sup>-5</sup>	7 ± 0
			14	6.2	60 ± 19	5.2 × 10 <sup>-4</sup>	23 ± 6
			28	6.2	33 ± 2.6	2.8 × 10 <sup>-4</sup>	14 ± 1
limestone	300	7.5	0.042	6.2	2.2 ± 0.5	7.6 × 10 <sup>-5</sup>	14 ± 3
			0.125	6.3	1.8 ± 0.2	6.4 × 10 <sup>-5</sup>	12 ± 1
			1	6.3	2.5 ± 0.2	8.7 × 10 <sup>-5</sup>	16 ± 1
			3	6.3	1.6 ± 1.1	5.6 × 10 <sup>-5</sup>	10 ± 7
			7	6.2	2.7	4.7 × 10 <sup>-5</sup>	17
			14	6.2	2.7	4.7 × 10 <sup>-5</sup>	17
			28	6.2	2.0 ± 0.3	7.0 × 10 <sup>-5</sup>	13 ± 2

- Sample volume = 200 mL; [Ni]=1×10<sup>-4</sup> mol/L

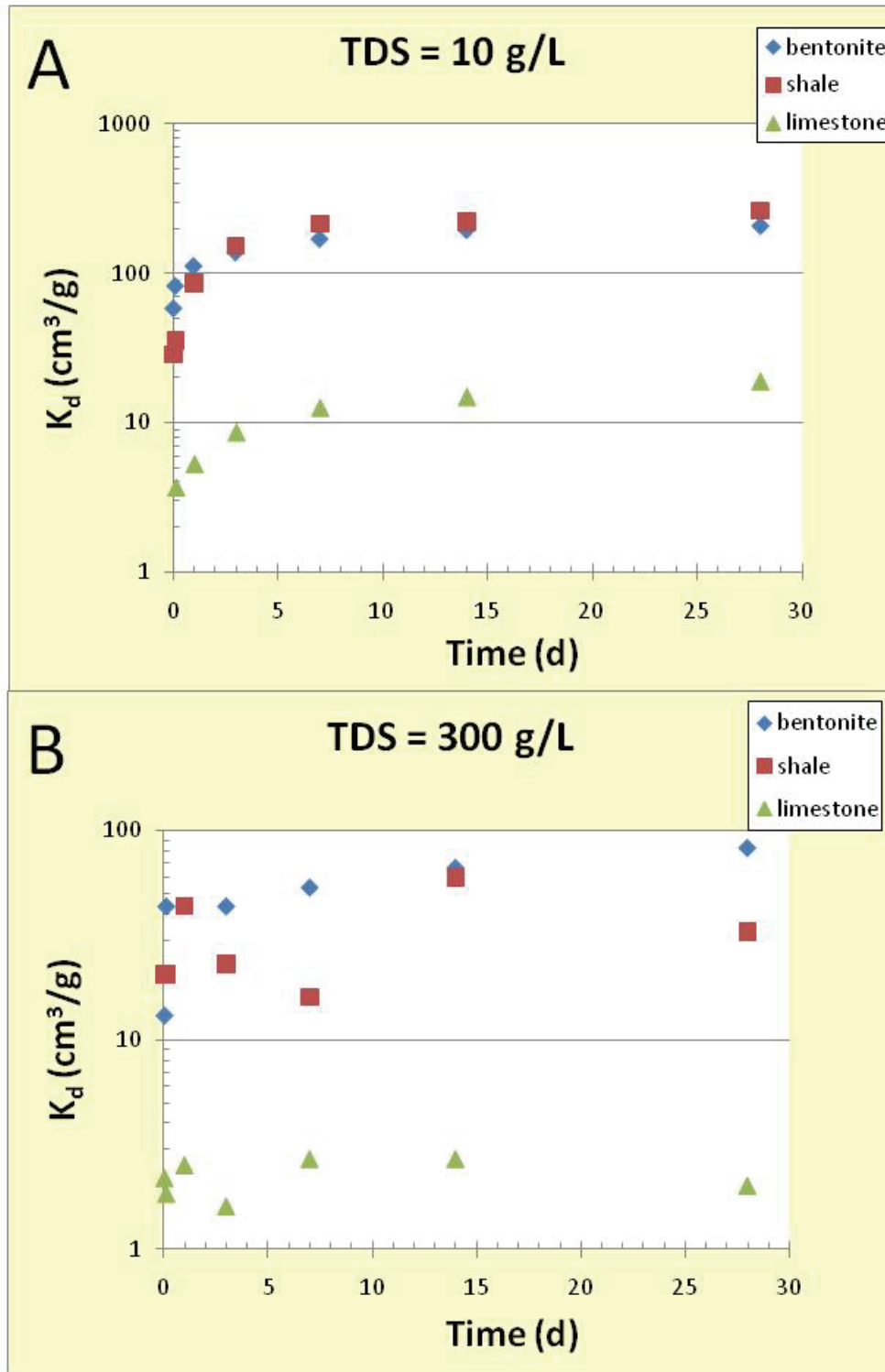


Figure 11: Average Nickel Sorption Coefficients as a Function of Time for 200 mL Volume Tests

The percent sorbed values for the 10 g/L solution ranged from 23 to 51% for bentonite, 13 to 57% for shale and 22 to 65% for limestone. This level of sorption produced a clear increase in sorption coefficients as a function of time (Figure 11A). However, the amount of Ni sorption in the 300 g/L solution was significantly less, with percent sorbed values of 6 to 29% for bentonite, 7 to 23% for shale and 10 to 14% for limestone. This low amount of sorption, combined with difficulties with the ICP analysis of 300 g/L solutions lead to high variability in derived sorption values and a less clear trend in sorption variation with time (Figure 11B). Sorption in the 10 g/L solution follows a typical pattern with respect to time in that there is a rapid sorption step lasting less than one hour, followed by a slower sorption process lasting several days. It may be of interest to quantify how close a given  $K_d$  value is to the maximum observed  $K_d$  value. This maximum  $K_d$  value might represent equilibrium, a steady state, or just the maximum value observed during the experimental period. The parameter used for this quantification is referred to as “percent complete,” and is the ratio of the given  $K_d$  value (for example the value at 7 days) and the maximum  $K_d$  value, expressed as a percent. By 7 days, the sorption appears to be about 82% complete for bentonite and shale, and 60% complete for limestone. Sorption continues to increase at a slow rate beyond 7 days, up to and probably exceeding 28 days. The effect of time is much less clear in the tests performed in the 300 g/L solution. Sorption on bentonite was about 64% complete after 7 days, followed by gradual increasing sorption up to 28 days. Maximum sorption values for limestone and shale were observed at 7 and 14 days, respectively. Due to the variability in measured sorption values, further increases in sorption on shale and limestone could not be identified.

*Nickel Sorption Kinetics Using Conditioned Solids:* The final set of tests measured Ni sorption on bentonite, shale and limestone using 4 different solution compositions. In these tests, the solid materials were conditioned with Ni-free brine solutions for 1 week before the start of sorption tests in order to minimize pH fluctuations and to evaluate the effect of sorption sites created by the rock grinding process. Freshly crushed rock samples are likely to contain a higher concentration of surface sites created by the crushing process. In theory, these new sites will react with the experimental solution and change with time. It was assumed that a 1 week contact would be sufficient to condition these sites and make the rock samples more representative of natural conditions. The solid/liquid ratios for bentonite and shale were increased in an attempt to optimize the percent sorbed for deriving better sorption coefficients. After the conditioning period one half of the Ni-free solution was removed and replaced with an equal amount of solution containing Ni. This initiated the sorption test. The sampling times were 0.125, 1, 3, 7, 14 and 28 days. Three samples were taken at 7 days in order to estimate the uncertainty due to sampling and analysis. The average and standard deviation of these replicates are reported in Table 13. In these tests, Ni analysis was performed with the spectroscopic method in order to improve results from the high TDS solutions. The experimental solutions included Na-Ca-Cl brines with TDS values of 10, 100 and 300 g/L, and a Na-Cl brine with a TDS of 100 g/L. The idea was to compare the results from the 100 g/L Na-Ca-Cl brine with those from the 100 g/L Na-Cl brine to evaluate the effect of  $\text{Ca}^{2+}$  on  $\text{Ni}^{2+}$  sorption. As discussed in Section 3.1, since the pH of brines in contact with rocks appears to be controlled by equilibrium with calcite, it was decided to add carbonate to the experimental solutions to minimize calcite dissolution and changes in the composition of the experimental solution. The amount of carbonate added to each solution was determined by the amount of Ca in solution and the equilibrium calculation by PHREEQC with respect to calcite in the brine solution. The concentration of  $\text{CO}_3$  in the 100 g/L Na-Cl solution was set at  $8 \times 10^{-3}$  mol/L, and the respective  $\text{CO}_3$  concentrations in the Na-Ca-Cl brines with TDS values of 10, 100 and 300 were set at  $4 \times 10^{-4}$ ,  $2 \times 10^{-4}$  and  $5 \times 10^{-5}$  mol/L to match predicted equilibrium  $\text{CO}_3$  values given in Table 6. The total Ni concentration used in these tests was  $1 \times 10^{-4}$  mol/L.

The results of these sorption tests are summarized in Table 13 and Figure 12. The tests with the 10 g/L solutions produced optimum amounts of sorption from an analytical perspective, with percent Ni sorbed values of 25 to 56% for bentonite, 29 to 82% for shale and 13 to 47% for limestone. The percent sorbed Ni values were a bit low in the 100 g/L solution, with percent sorbed values in the bentonite between 10 and 22%, shale between 10 and 36%, and limestone sorbing only 5 to 10% of the Ni. The fraction of Ni sorbed on bentonite and shale in the 300 g/L TDS solution was similar to that in the 100 g/L solution. As in 100 g/L TDS Na-Ca-Cl brine, the fraction of Ni sorbed on limestone (1 to 11%) in 300 g/L brine was very low, leading to a high level of uncertainty in the derived sorption coefficients. The tests with the NaCl solution displayed optimum percent sorbed values from an analytical perspective, which were 8 to 45% for bentonite, 22 to 69% for shale, and 18 to 44% for limestone.

The effect of sample conditioning before sorption tests can be evaluated by comparing the results of tests performed in 10 and 300 g/L TDS Na-Ca-Cl brines with unconditioned solids (Table 12) with those from this series using conditioned solids (Table 13). Table 14 compares the 7 day results from the tests with and without conditioning. Sorption was lower with preconditioned solids by a factor 2 to 7. Therefore, sample conditioning before the start of sorption tests is important to minimize artefacts associated with rock crushing.

**Table 13: Kinetic Study of Ni Sorption in 200 mL Volume with Conditioned Solids**

Solid	TDS (g/L)	Solids (g/100 mL)	Time (d)	pH	$K_d$ (cm <sup>3</sup> /g)	$K_a$ (cm)	% sorbed
bentonite	10	1	0.125	7.5	33	$1.3 \times 10^{-4}$	25
			1	7.5	45	$1.8 \times 10^{-4}$	31
			3	7.4	64	$2.6 \times 10^{-4}$	39
			7	7.4	$82 \pm 6$	$3.3 \times 10^{-4}$	$45 \pm 2$
			14	7.5	105	$4.2 \times 10^{-4}$	51
			28	7.4	128	$5.1 \times 10^{-4}$	56
shale	10	4	0.125	7.4	10	$8.7 \times 10^{-5}$	29
			1	7.4	17	$1.5 \times 10^{-4}$	44
			3	7.4	31	$2.7 \times 10^{-4}$	55
			7	7.4	$47 \pm 4$	$4.1 \times 10^{-4}$	$65 \pm 2$
			14	7.4	73	$6.3 \times 10^{-4}$	75
			28	7.4	111	$9.6 \times 10^{-4}$	82
limestone	10	8	0.125	7.4	1.8	$6.3 \times 10^{-5}$	13
			1	7.3	2.8	$9.5 \times 10^{-5}$	18
			3	7.4	4.3	$1.5 \times 10^{-4}$	25
			7	7.4	$6.1 \pm 0.7$	$2.1 \times 10^{-4}$	$33 \pm 3$
			14	7.4	8.0	$2.8 \times 10^{-4}$	39
			28	7.4	11	$3.8 \times 10^{-4}$	47
bentonite	100	1	0.125	7.3	11	$4.4 \times 10^{-5}$	10
			1	7.2	12	$4.6 \times 10^{-5}$	10
			3	7.1	17	$7.0 \times 10^{-5}$	10
			7	7.1	$22 \pm 2$	$8.7 \times 10^{-5}$	$18 \pm 1$
			14	7.0	26	$1.0 \times 10^{-4}$	21
			28	6.9	28	$1.1 \times 10^{-4}$	22
shale	100	4	0.125	7.0	2.7	$2.4 \times 10^{-5}$	10
			1	6.9	3.6	$3.1 \times 10^{-5}$	13
			3	6.9	6.3	$5.5 \times 10^{-5}$	20
			7	6.9	$8.3 \pm 0.5$	$7.2 \times 10^{-5}$	$25 \pm 1$
			14	6.6	10	$8.9 \times 10^{-5}$	29
			28	6.8	14	$1.2 \times 10^{-4}$	36
limestone	100	8	0.125	6.9	0.7	$2.5 \times 10^{-5}$	5
			1	6.9	0.7	$2.4 \times 10^{-5}$	5
			3	6.8	0.7	$2.4 \times 10^{-5}$	5
			7	6.8	$1.1 \pm 0.3$	$3.9 \times 10^{-5}$	$8 \pm 2$
			14	6.5	0.8	$2.7 \times 10^{-5}$	6
			28	6.7	1.5	$5.3 \times 10^{-5}$	10

- Sample volume = 200 mL
- [Ni]= $1 \times 10^{-4}$  mol/L

**Table 13: Kinetic Study of Ni Sorption in 200 mL Volume with Conditioned Solids (Continued)**

Solid	TDS (g/L)	Solids (g/100 mL)	Time (d)	pH	$K_d$ (cm <sup>3</sup> /g)	$K_a$ (cm)	% sorbed
bentonite	300	1	0.125	6.7	16	$6.4 \times 10^{-5}$	14
			1	6.6	28	$1.1 \times 10^{-4}$	22
			3	6.4	22	$8.9 \times 10^{-5}$	18
			7	6.4	$34 \pm 1$	$1.4 \times 10^{-4}$	$26 \pm 0$
			14	6.3	34	$1.4 \times 10^{-4}$	25
			28	6.4	40	$1.6 \times 10^{-4}$	29
shale	300	4	0.125	6.3	4.0	$3.5 \times 10^{-5}$	14
			1	6.3	4.6	$4.0 \times 10^{-5}$	15
			3	6.1	4.0	$3.4 \times 10^{-5}$	14
			7	6.2	$6.0 \pm 0.3$	$5.2 \times 10^{-5}$	$19 \pm 1$
			14	6.1	7.1	$6.2 \times 10^{-5}$	22
			28	6.1	9.0	$7.9 \times 10^{-5}$	27
limestone	300	8	0.125	6.2	1.2	$4.2 \times 10^{-5}$	9
			1	6.1	1.5	$5.2 \times 10^{-5}$	11
			3	5.9	0.2	$7.5 \times 10^{-6}$	2
			7	6.0	$0.4 \pm 0.2$	$1.5 \times 10^{-5}$	$3 \pm 2$
			14	6.0	0.2	$5.5 \times 10^{-6}$	1
			28	5.9	0.5	$1.6 \times 10^{-5}$	3
bentonite	NaCl 100	1	0.125	7.3	8.5	$3.4 \times 10^{-5}$	8
			1	7.2	21	$8.4 \times 10^{-5}$	17
			3	7.6	33	$1.3 \times 10^{-4}$	25
			7	7.0	$50 \pm 4$	$2.0 \times 10^{-4}$	$33 \pm 2$
			14	6.7	83	$3.3 \times 10^{-4}$	45
			28	6.7	76	$3.0 \times 10^{-4}$	43
shale	NaCl 100	4	0.125	7.3	7.0	$6.0 \times 10^{-5}$	22
			1	7.1	11	$9.7 \times 10^{-5}$	31
			3	7.5	18	$1.6 \times 10^{-4}$	42
			7	7.1	$31 \pm 2$	$2.7 \times 10^{-4}$	$55 \pm 2$
			14	7.1	47	$4.0 \times 10^{-4}$	65
			28	7.0	55	$4.8 \times 10^{-4}$	69
limestone	NaCl 100	8	0.125	7.2	2.8	$9.7 \times 10^{-5}$	18
			1	7.1	4.2	$1.5 \times 10^{-4}$	25
			3	no data	no data	no data	no data
			7	7.1	$8.0 \pm 1.0$	$2.6 \times 10^{-4}$	$38 \pm 3$
			14	7.1	8.6	$3.0 \times 10^{-4}$	41
			28	7.0	9.8	$3.4 \times 10^{-4}$	44

- Sample volume = 200 mL
- [Ni]= $1 \times 10^{-4}$  mol/L
- No data, because samples were lost

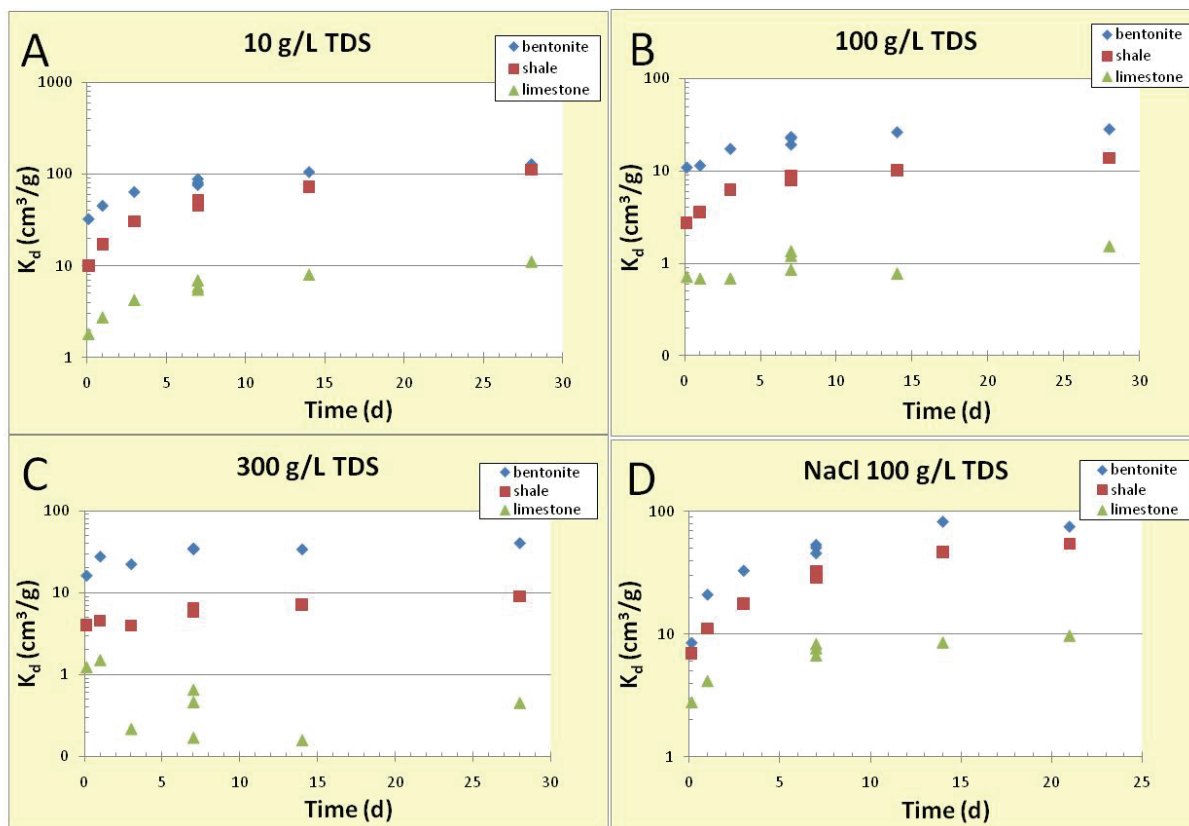


**Figure 12: Nickel Sorption as a Function of Time and Solution Composition Using Conditioned Solid Phases.**

**Table 14: Effect of Sample Preconditioning on Nickel Sorption**

Mineral	Solution (g/LTDS)	$K_d$ (cm <sup>3</sup> /g) Without Conditioning	$K_d$ (cm <sup>3</sup> /g) With Conditioning	Factor Lower With Conditioning
bentonite	10	169 ± 6	82 ± 6	2
bentonite	300	53 ± 18	34 ± 1	1.6
Shale	10	214 ± 0	47 ± 4	2.5
Shale	300	16 ± 0	6.0 ± 0.3	7
limestone	10	15 ± 1	6.1 ± 0.7	4.5
limestone	300	2.7 ± 0	0.4 ± 0.2	2.7

The shapes of the sorption curves tested with conditioned solids (Figure 12) are similar to the ones tested with non-conditioned solids (Figure 11). The 7 day sorption reaction in the 10 g/L solution was 80% complete for bentonite, 79% complete for shale and 70% complete for limestone in terms of the percent of sorbed within 28 days of experimental time period. At 7 days in the 100 g/L solution, sorption was 81% complete for bentonite, 69% complete for shale and 80% complete for limestone. In the 300 g/L solution, the increases in sorption for bentonite



and shale appear slower after the initial 3 h sorption. At 7 days sorption on bentonite appears to be 90% complete, while that on shale is 70% complete. Although sorption on limestone appears to be 80% complete at 7 days, it is difficult to draw conclusions regarding sorption kinetics given the variability in sorption values as a function of time and the high level of uncertainty due to the low percent sorbed Ni concentration. Sorption in the NaCl solution at 7 days was 73% complete for bentonite, 80% complete for shale and 86% complete for limestone. As observed in previous tests, a slow sorption process on bentonite, shale and limestone under these experimental conditions may continue beyond 28 days.

The effect of solution composition on Ni sorption is illustrated in Figure 13, where average values for sorption coefficients determined at reaction times of 7 days are plotted versus TDS, pH, and total CO<sub>3</sub> concentration. In Figure 13A and Figure 13B the data points from the Na-Cl brine are marked with NaCl. As before, Ni sorption decreased with TDS, but as previously noted, this was likely a pH effect as higher TDS solution has lower pH values (Table 6). Sorption values from the 100 g/L Na-Cl brine were higher than from the Na-Ca-Cl brine by a factor 2 to 7, suggesting that Ca competes with Ni for sorption sites. The difference in Ni sorption between the Na-Cl and Na-Ca-Cl brines does not appear to be a pH effect. The carbonate concentration did not have a significant effect on Ni sorption, which is not surprising given that the dominant Ni species were Ni<sup>+2</sup> and NiCl<sup>+</sup>.

*Desorption Test:* The reversibility of Ni sorption was tested by diluting the dissolved Ni concentration and observing the response of sorption coefficient values. If the sorption process is completely reversible, over a relatively short time period enough Ni will be desorbed to return the system to equilibrium and the observed sorption coefficients will be very similar to values before the desorption test. If the process is not reversible within the experimental time span, the observed sorption coefficient values will be higher because insufficient Ni would have desorbed to return the system to equilibrium.

The desorption test was performed using the experiment with 100 g/L Na-Ca-Cl brine after the sorption experiment was completed. Before the start of the desorption test the experimental volume was 120 mL. While the solids remained at the bottom of the reaction vessel, 95 mL of clear solution were removed and replaced with 95 mL of Ni-free 100 g/L Na-Ca-Cl brine. The dilution factor for Ni was 25/120. The reaction vessel was sampled as before after time intervals of 0.13, 1, 3, 7 and 14 days. The results of the desorption test are summarized in Table 15 as  $K_d$  values and as the ratio of the values with respect to the sorption value before desorption ( $K_d^0$ ). The ratio ( $K_d/K_d^0$ ), plotted in Figure 14, should approach a value of 1 when the system comes close to equilibrium. Nickel sorption on bentonite was the closest to achieving equilibrium after desorption with a  $K_d/K_d^0$  ratio of 4.7 observed after 14 days. The  $K_d$  values were all significantly higher than before the desorption test. Sorption on limestone and shale was significantly less reversible with  $K_d/K_d^0$  values that were about an order of magnitude higher than that on bentonite. Based on the trends in Figure 14, it may take months to years for Ni to desorb from shale and limestone. These results suggest that bentonite has a high concentration of sites where Ni is held in a configuration that is exchangeable, whereas limestone and shale have sites that strongly retain Ni and resist desorption in response to a drop in dissolved Ni concentration.

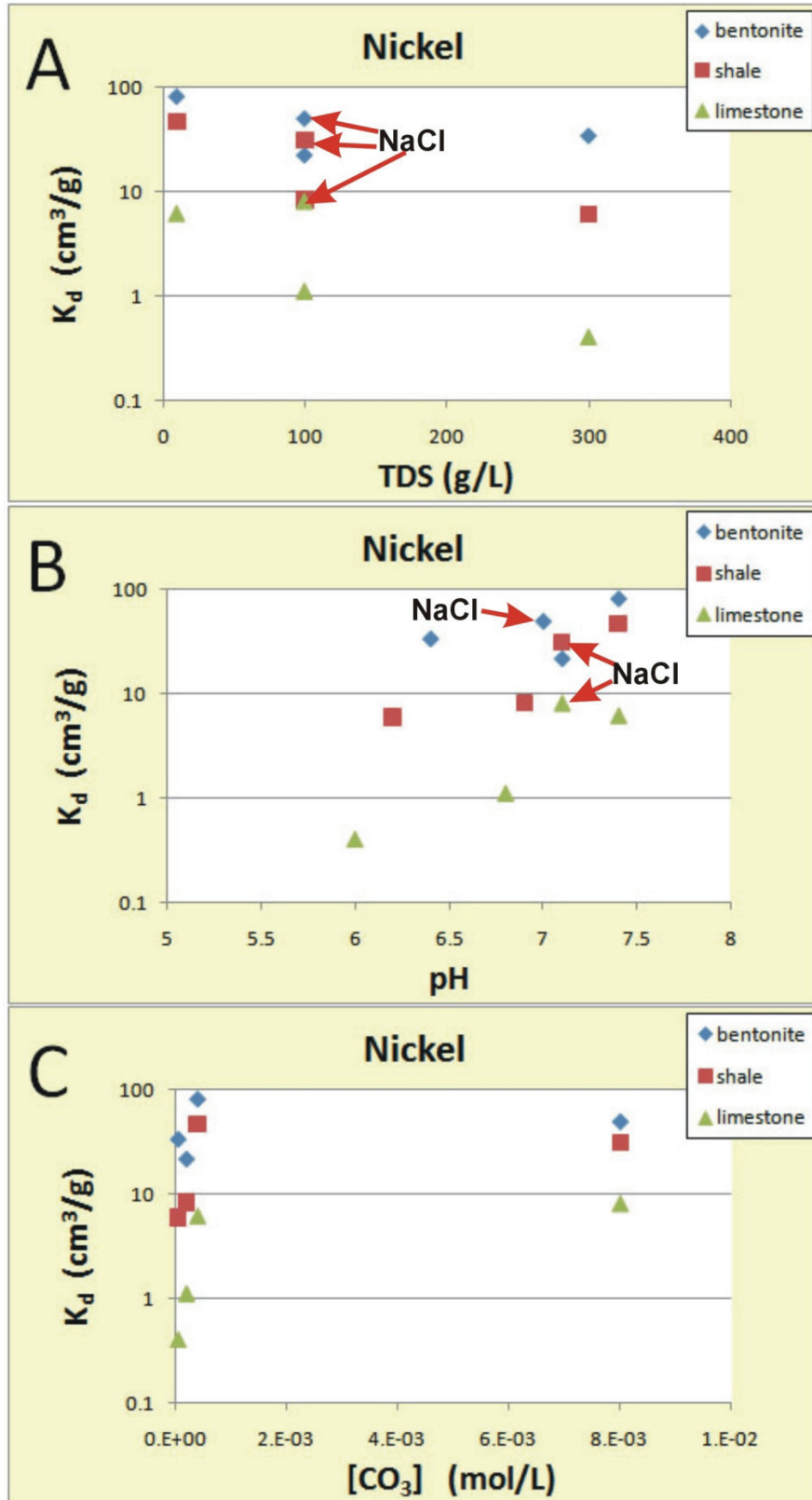
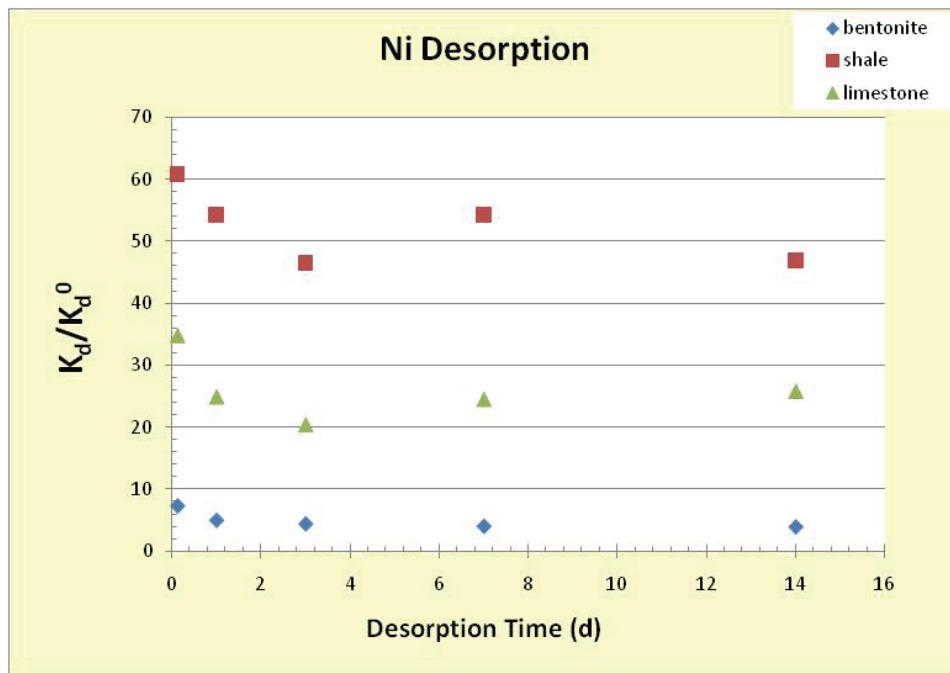


Figure 13: Ni Sorption Coefficients as a Function of (A) TDS, (B) pH, and (C) [CO<sub>3</sub>]

**Table 15: Nickel Desorption Experiment in 100 g/L TDS Na-Ca-Cl Brine**

Rock	Time (d)	$K_d$ (cm <sup>3</sup> /g)	$K_d/K_d^0$
Bentonite	Before desorption ( $K_d^0$ )	99	
	0.13	843	8.5
	1	585	5.9
	3	521	5.3
	7	478	4.8
	14	468	4.7
Shale	Before desorption ( $K_d^0$ )	31	
	0.13	2170	70
	1	1940	62
	3	1660	53
	7	1940	62
	14	1680	54
Limestone	Before desorption ( $K_d^0$ )	13	
	0.13	538	41
	1	389	29
	3	321	24
	7	383	29
	14	402	30

- Desorption at pH=6.9



**Figure 14: Nickel Desorption Test**

*Summary:* Comparing nickel sorption on bentonite, shale and limestone in Na-Ca-Cl brine to that of Na-Cl brine at the same TDS (100 g/L), it is demonstrated that nickel sorption is affected by brine composition. The presence of Ca in Na-Ca-Cl brine reduced Ni sorption by a factor 2 to 7. In Na-Ca-Cl solutions the pH probably has a more important effect than the TDS, as indicated by the literature (Bradbury and Baeyans, 2005; Gu et al., 2010) and by observed variations with pH in this study. This should be verified with short time span tests on conditioned solids covering a pH interval from 5.5 to 8, using the same brine composition. Nickel sorption increases with time and by 7 days it achieves a level that is 70 to 90 percent of the sorption observed by 28 days. Sorption probably continues at a very slow rate beyond 28 days. The nature of the mechanism(s) responsible for the slow sorption has not been identified. Nickel sorption on bentonite is close to being reversible, but sorption on shale and limestone does not appear to be reversible in the experimental time frame.

In the interests of selecting Ni sorption data that would be the most relevant for performance assessment, the data from the experiments with conditioned solids are considered the most useful, since artefacts from rock crushing have been reduced. Sorption data from these tests are summarized in Table 16 in the form of average  $K_d$  values determined with reaction times of 7 days. The 7 day reaction time is conservative since longer times would produce higher values. These average values include variability associated with changes in TDS, Ca/Na ratio, and pH. These average values cover a pH range from 6.0 to 7.4, and ionic strengths of 0.2 to 7.5 (mol/kg). The geometric mean is included, along with the geometric standard deviation in parentheses.

**Table 16: Average Ni Sorption  $K_d$  Values ( $\text{cm}^3/\text{g}$ ) for Brine Solutions**

<b>Mineral</b>	<b>Average</b>	<b>Geometric Mean</b>
Bentonite	47 ± 26	42 (1.8)
Shale	23 ± 20	16 (2.7)
Limestone	3.9 ± 3.7	2.2 (4.2)

Note: The standard deviation is given as the error for the average, and the geometric standard deviation is in parentheses beside the geometric mean.

### 4.2.3 Copper

Copper is a transition element which will be present as a divalent cation under oxidizing conditions. The dominant copper species in the brine solutions used in this study is predicted to be  $\text{Cu}^{+2}$ . Solubility is limited by malachite ( $\text{Cu}_2(\text{CO}_3)(\text{OH})_2$ ). Therefore, Cu chemistry will be affected by pH and total carbonate concentration. Furthermore, Cu is likely to sorb to exposed oxygen sites on silicate minerals, and carbonate sites in calcite or dolomite. Although Cu could be expected to sorb by a combination of surface complexation and cation exchange, the latter is probably suppressed in brine solutions due to the mass action of salts. The sorption properties of  $\text{Cu}^{+2}$  are likely to be similar to those of  $\text{Ni}^{+2}$ .

*Initial Sorption Tests with Cu:* The initial Cu sorption tests were performed in the 300 g/L brine solution using 10 mL sample volumes, a solid/liquid ratio of 10 g/100 mL (i.e. 1 g/10 mL), and total Cu concentrations ranging from  $6 \times 10^{-5}$  to  $8 \times 10^{-4}$  mol/L. The purpose of these tests was to identify an ideal range of Cu concentrations to use for measuring sorption on bentonite, shale and limestone. Initial tests with Cu concentrations of  $1 \times 10^{-3}$  mol/L demonstrated that the Cu solubility was exceeded and a green mineral, likely malachite, precipitated. Therefore, a concentration of  $1 \times 10^{-4}$  mol/L was deemed to be the highest Cu concentration that can be used in sorption tests.

Results for a 10 day reaction time are presented in Table 17. The table includes the total Cu concentration that was available for sorption onto the solid (determined from blanks), pH values which correspond to measurements at the end of the experiment, sorption coefficients ( $K_d$ ) and the percent of total Cu that was sorbed. The percent sorbed values were all high, ranging from 81 to 99 percent. Since the percent sorbed approached 100 percent, there is uncertainty as to what is the actual Cu concentration in solution that was in equilibrium with the solid. This suggests that the sorption values in Table 17 could be overestimates, particularly if the sorption reaction is slow to reach equilibrium. Figure 15 illustrates the variation of Cu sorption coefficients with the total amount of Cu in the system. The increase in sorption coefficients with higher Cu concentrations suggests that Cu is being precipitated. Even though the Cu concentration is predicted to be below the malachite solubility limit, the presence of mineral surfaces could induce precipitation. Ion concentrations close to mineral surfaces are often higher than in the bulk solution due to the accumulation of cations and anions close to charged surfaces. The resulting increase in the local concentration of Cu and carbonate might induce precipitation. Since Cu is associated with carbonate minerals, it is likely that it will become strongly attached to the surfaces of carbonate minerals found in the limestone, shale and bentonite. If the total mass of Cu precipitated on a mineral surface is small it is likely that it cannot be experimentally distinguished from sorption. Given that surface induced precipitation is a possibility, the sorption coefficients from the lowest copper concentrations are likely to be the most reliable in terms of being unaffected by surface precipitation.

**Table 17: Copper Sorption Results with the 300 g/L TDS Na-Ca-Cl Brine**

Solid	Total [Cu] (mol/L)	pH	$K_d$ (cm <sup>3</sup> /g)	% sorbed
bentonite	$2.50 \times 10^{-4}$	6.03	1577	99
bentonite	$1.00 \times 10^{-4}$	6.33	696	99
bentonite	$6.14 \times 10^{-5}$	6.14	379	97
shale	$5.00 \times 10^{-4}$	5.78	846	99
shale	$3.05 \times 10^{-4}$	5.83	363	97
shale	$6.14 \times 10^{-5}$	5.92	41	81
limestone	$7.87 \times 10^{-4}$	5.81	1842	99
limestone	$3.05 \times 10^{-4}$	5.74	635	98
limestone	$6.14 \times 10^{-5}$	6.01	46	82

- Reaction time = 10 days
- Solid/liquid ratio = 10 g/100 mL
- Experimental volume = 10 mL

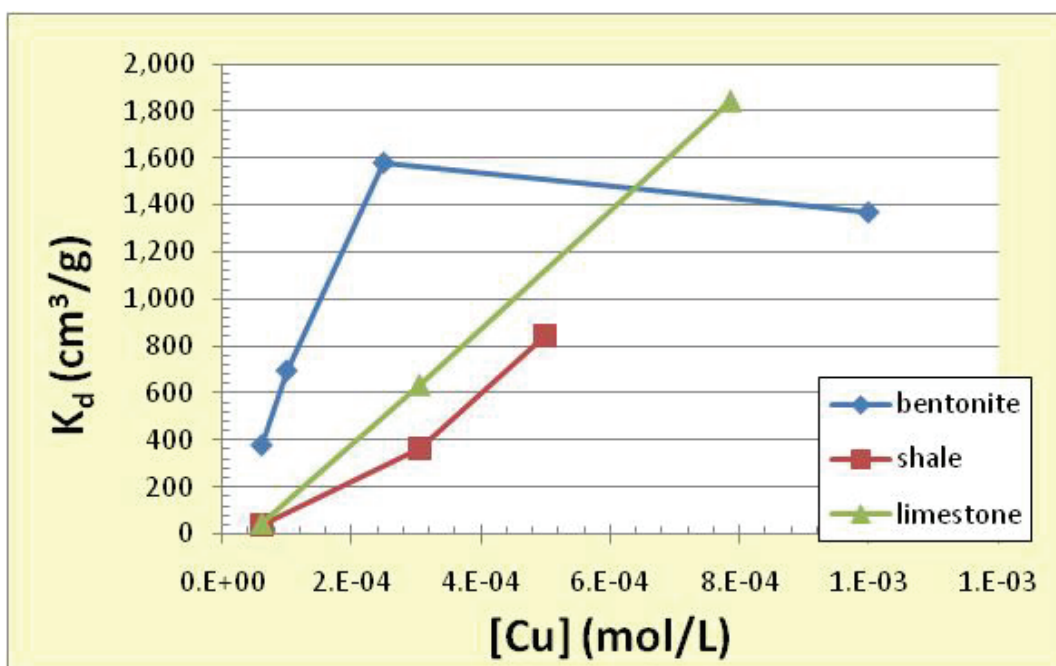


**Figure 15: Copper Sorption Coefficient Versus Total Copper in the 300 g/L Brine System**

*Sorption as a Function of Brine Composition:* An experiment was performed to evaluate Cu sorption on bentonite, shale and limestone as a function of brine concentrations using TDS values of 10, 25, 100, 200 and 300 g/L. The tests used nominal Cu concentration of  $1 \times 10^{-5}$  mol/L, and solid to liquid ratios of 1 g in 10 mL (i.e. 10 g/100 mL). The reaction volume was 10 mL, and the sorption time was 7 days. The experimental results are presented in Table 18 and Figure 16. The  $K_a$  values were calculated using BET surface areas of solids (Table 5).

With the exception of measurements in the 10 g/L solution, the values of percent sorbed Cu were in a good range. Results from Figure 16 show that when the TDS is 100 g/L and lower, the Cu sorption on shale and limestone is as high as on bentonite even though bentonite has a much higher surface area (Table 5). Sorption on limestone appears particularly high when sorption is expressed as a function of surface area. This suggests that Cu has a strong affinity for carbonate surfaces. As with Ni, Cu sorption appears to decrease with TDS. However, when Cu  $K_d$  values are plotted versus pH (Figure 17), a strong increase in sorption with pH is noted in the pH interval from 6 to 8. The sorption values determined for the 25 g/L solution are a bit low when compared to the sorption trends of other TDS and pH solutions. The reason for this is not known at the present time. Although the sorption edge for Cu on Fe oxide is in the pH range of 4.5 to 6 (Stumm, 1992), the variation of  $K_d$  values in Figure 17 suggests that the sorption edge on sedimentary rocks may be from pH 6 to 8, and that pH determines the variation in Cu sorption values in brine solutions. Nonspecific coulombic sorption of Cu may have already been eliminated in the presence of 10 g/L TDS. The effect of pH on Cu sorption needs to be addressed by measuring sorption in a given brine solution over a pH range of 5.5 to 8, using short term tests in which the pH can be maintained at target values.

**Table 18: Copper Sorption as a Function of TDS**

Solid	Total [Cu] (mol/L)	TDS (g/L)	pH	$K_d$ (cm <sup>3</sup> /g)	$K_a$ (cm)	% sorbed
bentonite	$1 \times 10^{-5}$	300	6.83	6.5	$2.6 \times 10^{-5}$	40
		200	7.13	10	$4.1 \times 10^{-5}$	51
		100	7.43	21	$8.3 \times 10^{-5}$	68
		25	7.76	14	$5.6 \times 10^{-5}$	58
		10	7.96	256	$1.0 \times 10^{-3}$	96
shale	$1 \times 10^{-5}$	300	6.35	0	0	0
		200	6.64	3.3	$2.8 \times 10^{-5}$	25
		100	6.99	33	$2.9 \times 10^{-4}$	77
		25	7.31	8.3	$7.2 \times 10^{-5}$	45
		10	7.53	489	$4.3 \times 10^{-3}$	98
limestone	$1 \times 10^{-5}$	300	6.21	0.2	$7.8 \times 10^{-6}$	2
		200	6.55	9.2	$3.2 \times 10^{-4}$	48
		100	6.91	64	$2.2 \times 10^{-3}$	86
		25	7.28	7.5	$2.6 \times 10^{-4}$	43
		10	7.47	123	$4.3 \times 10^{-3}$	93

- Reaction time = 7 days
- Solid/liquid ratio = 10 g/100 mL
- Experimental volume = 10 mL

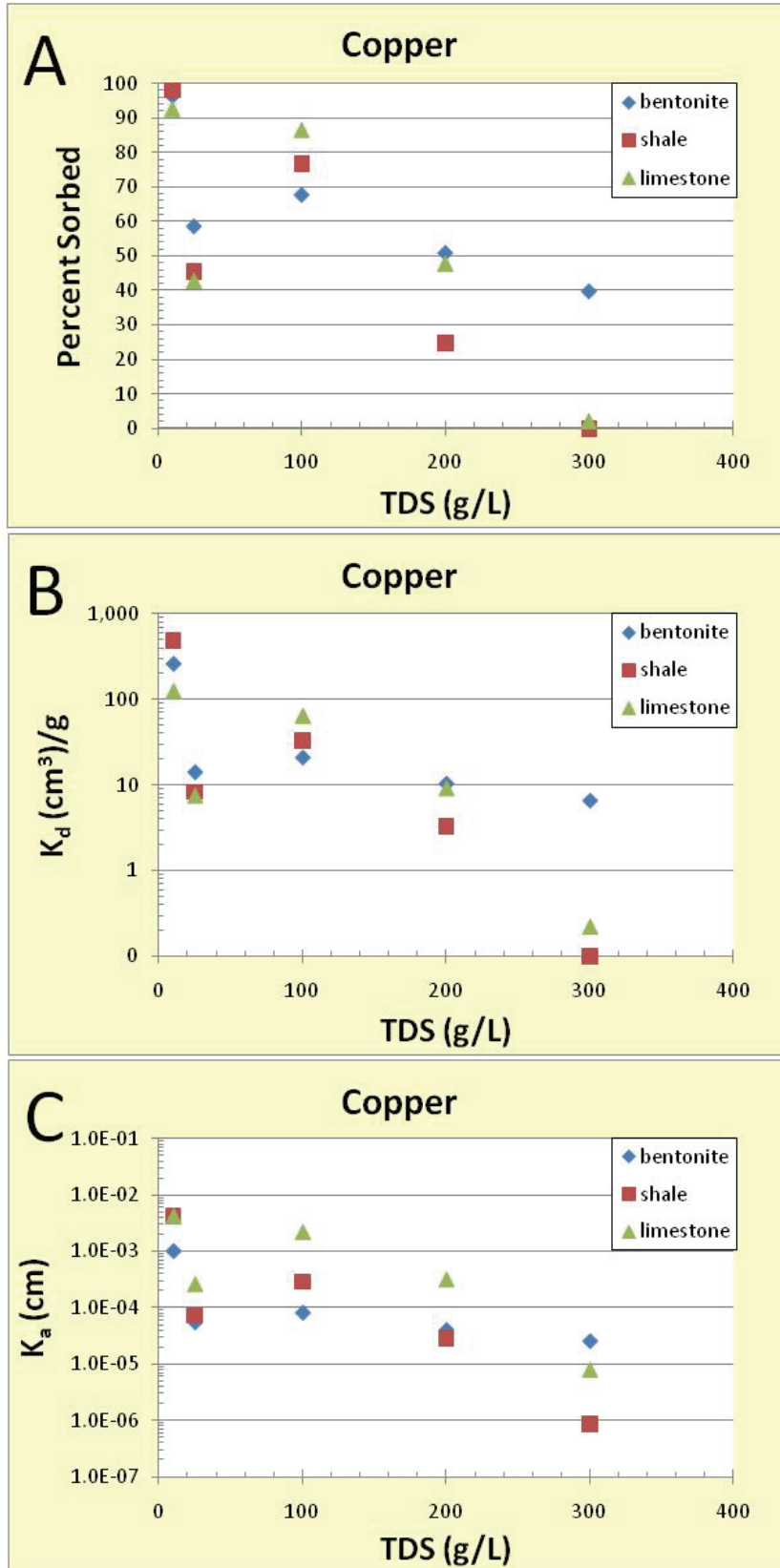
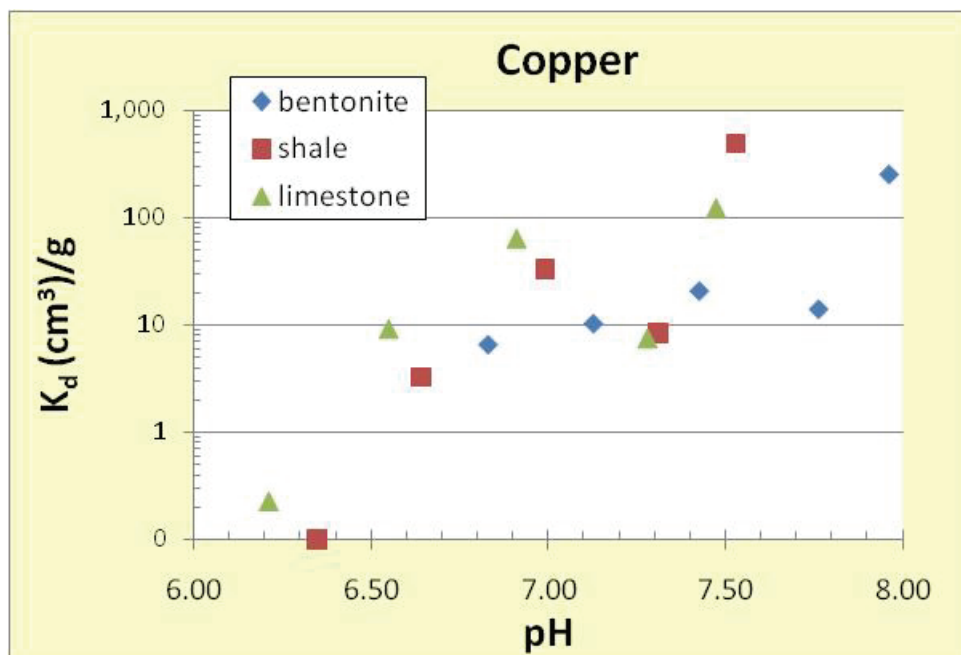


Figure 16: Copper Sorption as a Function of TDS





**Figure 17: Copper Sorption Variation with pH**

*Summary:* Copper sorption on bentonite, shale and limestone is affected by the salinity of the brine. The pH probably has a stronger effect than the TDS, as indicated by the observed variations with pH in this study and by the argument that the mass action of salt had already suppressed non-specific coulombic attraction in the solution with the lowest TDS. This should be verified with short time tests covering a pH interval from 5.5 to 8, using the same brine composition.

In the interests of selecting Cu sorption data for performance assessment, the data from the experiments with the lowest Cu concentrations were considered to be the most useful to avoid artefacts from potential surface precipitation. The sorption data from these tests are summarized in Table 19 in the form of average  $K_d$  values determined with reaction times of 7 days. These average values include variability associated with changes in TDS and pH. These average values cover a pH range from 6.2 to 8.0, and ionic strengths of 0.2 to 7.5 (mol/kg). The average Cu  $K_d$  values for sorption on bentonite and shale were not significantly different from those of Ni sorption, although the geometric mean values of Ni sorption were slightly higher. While the sorption of Ni was about a factor 10 lower on limestone compared to the other solids, Cu sorption values on limestone were not that much lower compared to Cu sorption values on the other solids. As Cu chemistry will be affected by carbonate concentration in solution, the effect of carbonate concentration on Cu sorption should be investigated in the future. One must also consider that the Cu sorption values in Table 19 were from tests with unconditioned solids. Ni sorption values on conditioned solids were on average a factor 3 lower than on the unconditioned solids. If the effect of conditioning solids is the same for both Ni and Cu, then the values in Table 19 could be a factor 3 lower.

**Table 19: Average Cu Sorption  $K_d$  Values ( $\text{cm}^3/\text{g}$ ) for Brine Solutions**

<b>Mineral</b>	<b>Average</b>	<b>Geometric Mean</b>
Bentonite	62 ± 109	22 (4.2)
Shale	107 ± 214	8 (23)
Limestone	41 ± 53	10 (12)

Note: The standard deviation is given as the error for the average, and the geometric standard deviation is in parentheses beside the geometric mean.

#### 4.2.4 Uranium

Although U may occur in the IV, V and VI oxidation states, only the VI species are likely to be present under the oxidizing conditions of these sorption experiments. Depending upon pH and carbonate concentration, the dissolved uranium chemistry is dominated by carbonate species such as  $\text{UO}_2(\text{CO}_3)_2^{-2}$ ,  $\text{UO}_2(\text{CO}_3)_3^{-4}$ , and  $(\text{UO}_2)_3(\text{CO}_3)_6^{-6}$ . Solubility is limited by schoepite,  $\text{UO}_2(\text{OH})_2 \cdot \text{H}_2\text{O}$ . The dominant solution species and the solubility limiting solid suggest that U would sorb to oxygen sites coordinated to Si or Al, and possibly to carbonate sites.

*Sorption as a Function of Brine Solution:* The sorption of U on bentonite, shale and limestone was evaluated as a function of Na-Ca-Cl brine concentration for TDS values of 10, 25, 100, 200 and 300 g/L. The reaction time was 7 days. The experimental volume was 20 mL and the solid/liquid ratio was 0.5 g/100 mL (i.e. 0.1 g/20 mL). The total U concentration was  $1 \times 10^{-5}$  mol/L, low enough to avoid problems with solubility limits of schoepite. Duplicate tests were used for each solution composition.

Experimental results are summarized in Table 20: as average values of two measurements and plotted as individual results in Figure 18. The percent sorbed values were in a good range for bentonite (46-72%), and a little bit low for shale (11-26%). The percent sorbed values were low for limestone (6-14%), suggesting that the solid/liquid ratio of 0.5 g/100 mL is too low for limestone and a higher solid/liquid ratio should be used. Uranium sorption on bentonite was significantly higher compared to sorption on shale and limestone. Expressing sorption with respect to surface area (Figure 18B) showed that the sorbed U density on limestone was often greater than on shale, but bentonite continued to have the highest density of sorbed U. Unlike Ni and Cu, U sorption on bentonite increased with higher TDS (Figure 18A) and lower pH (Figure 18C). This indicates that the mass action of Na and Ca did not reduce U sorption on bentonite. Furthermore, one would expect that in this pH range, U sorption would have increased with pH, but this was not the case. This suggests that U sorption on bentonite was affected by another factor, uranium carbonate complexation which is more important than salt concentration or pH. U sorption on shale and limestone did not vary significantly with solution composition when the TDS value was 25 g/L and higher. Sorption on limestone at a TDS of 300 g/L was an exception which has  $K_d$  value of 0. An increase in sorption on shale and limestone was noted when the pH increased above 7.5.

**Table 20: Uranium Sorption as a Function of TDS**

<b>Solid</b>	<b>TDS (g/L)</b>	<b>pH</b>	<b>K<sub>d</sub> (cm<sup>3</sup>/g)</b>	<b>K<sub>a</sub> (cm)</b>	<b>% sorbed (n=2)</b>
bentonite	300	6.8	450 ± 38	1.8 × 10 <sup>-3</sup>	72 ± 1
	200	7.1	269 ± 51	1.1 × 10 <sup>-3</sup>	58 ± 3
	100	7.6	233 ± 15	9.3 × 10 <sup>-4</sup>	55 ± 1
	25	7.8	167 ± 8	6.7 × 10 <sup>-4</sup>	46 ± 1
	10	8.0	211 ± 14	8.4 × 10 <sup>-4</sup>	52 ± 1
shale	300	6.4	24 ± 10	2.1 × 10 <sup>-4</sup>	11 ± 3
	200	6.8	32 ± 6	2.8 × 10 <sup>-4</sup>	14 ± 2
	100	7.2	25 ± 1	2.2 × 10 <sup>-4</sup>	11 ± 0
	25	7.5	39 ± 21	3.4 × 10 <sup>-4</sup>	16 ± 5
	10	7.7	69 ± 5	6.0 × 10 <sup>-4</sup>	26 ± 1
limestone	300	6.4	0	0	0
	200	6.7	13 ± 5	4.6 × 10 <sup>-4</sup>	6 ± 2
	100	7.2	11 ± 0	4.0 × 10 <sup>-4</sup>	6 ± 0
	25	7.5	15 ± 3	5.1 × 10 <sup>-4</sup>	7 ± 1
	10	7.7	33 ± 0	1.1 × 10 <sup>-3</sup>	14 ± 0

- Na-Ca-Cl brines
- Reaction time = 7 days
- Total uranium concentration = 1 × 10<sup>-5</sup> mol/L
- Solid/liquid ratio = 0.5 g/100 mL
- Average of two measurements

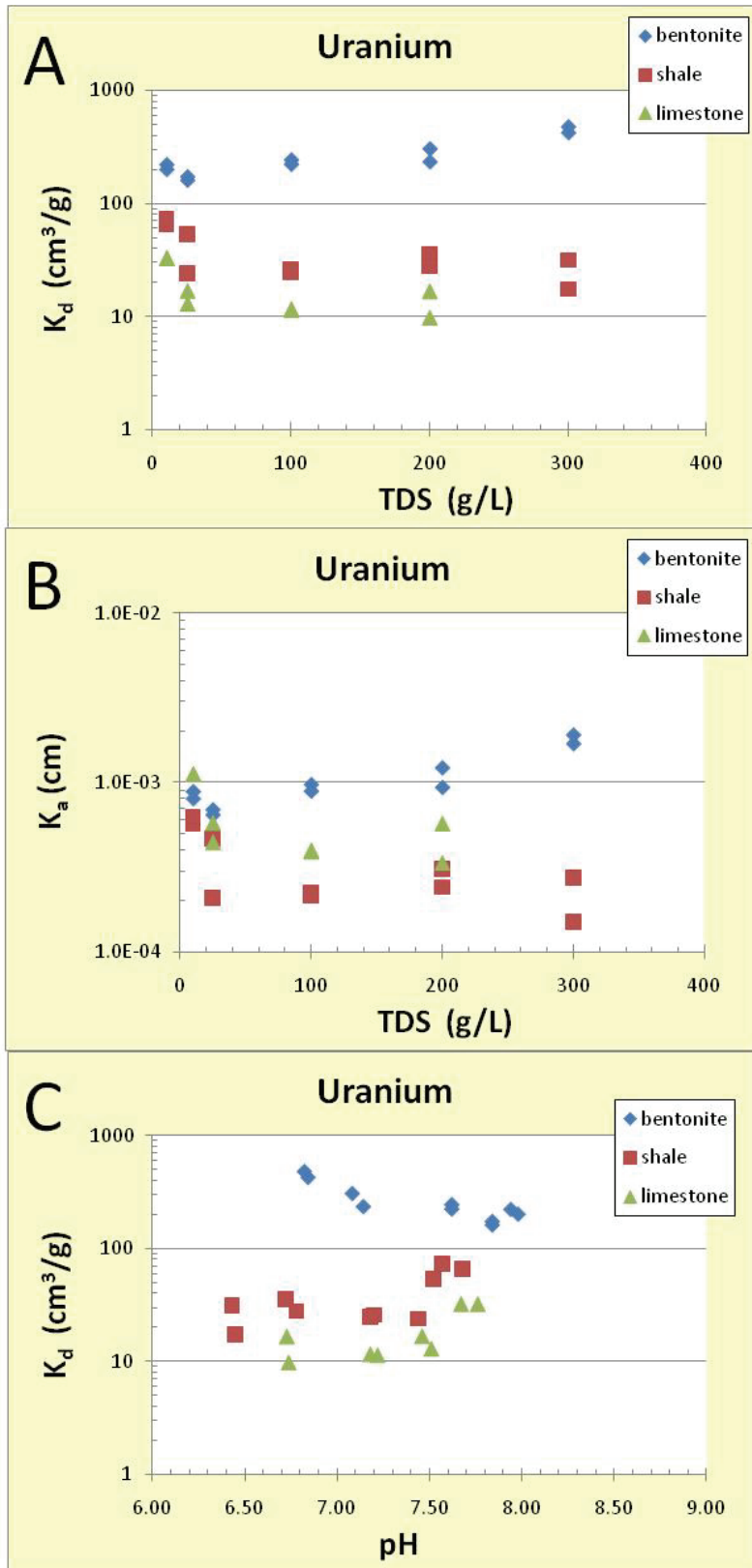
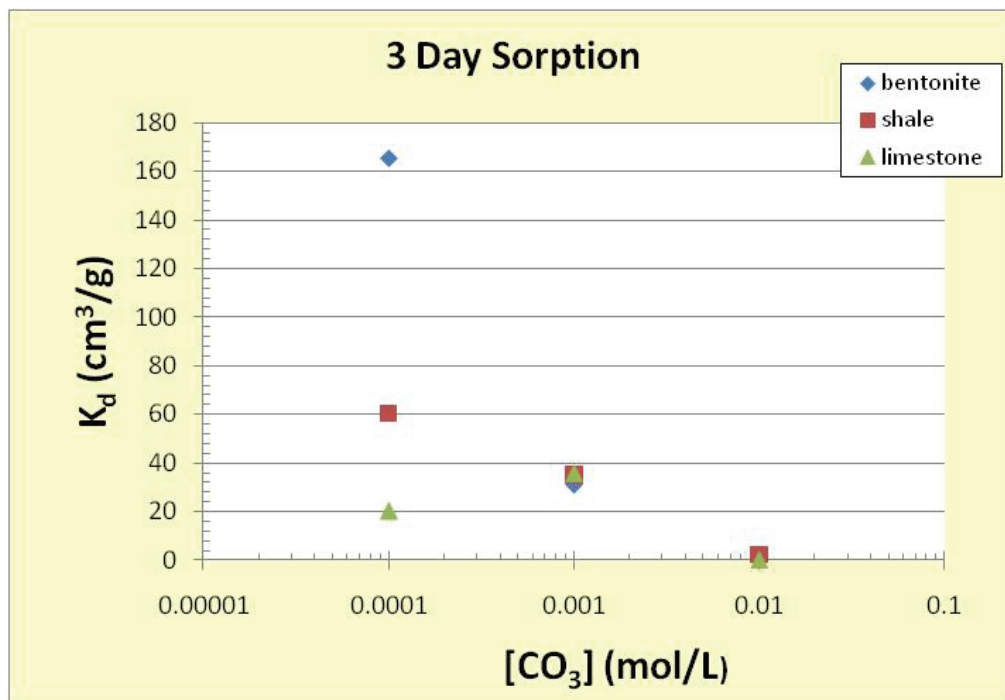


Figure 18: Uranium Sorption as a Function of TDS

*Effect of Total Dissolved Carbonate on U Sorption:* In aqueous solution containing carbonate, uranium will complex with carbonate and decrease its sorption on solids. An experiment was performed to evaluate the sensitivity of U sorption to carbonate concentration in the 10 g/L TDS solution, where the Ca concentration was low enough to permit the use of a broad range of carbonate concentrations below the solubility limit of calcite. The experimental volume was 20 mL and the solid/liquid ratio was 0.5 g/100 mL (i.e. 0.1 g/20 mL). The total U concentration was  $1 \times 10^{-5}$  mol/L. Reaction times were 0.125 and 3 days.

Sorption results are summarized in Table 21 and 3 day sorption  $K_d$  values are plotted in Figure 19. The results clearly show that increased carbonate concentrations will reduce U sorption. Uranium sorption dropped to 0 in most cases when the carbonate concentration was increased to  $1 \times 10^{-2}$  mol/L. Carbonate had the strongest effect for reducing sorption on bentonite, followed by shale. The effect of carbonate on U sorption on limestone was less clear, but sorption did drop to 0 at the highest carbonate concentration. These results are consistent with the previous experiment, in that sorption on bentonite in the 300 g/L brine has the highest  $K_d$  value due to the lowest carbonate concentrations expected in the 300 g/L brine (Table 6).



**Figure 19: Uranium Sorption in 10 g/L Brine as a Function of Carbonate Concentration**

**Table 21: Uranium Sorption in 10 g/L TDS as a Function of Total Carbonate in Solution**

Solid	[CO <sub>3</sub> ] (mol/L)	Time (d)	pH	K <sub>d</sub> (cm <sup>3</sup> /g)	K <sub>a</sub> (cm)	% sorbed
bentonite	1 x 10 <sup>-4</sup>	0.125	7.8	46	4.0 x 10 <sup>-4</sup>	19
bentonite		3	7.7	165	1.4 x 10 <sup>-3</sup>	46
shale		0.125	7.8	25	2.2 x 10 <sup>-4</sup>	11
shale		3	7.6	60	5.3 x 10 <sup>-4</sup>	24
limestone		0.125	7.9	0	0	0
limestone		3	7.5	20	1.8 x 10 <sup>-4</sup>	9
bentonite	1 x 10 <sup>-3</sup>	0.125	7.5	0	0	0
bentonite		3	7.6	31	1.9 x 10 <sup>-4</sup>	13
shale		0.125	7.4	19	1.2 x 10 <sup>-4</sup>	9
shale		3	7.5	35	2.2 x 10 <sup>-4</sup>	15
limestone		0.125	7.4	5	3.8 x 10 <sup>-5</sup>	3
limestone		3	7.5	36	2.2 x 10 <sup>-4</sup>	15
bentonite	1 x 10 <sup>-2</sup>	0.125	6.9	0	0	0
bentonite		3	7.2	0	0	0
shale		0.125	6.9	0	0	0
shale		3	7.1	2	1.4 x 10 <sup>-5</sup>	1
limestone		0.125	6.9	0	0	0
limestone		3	7.0	0	0	0

- 10 g/L Na-Ca-Cl brine
- Solid/liquid ratio = 0.5 g/100 mL
- Total uranium = 1 x 10<sup>-5</sup> mol/L

*Uranium Sorption Kinetics Using Conditioned Solids:* The final series of tests measured U sorption on bentonite, shale and limestone using 4 different solution compositions. In these tests, the solid materials were conditioned with U-free brine solutions for 1 week before the start of sorption tests in order to minimize pH fluctuations and to allow surface sites created by rock crushing to equilibrate with solutions before starting sorption tests. The solid/liquid ratios for shale and limestone were increased to optimize the percent sorbed to improve estimates of sorption coefficients. The experimental volume was 200 mL, and samples were taken at reaction times of 0.125, 1, 3, 7, 14 and 28 days. Three samples were taken at 7 days in order to estimate the uncertainty due to sampling and analysis. The average and standard deviations of these replicates are reported in the data table. The experimental solutions included Na-Ca-Cl brines with TDS values of 10, 100 and 300 g/L, and a Na-Cl brine with a TDS of 100 g/L. The total U concentration used in these tests was 1 x 10<sup>-5</sup> mol/L. The results of these sorption tests are summarized in Table 22 and Figure 20 and Figure 21.

**Table 22: Kinetic Study of U Sorption in 200 mL Volume with Conditioned Solids**

Solid	TDS (g/L)	Solids (g/100 mL)	Time (d)	pH	K <sub>d</sub> (cm <sup>3</sup> /g)	K <sub>a</sub> (cm)	% sorbed
bentonite	10	0.5	0.125	7.5	46	1.8 x 10 <sup>-4</sup>	19
			1	7.5	98	3.9 x 10 <sup>-4</sup>	33
			3	7.5	155	6.2 x 10 <sup>-4</sup>	44
			7	7.5	186 ± 12	7.5 x 10 <sup>-4</sup>	48 ± 2
			14	7.5	210	8.4 x 10 <sup>-4</sup>	51
			28	7.4	189	7.6 x 10 <sup>-4</sup>	49
shale	10	1	0.125	7.5	7.7	6.6 x 10 <sup>-5</sup>	7
			1	7.5	16	1.4 x 10 <sup>-4</sup>	14
			3	7.5	20	1.7 x 10 <sup>-4</sup>	16
			7	7.5	20 ± 3	1.8 x 10 <sup>-4</sup>	17 ± 2
			14	7.5	21	1.8 x 10 <sup>-4</sup>	17
			28	7.5	19	1.6 x 10 <sup>-4</sup>	16
limestone	10	2.5	0.125	7.5	3.8	1.3 x 10 <sup>-4</sup>	9
			1	7.5	7.1	2.5 x 10 <sup>-4</sup>	15
			3	7.5	8.5	2.9 x 10 <sup>-4</sup>	18
			7	7.5	9.0 ± 1.0	3.2 x 10 <sup>-4</sup>	19 ± 1
			14	7.4	9.0	3.1 x 10 <sup>-4</sup>	18
			28	7.4	8.2	2.8 x 10 <sup>-4</sup>	17
bentonite	100	0.5	0.125	7.0	23	9.1 x 10 <sup>-5</sup>	10
			1	7.1	79	3.1 x 10 <sup>-4</sup>	28
			3	7.0	151	6.1 x 10 <sup>-4</sup>	43
			7	7.0	183 ± 14	4.9 x 10 <sup>-4</sup>	48 ± 2
			14	6.9	206	8.2 x 10 <sup>-4</sup>	51
			28	6.9	141	5.7 x 10 <sup>-4</sup>	41
shale	100	1	0.125	6.9	1.5	1.3 x 10 <sup>-5</sup>	1
			1	7.0	1.3	1.1 x 10 <sup>-4</sup>	11
			3	7.0	1.3	1.1 x 10 <sup>-4</sup>	11
			7	7.0	6.0 ± 5.0	5.3 x 10 <sup>-5</sup>	6 ± 4
			14	6.9	7.4	6.5 x 10 <sup>-5</sup>	7
			28	7.0	25	2.2 x 10 <sup>-4</sup>	20
limestone	100	2.5	0.125	6.9	0	0	0
			1	7.0	2.0	6.9 x 10 <sup>-5</sup>	5
			3	7.0	3.0	1.0 x 10 <sup>-4</sup>	7
			7	7.0	2.0 ± 1.0	8.3 x 10 <sup>-5</sup>	6 ± 2
			14	6.9	1.7	6.0 x 10 <sup>-5</sup>	4
			28	6.9	1.2	4.0 x 10 <sup>-5</sup>	3

- Sample volume = 200 mL
- [U]=1×10<sup>-5</sup> mol/L
- Average of three measurements at 7 days

**Table 22: Kinetic Study of U Sorption in 200 mL Volume with Conditioned Solids (Continued)**

Solid	TDS (g/L)	Solids (g/100 mL)	Time (d)	pH	$K_d$ (cm <sup>3</sup> /g)	$K_a$ (cm)	% sorbed
bentonite	300	0.5	0.125	6.5	16	$6.4 \times 10^{-5}$	7
			1	6.5	47	$1.9 \times 10^{-4}$	19
			3	6.4	106	$4.2 \times 10^{-4}$	35
			7	6.5	$565 \pm 46$	$2.3 \times 10^{-3}$	$74 \pm 2$
			14	6.6	1590	$6.4 \times 10^{-3}$	89
			28	6.4	1370	$5.5 \times 10^{-3}$	87
shale	300	1	0.125	6.2	6.6	$5.7 \times 10^{-5}$	6
			1	6.2	11	$9.3 \times 10^{-5}$	10
			3	6.2	20	$1.7 \times 10^{-4}$	17
			7	6.2	$51 \pm 2$	$4.4 \times 10^{-4}$	$34 \pm 1$
			14	6.2	57	$5.0 \times 10^{-4}$	36
			28	6.2	54	$4.7 \times 10^{-4}$	35
limestone	300	2.5	0.125	6.2	1.1	$3.8 \times 10^{-5}$	3
			1	6.2	4.3	$1.5 \times 10^{-4}$	10
			3	6.1	7.9	$2.7 \times 10^{-4}$	17
			7	6.1	$17 \pm 0$	$5.9 \times 10^{-4}$	$30 \pm 0$
			14	6.1	20	$6.9 \times 10^{-4}$	33
			28	6.1	24	$8.1 \times 10^{-4}$	37
bentonite	NaCl 100	0.5	0.125	7.1	10	$4.0 \times 10^{-5}$	5
			1	7.1	17	$6.8 \times 10^{-5}$	8
			2	7.1	14	$5.4 \times 10^{-5}$	6
			6	7.2	0	0	0
			7	7.3	14	$5.4 \times 10^{-5}$	6
shale	NaCl 100	1	0.125	7.1	6.7	$5.9 \times 10^{-5}$	6
			1	7.1	8.6	$7.4 \times 10^{-5}$	8
			2	7.1	5.0	$4.4 \times 10^{-5}$	5
			6	7.2	$3.9 \pm 2.6$	$3.4 \times 10^{-5}$	$4 \pm 2$
			7	7.3	1.7	$1.4 \times 10^{-5}$	2
limestone	NaCl 100	2.5	0.125	7.0	4.2	$1.4 \times 10^{-4}$	9
			1	7.1	4.2	$1.4 \times 10^{-4}$	9
			2	7.1	4.2	$1.4 \times 10^{-4}$	9
			6	7.2	$2.9 \pm 0.5$	$8.2 \times 10^{-5}$	$7 \pm 1$
			7	7.3	4.9	$1.7 \times 10^{-4}$	11

- Sample volume = 200 mL
- [U]= $1 \times 10^{-5}$  mol/L
- Average of three measurements at 7 days, except for NaCl brine (6 days)



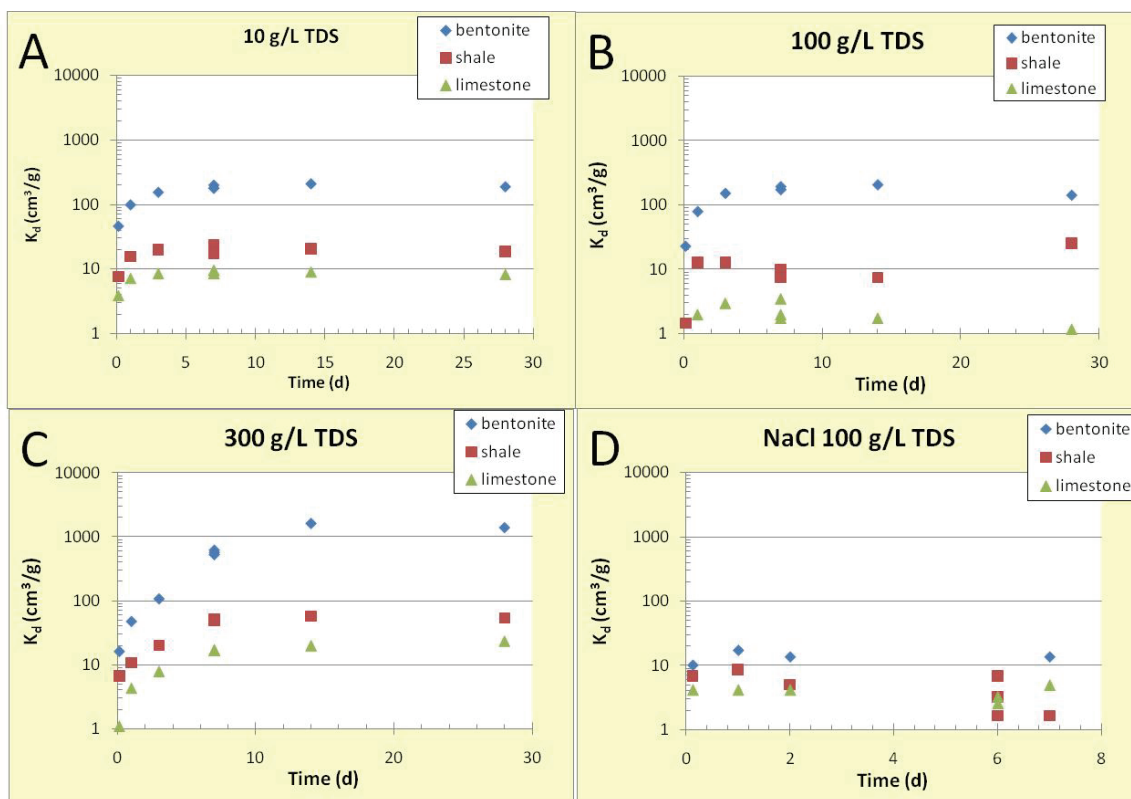


**Figure 20: Uranium Sorption as a Function of Time and Solution Composition using Conditioned Solids; the Solid/Liquid Ratios are 0.5, 1 and 2.5 g/100 mL for Bentonite, Shale and Limestone**

Uranium sorption in the 10 g/L and 100 g/L TDS Na-Ca-Cl solutions appeared to be complete within 7 to 14 days (Figure 20A, Figure 20B and Table 22) except for shale. The sorption reaction was slower in the 300 g/L TDS solutions, with sorption reaching apparent equilibrium within 14 days for bentonite and shale, and over 28 days for limestone (Figure 20C). Uranium sorption on bentonite in the 100 g/L Na-Cl solution was significantly lower than that in 100 g/L TDS Ca-Na-Cl solution within the experimental conditions (Table 22), and the test was run for only 7 days (Figure 20D).

Uranium  $K_d$  values (7 day) are plotted against solution composition parameters in Figure 21. The variation of sorption values with TDS in Na-Ca-Cl brines was similar to the results without pre-conditioning (Figure 18), except sorption on limestone was not 0 as that without pre-conditioning. In Figure 21A the sample points representing the 100 g/L TDS Na-Cl brine are marked, showing significantly reduced sorption on bentonite. The reduced sorption in the 100 g/L TDS Na-Cl brine can be explained by the higher carbonate concentration of  $8 \times 10^{-3}$  mol/L compared to that of  $2 \times 10^{-4}$  mol/L for 100 g/L TDS Na-Ca-Cl solution (Table 6). The higher carbonate concentration in 100 g/L TDS Na-Cl brine induces the formation of more uranium carbonate complexes and reduces the uranium sorption on bentonite. Uranium sorption on limestone and shale was not significantly different in the Na-Cl brine compared to the 100 g/L TDS Na-Ca-Cl brine. The sorption behaviour of limestone and shale could perhaps be explained by U sorbing on carbonate sites, so that changes in solution carbonate had a minimal

effect. Furthermore, the interaction of Ca with carbonate surfaces in the Na-Ca-Cl brine could have reduced uranium sorption.

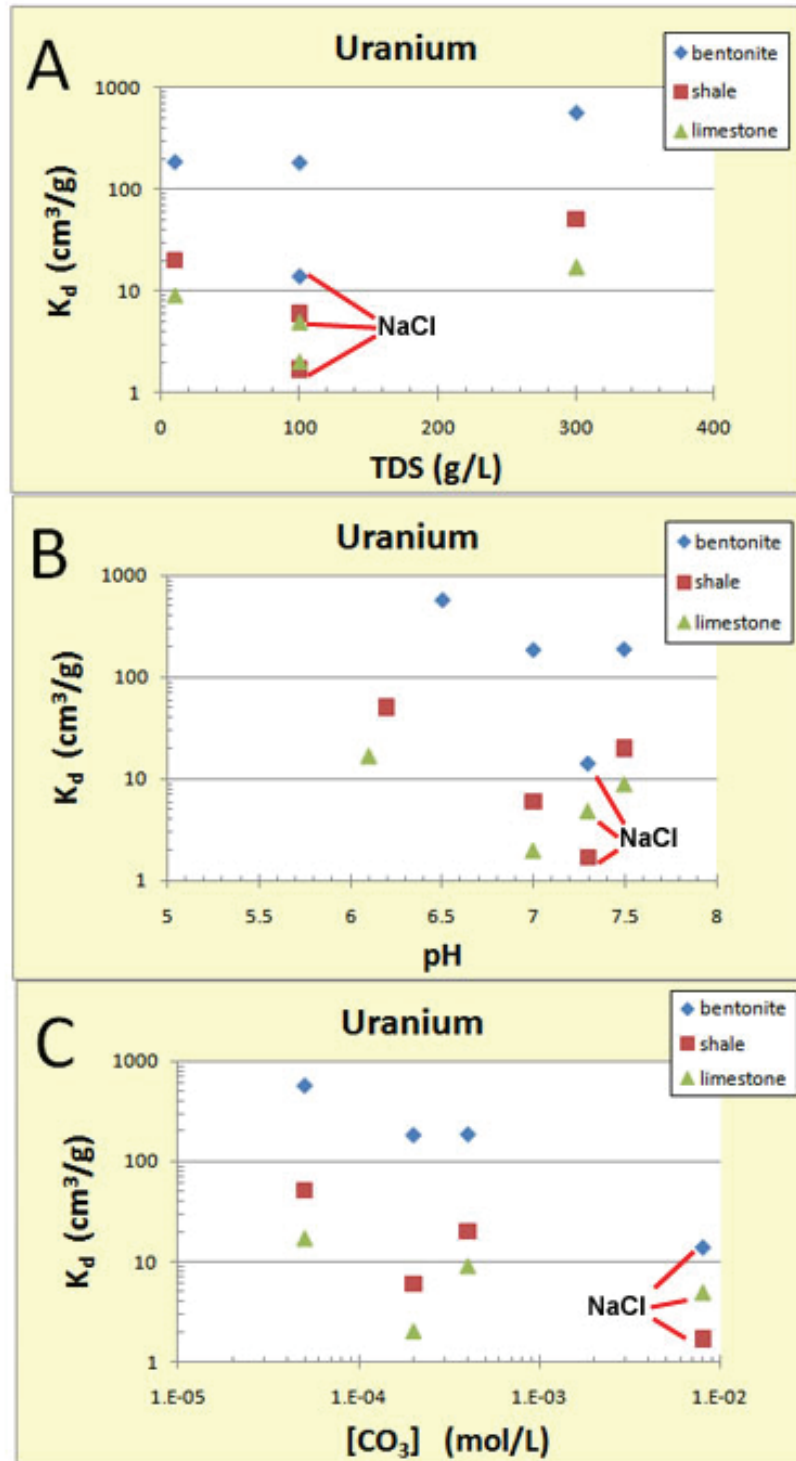


Figure 21: Seven Day Uranium  $K_d$  Values as a Function of (A) TDS, (B) pH, and (C)  $[\text{CO}_3]$ , the Solid/Liquid Ratios are 0.5, 1 and 2.5 g/100 mL for Bentonite, Shale and Limestone

*Desorption Test:* The desorption test was performed using the experiment with 100 g/L TDS Na-Ca-Cl brine after that sorption experiment was completed. The desorption test used the same experimental procedure as Ni. The reaction vessel was sampled as before after time intervals of 0.13, 1, 2, and 7 days. At 7 days the sorption reaction was sampled in triplicate to estimate uncertainty due to sampling and analyses. The results of the desorption test are summarized in Table 23 as  $K_d$  values and as the ratio of the measured  $K_d$  values with respect to the sorption value before desorption ( $K_d^0$ ). The ratio ( $K_d/K_d^0$ ), plotted in Figure 22, would approach a value of 1 when the system comes close to equilibrium.

**Table 23: Uranium Desorption Experiment in 100 g/L TDS Na-Ca-Cl Brine**

Rock	Time (d)	$K_d$ (cm <sup>3</sup> /g)	$K_d/K_d^0$
Bentonite	Before desorption ( $K_d^0$ )	53	
	0.13	2040	38
	1	1040	19
	2	452	8
	*7	215 ± 74	4 ± 1
Shale	Before desorption ( $K_d^0$ )	25	
	0.13	686	27
	1	686	27
	2	325	13
	*7	221 ± 90	9 ± 4
Limestone	Before desorption ( $K_d^0$ )	1.2	
	0.13	377	321
	1	377	324
	2	288	246
	*7	88 ± 20	71 ± 17

- \* average of three measurements
- Desorption at pH= 7

At the initiation of the desorption test, U sorption on limestone displayed the furthest deviation from equilibrium with a  $K_d/K_d^0$  ratio of 321. However, over a 7 day period the  $K_d/K_d^0$  ratio dropped significantly, and following its observed trend (Figure 22), U desorption from limestone will likely reach equilibrium after 2 weeks. Although U desorption from limestone doesn't occur in the short term, over long time periods U sorption appears to be reversible. In the initial time frame at the start of the desorption experiment, U sorption on bentonite and shale was significantly closer to equilibrium than limestone with  $K_d/K_d^0$  ratios of 38 and 27, respectively. With prolonged desorption, U sorption on bentonite and shale appeared to be approaching equilibrium. Comparing the  $K_d/K_d^0$  ratios of U desorption and their changes with time to that of Ni desorption (Table 15), it suggests that U sorption is more reversible than that of Ni.

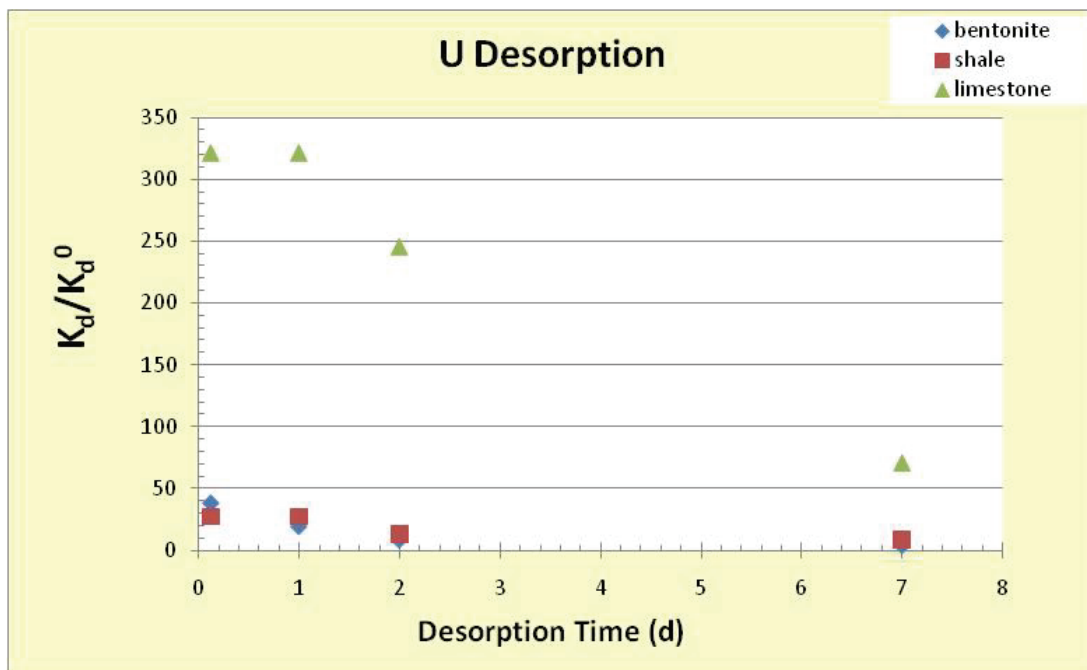


**Figure 22: Uranium Desorption Experiment**

*Summary:* Uranium sorption on bentonite and shale is reduced when dissolved carbonate concentrations increase and promote the formation of more uranium carbonate complexes in solution. This effect was less pronounced with limestone, although when the carbonate concentration was as high as  $1 \times 10^{-2}$  mol/L U sorption on limestone was eliminated. The TDS does not appear to affect U sorption. Uranium sorption did not vary with pH in a consistent manner, probably because other solution parameters such as carbonate concentration influenced the variability in U sorption values. The variation in U sorption with pH needs to be investigated using solutions in which only the pH is a variable. These tests need to have a short experimental duration to get around the problem of drifting pH caused by reactions with mineral surfaces. Uranium sorption appears to reach equilibrium within 7 to 14 days, in contrast to that of Ni which continues to increase with time for a period that likely exceeds 28 days. Uranium sorption appears to be reversible.

In the interests of selecting U sorption data for performance assessment, the data from the experiments with conditioned solids were considered to be the most useful since artefacts from rock crushing have been reduced. The sorption data from these tests are summarized in Table 24 in the form of average  $K_d$  values determined with reaction times of 7 days. These average values include variability associated with changes in TDS, Ca/Na ratio, and pH. These average values cover a pH range from 6.0 to 7.5, and ionic strengths of 0.2 to 7.5 (mol/kg).

**Table 24: Average U Sorption  $K_d$  Values ( $\text{cm}^3/\text{g}$ ) for Brine Solutions**

Mineral	Average	Geometric Mean
Bentonite	240 ± 230	130 (6.7)
Shale	20 ± 22	10 (5.6)
Limestone	8 ± 7	6 (3)

Note: The standard deviation is given as the error for the average, and the geometric standard deviation is in parentheses beside the geometric mean.

#### 4.2.5 Europium

Europium is a Group 9, lanthanide series rare earth element, with a dominant III oxidation state. The major soluble species that could be expected to be present in brine solutions are predicted to be  $\text{Eu}^{+3}$ ,  $\text{EuCl}^{+2}$ ,  $\text{Eu}(\text{CO}_3)^+$ ,  $\text{Eu}(\text{CO}_3)_2^-$ , and  $\text{Eu}(\text{OH})^{+2}$ . The presence of europium carbonate species depends on the carbonate concentration in the brine. Solubility is limited by carbonate and mixed carbonate-hydroxide solids such as  $\text{Eu}_2(\text{CO}_3)_3 \cdot \text{H}_2\text{O}$  and  $\text{Eu}(\text{CO}_3)(\text{OH})$ . This suggests that Eu sorption will be affected by pH, and the concentrations of chloride and carbonate. Europium is likely to sorb by complexation with oxygen coordinated with Al and Si, and with carbonate sites.

*Initial Test to Evaluate Eu Sorption Kinetics:* Europium sorption on bentonite, shale and limestone in the 300 g/L TDS brine was studied as a function of time for up to 28 days. The nominal Eu concentrations were  $4.39 \times 10^{-4}$  and  $5.28 \times 10^{-5}$  mol/L. The reaction test volume was 10 mL and the solid/liquid ratio was 10 g/100 mL (i.e. 1 g/10 mL).

Experimental results are presented in Table 25 and in Figure 23 as a function of time in the form of percent sorbed,  $K_d$  values and  $K_a$  values. The percent sorbed (89 to 99%) was significantly higher in tests with a total Eu concentration of  $5.28 \times 10^{-5}$  mol/L, compared with tests with a total Eu concentration of  $4.39 \times 10^{-4}$  mol/L (54 to 98% sorbed). The high percent sorbed values ( $\geq 90\%$ ) increased the uncertainty in dissolved Eu concentrations and the resulting  $K_d$  values. Focusing on the results from tests with a total Eu concentration of  $4.39 \times 10^{-4}$  mol/L (Figure 23:), sorption was the highest on bentonite, followed by shale and limestone with similar amounts of sorbed Eu. When sorption is expressed in relation to surface area (Figure 23:C), bentonite still had the highest Eu density, followed closely by limestone and shale. Limestone had a significantly higher Eu surface density compared to shale, indicating that Eu may have a strong affinity for carbonate surface sites. Europium sorption increased with time, possibly reaching a steady-state with shale and limestone after 14 days. Europium might continue to sorb on bentonite after 28 days. If one were to assume that sorption reaches equilibrium by 28 days, then at 7 days the sorption coefficient could be considered to be 46 percent complete for bentonite, and about 87 percent complete for limestone and shale in terms of  $K_d$  values.

**Table 25: Europium Sorption as a Function of Time in 300 g/L TDS Na-Ca-Cl Brine**

<b>Solid</b>	<b>Total [Eu] (mol/L)</b>	<b>Time (d)</b>	<b>pH</b>	<b>K<sub>d</sub> (cm<sup>3</sup>/g)</b>	<b>K<sub>a</sub> (cm)</b>	<b>% sorbed</b>
bentonite	4.39 x 10 <sup>-4</sup>	0.13	6.10	21	8.5 x 10 <sup>-5</sup>	68
		1	6.17	25	9.9 x 10 <sup>-5</sup>	71
		3	6.41	85	3.4 x 10 <sup>-4</sup>	90
		7	6.68	283	1.1 x 10 <sup>-3</sup>	97
		14	6.59	465	1.9 x 10 <sup>-3</sup>	98
		28	6.62	615	2.5 x 10 <sup>-3</sup>	98
shale	4.39 x 10 <sup>-4</sup>	0.13	5.92	13	1.1 x 10 <sup>-4</sup>	57
		1	6.02	18	1.5 x 10 <sup>-4</sup>	64
		3	6.10	23	2.0 x 10 <sup>-4</sup>	69
		7	6.20	27	2.4 x 10 <sup>-4</sup>	73
		14	6.11	35	3.0 x 10 <sup>-4</sup>	78
		28	6.08	31	2.7 x 10 <sup>-4</sup>	75
limestone	4.39 x 10 <sup>-4</sup>	0.13	5.97	12	4.0 x 10 <sup>-4</sup>	54
		1	5.98	12	4.3 x 10 <sup>-4</sup>	56
		3	6.08	19	6.6 x 10 <sup>-4</sup>	66
		7	6.16	20	7.1 x 10 <sup>-4</sup>	67
		14	6.07	31	1.1 x 10 <sup>-3</sup>	76
		28	6.03	23	8.1 x 10 <sup>-4</sup>	70
bentonite	5.28 x 10 <sup>-5</sup>	0.13	6.44	166	6.6 x 10 <sup>-4</sup>	94
		1	6.57	268	1.1 x 10 <sup>-3</sup>	96
		3	6.71	528	2.1 x 10 <sup>-3</sup>	98
		7	6.86	544	2.2 x 10 <sup>-3</sup>	98
		14	6.73	470	1.9 x 10 <sup>-3</sup>	98
		28	6.73	631	2.5 x 10 <sup>-4</sup>	98
shale	5.28 x 10 <sup>-5</sup>	0.13	6.24	78	6.7 x 10 <sup>-4</sup>	89
		1	6.26	172	1.5 x 10 <sup>-3</sup>	95
		3	6.39	210	1.8 x 10 <sup>-3</sup>	95
		7	6.31	341	3.0 x 10 <sup>-3</sup>	97
		14	6.33	394	3.4 x 10 <sup>-3</sup>	98
		28	6.27	1066	9.3 x 10 <sup>-3</sup>	99
limestone	5.28 x 10 <sup>-5</sup>	0.13	6.22	118	4.1 x 10 <sup>-3</sup>	92
		1	6.25	192	6.7 x 10 <sup>-3</sup>	95
		3	6.34	527	1.8 x 10 <sup>-2</sup>	98
		7	6.28	682	2.4 x 10 <sup>-2</sup>	99
		14	6.22	1067	3.7 x 10 <sup>-2</sup>	99
		28	6.14	1066	3.7 x 10 <sup>-2</sup>	99

- Solid/liquid ratio = 10 g/100 mL

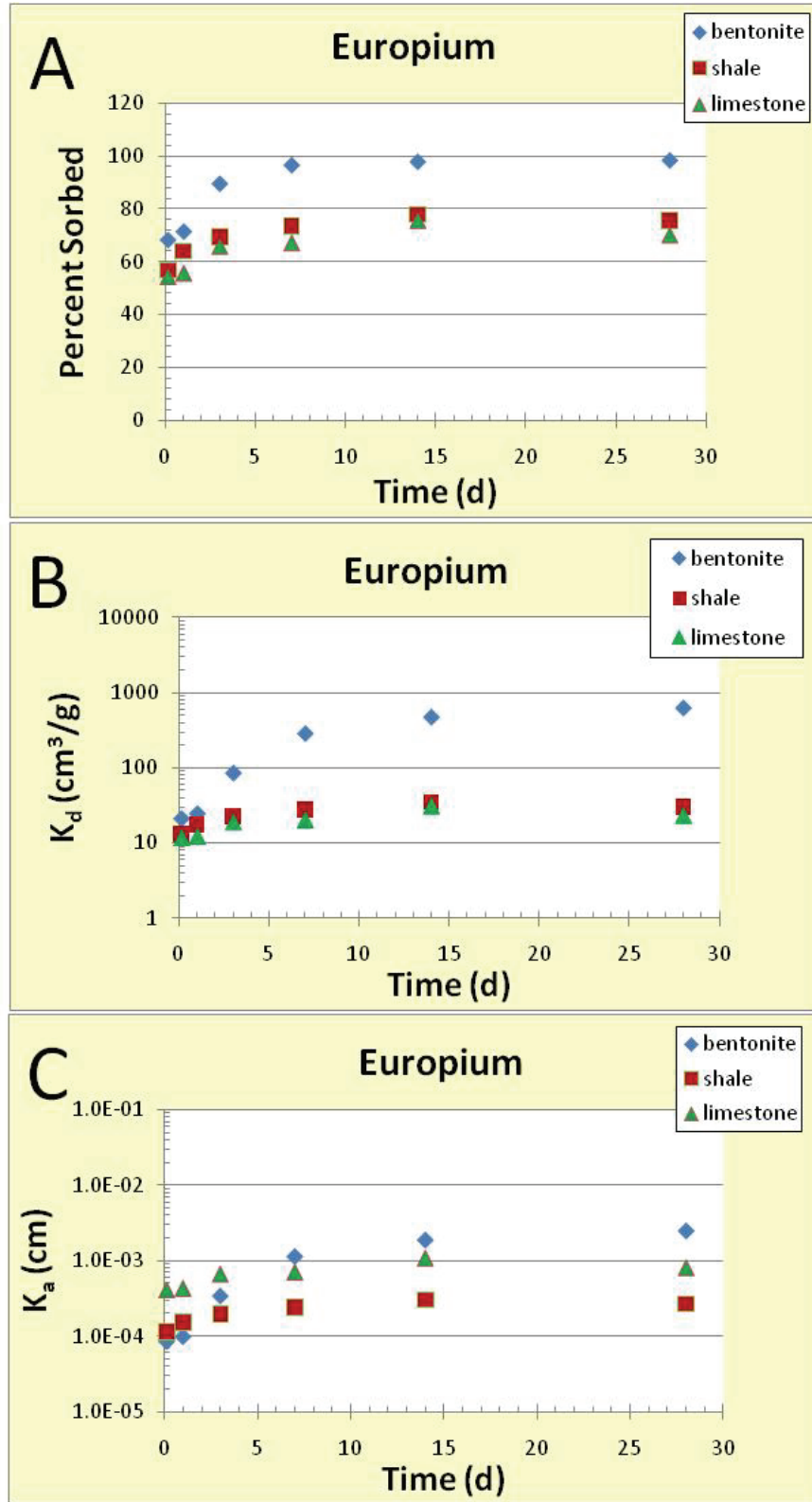


Figure 23: Europium Sorption with Time Shown as Percent Sorbed,  $K_d$  Values and  $K_a$  Values. Data are from the Tests with a Total Eu Concentration of  $4.39 \times 10^{-4}$  mol/L

*Variation in Europium Sorption with Solid/Liquid Ratio.* An experiment was performed to evaluate the effect of the solid/liquid ratio on Eu sorption to help define ideal solid/liquid ratios that would lead to percent sorbed values in the range of 40 to 60 percent. There is also an interest in checking whether solid/liquid ratios have an impact on measured sorption coefficients. The sorption tests were performed with the 300 g/L brine, using a reaction volume of 20 mL. The total Eu concentration was  $5 \times 10^{-4}$  mol/L, and the reaction time was 7 days.

The results are presented in Table 26 and illustrated in Figure 24. The percent sorbed values were improved over the previously described test with 300 g/L TDS and were used as a guide for selecting solid/liquid ratios for the final Eu sorption tests. Although percent sorbed values increased with higher solid/liquid ratios, the  $K_d$  values decreased with increasing solid/liquid ratio for all solids. Since the percent sorbed values were not high and the dissolved Eu concentrations were not a limit to sorption, it may be that that some sorption sites were blocked at higher solid/liquid ratios by particle-particle interactions. Sorption coefficients determined with a solid/liquid ratio of 2.5 g/100 mL were lower than those determined with a ratio of 0.25 g/100 mL by factors of 2 for bentonite, 3.5 for shale and 3.3 for limestone. Sorption on bentonite may be less affected by the solid/liquid ratio because bentonite has a very large surface area and/or bentonite particles were flocs, with internal sites that were not blocked by interactions with other particles. Focusing on the percent sorbed values, the results in Table 26 were used to select the solid/liquid ratios reported for Eu sorption in Table 27.

**Table 26: Europium Sorption Variation with Solid/Liquid Ratio in 300 g/L TDS Brine**

Solid	Solids (g/100 mL)	pH	$K_d$ (cm <sup>3</sup> /g)	$K_a$ (cm)	% sorbed
benonite	0.25	6.1	120	$4.8 \times 10^{-4}$	23
	0.51	6.2	84	$3.3 \times 10^{-4}$	30
	0.98	6.3	71	$2.8 \times 10^{-4}$	41
	2.54	6.4	60	$2.4 \times 10^{-4}$	60
shale	0.25	6.1	77	$3.1 \times 10^{-4}$	16
	0.50	6.2	44	$1.8 \times 10^{-4}$	18
	1.00	6.2	37	$1.5 \times 10^{-4}$	27
	2.49	6.2	22	$8.9 \times 10^{-5}$	36
limestone	0.25	6.1	93	$3.7 \times 10^{-4}$	19
	0.52	6.2	59	$2.4 \times 10^{-4}$	24
	1.02	6.2	44	$1.7 \times 10^{-4}$	31
	2.50	6.2	28	$1.1 \times 10^{-4}$	41

- Reaction time = 7 days
- [Eu] =  $5 \times 10^{-4}$  mol/L



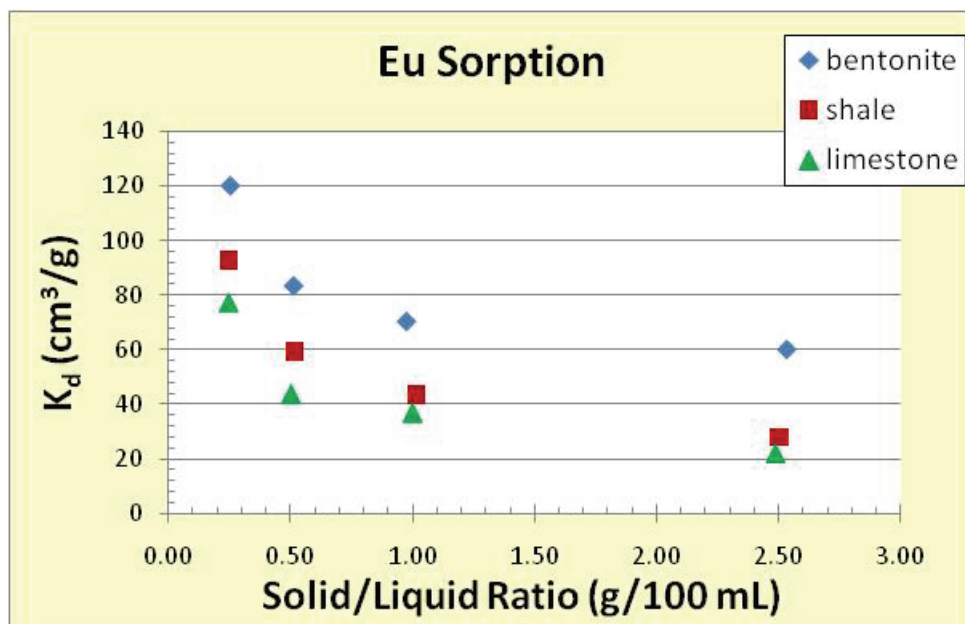


**Figure 24: Europium Sorption K<sub>d</sub> Values as a Function of Solid/Liquid Ratio**

*Europium Sorption Kinetics Using Conditioned Solids:* The final set of tests measured Eu sorption on bentonite, shale and limestone using different solution compositions. In these tests, the solid materials were conditioned with Eu-free brine solutions for 1 week before the start of sorption tests in order to minimize pH fluctuations and to allow the new sorption sites created by the rock grinding to equilibrate with brine solution. The solid/liquid ratios for bentonite and shale were increased in an attempt to optimize the percent sorbed for deriving better sorption coefficients. The experimental volume was 200 mL, and samples were taken at sorption times of 0.125, 1, 3, 7, 14 and 28 days. Three samples were taken at 7 days in order to estimate the uncertainty due to sampling and analysis. The average and standard deviation of these replicates are reported in the data table. The experimental solutions included Na-Ca-Cl brines with TDS values of 10, 100 and 300 g/L, and a Na-Cl brine with a TDS of 100 g/L. The total Eu concentration used in these tests was  $1 \times 10^{-5}$  mol/L to keep the Eu concentration as low as possible.

The results of these sorption tests are summarized in Table 27 and Figure 25. Note that there are no results from the 100 g/L TDS Na-Cl solution because the carbonate concentration was high enough to induce Eu precipitation as  $\text{Eu}_2(\text{CO}_3)_3 \cdot 3\text{H}_2\text{O}$ . The tests with the 10 g/L TDS solution produced optimum amounts of sorption, with percent Eu sorbed ranging from 31 to 78 percent for all solids. The percent Eu sorbed values were slightly higher in the 100 g/L solution, ranging from 37 and 79% for bentonite and shale, and from 62 to 92% for limestone. The amount of Eu sorption in the 300 g/L TDS solution was higher, with percent sorbed values of 47 to 97% for bentonite, 29 to 55% for shale and 49 to 92% for limestone. These results indicate that the choice of solid/liquid ratios (0.5-2.5 g/100 mL) was better than in the initial Eu sorption tests (10 g/100 mL).

**Table 27: Kinetic Study of Eu Sorption in 200 mL Volume with Conditioned Solids**

Solid	TDS (g/L)	Solids (g/100 mL)	Time (d)	pH	$K_d$ (cm <sup>3</sup> /g)	$K_a$ (cm)	% sorbed
Bentonite	10	0.5	0.125	7.1	1.6	$6.2 \times 10^{-6}$	1
			1	7.2	89	$3.6 \times 10^{-4}$	31
			3	7.2	110	$4.4 \times 10^{-4}$	35
			7	7.3	$97 \pm 55$	$3.9 \times 10^{-4}$	$31 \pm 13$
			14	7.3	313	$1.3 \times 10^{-3}$	61
			28	7.3	300	$1.2 \times 10^{-3}$	60
Shale	10	1	0.125	7.1	136	$1.2 \times 10^{-3}$	58
			1	7.2	205	$1.8 \times 10^{-3}$	67
			3	7.3	no data	no data	no data
			7	7.3	$179 \pm 48$	$1.5 \times 10^{-3}$	$63 \pm 7$
			14	7.3	355	$3.1 \times 10^{-3}$	78
			28	7.3	213	$1.9 \times 10^{-3}$	68
Limestone	10	2.5	0.125	7.2	38	$1.3 \times 10^{-3}$	49
			1	7.2	96	$3.4 \times 10^{-3}$	71
			3	7.3	41	$1.4 \times 10^{-3}$	51
			7	7.5	$93 \pm 58$	$3.2 \times 10^{-3}$	$67 \pm 15$
			14	7.4	71	$2.5 \times 10^{-3}$	64
			28	7.5	116	$4.0 \times 10^{-3}$	74
Bentonite	100	0.5	0.125	6.9	119	$4.8 \times 10^{-4}$	37
			1	6.7	372	$1.5 \times 10^{-3}$	65
			3	6.9	525	$2.1 \times 10^{-3}$	72
			7	6.9	$763 \pm 72$	$3.1 \times 10^{-3}$	$79 \pm 2$
			14	6.9	615	$2.5 \times 10^{-3}$	75
			28	6.9	645	$2.6 \times 10^{-3}$	76
shale	100	1	0.125	6.8	56	$4.8 \times 10^{-4}$	36
			1	6.7	128	$1.1 \times 10^{-3}$	56
			3	6.8	177	$1.5 \times 10^{-3}$	64
			7	6.9	$215 \pm 3$	$1.9 \times 10^{-3}$	$68 \pm 0$
			14	6.9	298	$2.6 \times 10^{-3}$	75
			28	6.9	316	$2.7 \times 10^{-3}$	76
limestone	100	2.5	0.125	6.7	64	$2.2 \times 10^{-3}$	62
			1	6.6	119	$4.1 \times 10^{-3}$	75
			3	6.8	168	$5.8 \times 10^{-3}$	81
			7	6.9	$293 \pm 26$	$1.0 \times 10^{-2}$	$88 \pm 1$
			14	6.9	354	$1.2 \times 10^{-2}$	90
			28	6.9	433	$1.5 \times 10^{-2}$	92

- Sample volume = 200 mL
- Average of three measurements at 7 days
- [Eu]= $1 \times 10^{-5}$  mol/L
- No data, because samples were lost

**Table 27: Kinetic Study of Eu Sorption in 200 mL Volume with Conditioned Solids (Continued)**

Solid	TDS (g/L)	Solids (g/100 mL)	Time (d)	pH	K <sub>d</sub> (cm <sup>3</sup> /g)	K <sub>a</sub> (cm)	% sorbed
bentonite	300	0.5	0.125	6.3	181	7.2 x 10 <sup>-4</sup>	47
			1	6.2	221	8.9 x 10 <sup>-4</sup>	53
			3	6.3	708	2.8 x 10 <sup>-3</sup>	78
			7	6.4	5700 ± 0	2.3 x 10 <sup>-2</sup>	97 ± 0
			14	6.4	3730	1.5 x 10 <sup>-2</sup>	95
			28	6.4	2750	1.1 x 10 <sup>-2</sup>	93
shale	300	1	0.125	6.1	41	3.6 x 10 <sup>-4</sup>	29
			1	5.9	55	4.8 x 10 <sup>-4</sup>	35
			3	5.9	81	7.0 x 10 <sup>-4</sup>	45
			7	6.1	108 ± 8	9.3 x 10 <sup>-4</sup>	52 ± 2
			14	6.1	103	9.0 x 10 <sup>-4</sup>	51
			28	6.1	124	1.1 x 10 <sup>-3</sup>	55
limestone	300	2.5	0.125	6.0	39	1.3 x 10 <sup>-3</sup>	49
			1	5.9	68	2.4 x 10 <sup>-3</sup>	63
			3	5.9	97	3.4 x 10 <sup>-3</sup>	71
			7	6.0	150 ± 8	5.2 x 10 <sup>-3</sup>	79 ± 1
			14	6.0	249	8.6 x 10 <sup>-3</sup>	86
			28	6.1	480	1.7 x 10 <sup>-2</sup>	92

- Sample volume = 200 mL
- Average of three measurements at 7 days
- [Eu]=1×10<sup>-5</sup> mol/L

The time for Eu sorption to achieve a steady state varied from 7 to over 28 days (Figure 25). In the 10 g/L TDS solution, sorption on limestone had reached steady-state by 7 days, while 14 days were required to reach steady-state for bentonite and shale. The maximum K<sub>d</sub> value of these tests was used as a reference to calculate the percent complete. In the 10 g/L TDS solution the 7 day K<sub>d</sub> values were 31 percent complete for bentonite, 80 percent complete for limestone and 50 percent complete for shale. In the 100 g/L solution, Eu sorption reached steady-state by 7 days for bentonite, but took longer than 28 days for shale and limestone. The 7 day K<sub>d</sub> values for shale and limestone were approximately 68 percent complete. Europium sorption in the 300 g/L TDS solution reached steady-state after 7 days for bentonite and didn't reach steady-state within the 28 day experimental time for shale and limestone. The 7 day K<sub>d</sub> value was 87 percent complete for shale and 31 percent complete for limestone.

The effect of solution composition is illustrated in Figure 26, where 7 day average K<sub>d</sub> values (3 tests) are plotted versus (A) TDS, (B) pH, and (C) carbonate concentration. Again one must bear in mind that the TDS, pH and carbonate concentration were not independent variables. As with U, the Eu K<sub>d</sub> values for sorption on bentonite increased with increasing TDS and decreasing pH. This is counter intuitive because one would expect the mass action of the salt to reduce sorption, and the higher pH to promote more sorption by surface complexation reactions. This suggests that it was the decreasing carbonate concentration in the higher TDS solutions (Table 6) that increased sorption on bentonite. Europium complexes with carbonate in

aqueous solution. Europium sorption in bentonite was strongly correlated with the total carbonate in solution. This is supported by geochemical simulations with PHREEQC that showed an increased fraction of europium carbonate complexes and a reduced concentration of  $\text{Eu}^{+3}$  that would be available for sorption in the 10 g/L TDS solution (The results are not shown). Europium sorption on shale and limestone showed significantly less variability with solution composition, with no clear trends with any of the solution parameters. The increased carbonate did not affect sorption on limestone and shale, possibly because Eu was complexing with carbonate sites in both of these rocks or TDS and pH impacted Eu sorption when carbonate concentrations were low.

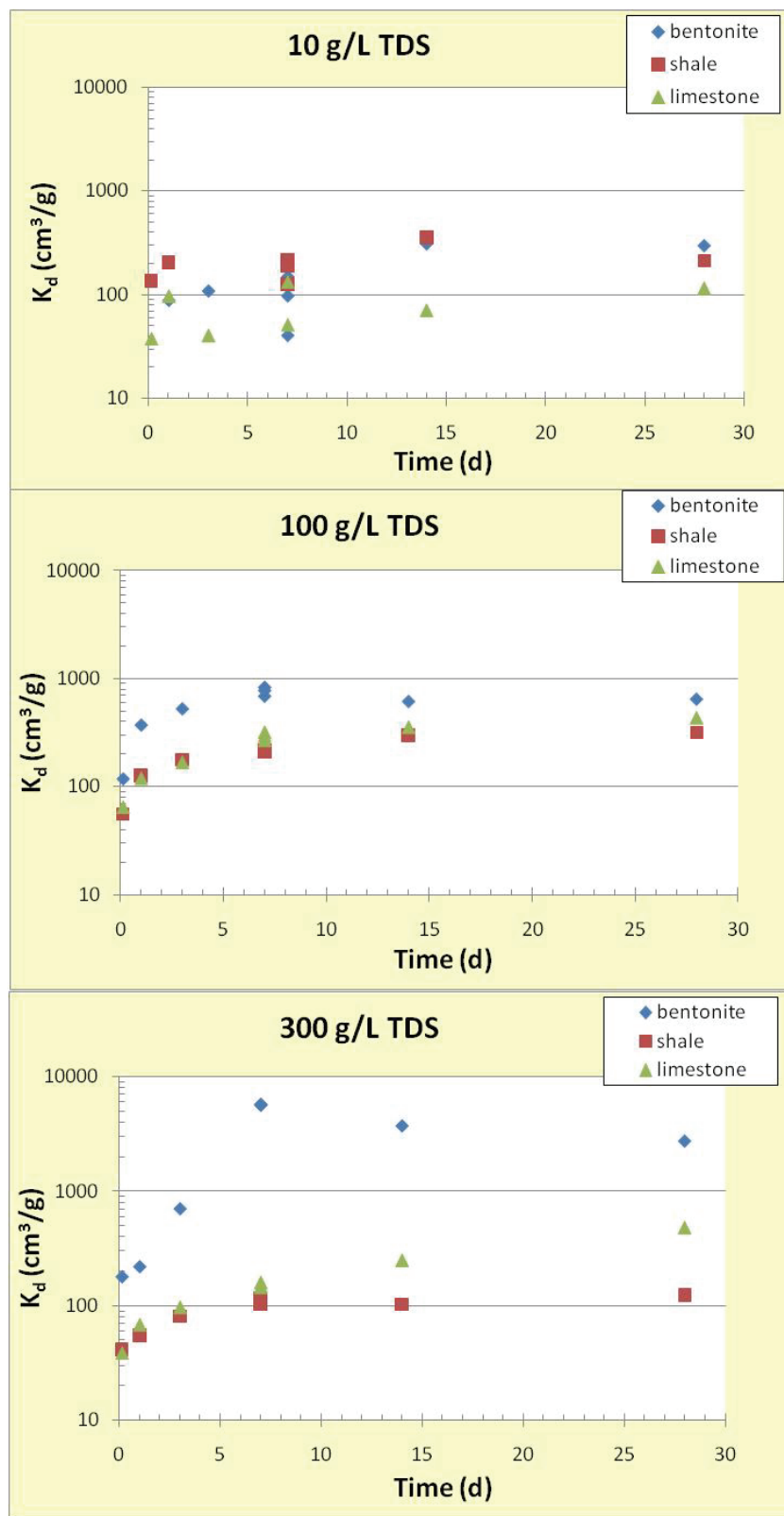


Figure 25: Kinetic Study of Eu Sorption in 200 mL Volume with Conditioned Solids, the Solid/Liquid Ratios are 0.5, 1 and 2.5 g/100 mL for Bentonite, Shale and Limestone

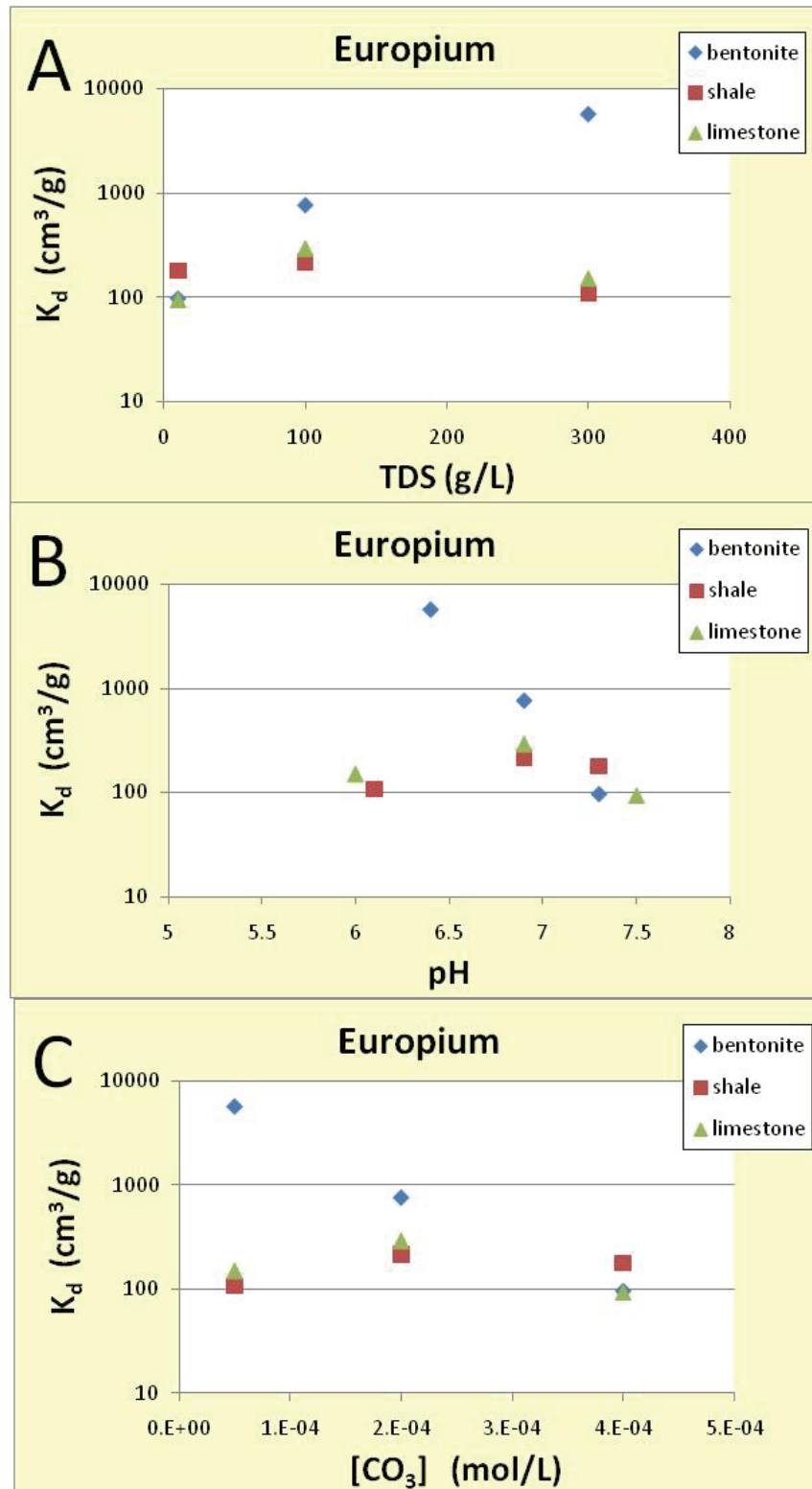


Figure 26: Seven Day Europium Sorption Coefficients as a Function of (A) TDS, (B) pH, and (C)  $[\text{CO}_3]$ , the Solid/Liquid Ratios are 0.5, 1 and 2.5 g/100 mL for Bentonite, Shale and Limestone

*Desorption Test:* The desorption test was performed using the experiment with the 100 g/L Na-Ca-Cl brine after that sorption experiment was completed, and followed the same experimental procedure as Ni and U. The reaction vessel was sampled as before after time intervals of 0.13, 1, 3, 7 and 14 days. The results of the desorption test are summarized in Table 28 as  $K_d$  values and as the ratio of the measured  $K_d$  values with respect to the sorption value before desorption ( $K_d^0$ ). The ratios of  $K_d/K_d^0$  were plotted in Figure 27.

At the initiation of the desorption test, Eu sorption on limestone displayed the furthest deviation from equilibrium with a  $K_d/K_d^0$  ratio of 5, which remained constant for 14 days. In the initial time frame of the desorption experiment, Eu sorption on bentonite and shale was closer to equilibrium with  $K_d/K_d^0$  ratios of 4.0 and 4.5, respectively. With prolonged desorption, the  $K_d/K_d^0$  values decreased slightly, but did not show any trends that would indicate that the  $K_d$  values would return to equilibrium with  $K_d/K_d^0$  ratio approaching to 1.

**Table 28: Europium Desorption Experiment in 100 g/L TDS Na-Ca-Cl Brine**

Rock	Time (d)	$K_d$ (cm <sup>3</sup> /g)	$K_d/K_d^0$
Bentonite	Before desorption ( $K_d^0$ )	645	
	0.13	2340	4.0
	1	2560	4.4
	3	1800	3.1
	7	2340	4.0
	14	1720	3.0
Shale	Before desorption ( $K_d^0$ )	316	
	0.13	1290	4.5
	1	1060	3.7
	3	790	2.8
	7	810	2.8
	14	1110	3.9
Limestone	Before desorption ( $K_d^0$ )	433	
	0.13	2220	5
	1	2220	5
	3	2220	5
	7	2220	5
	14	2220	5

- Desorption at pH=6.9

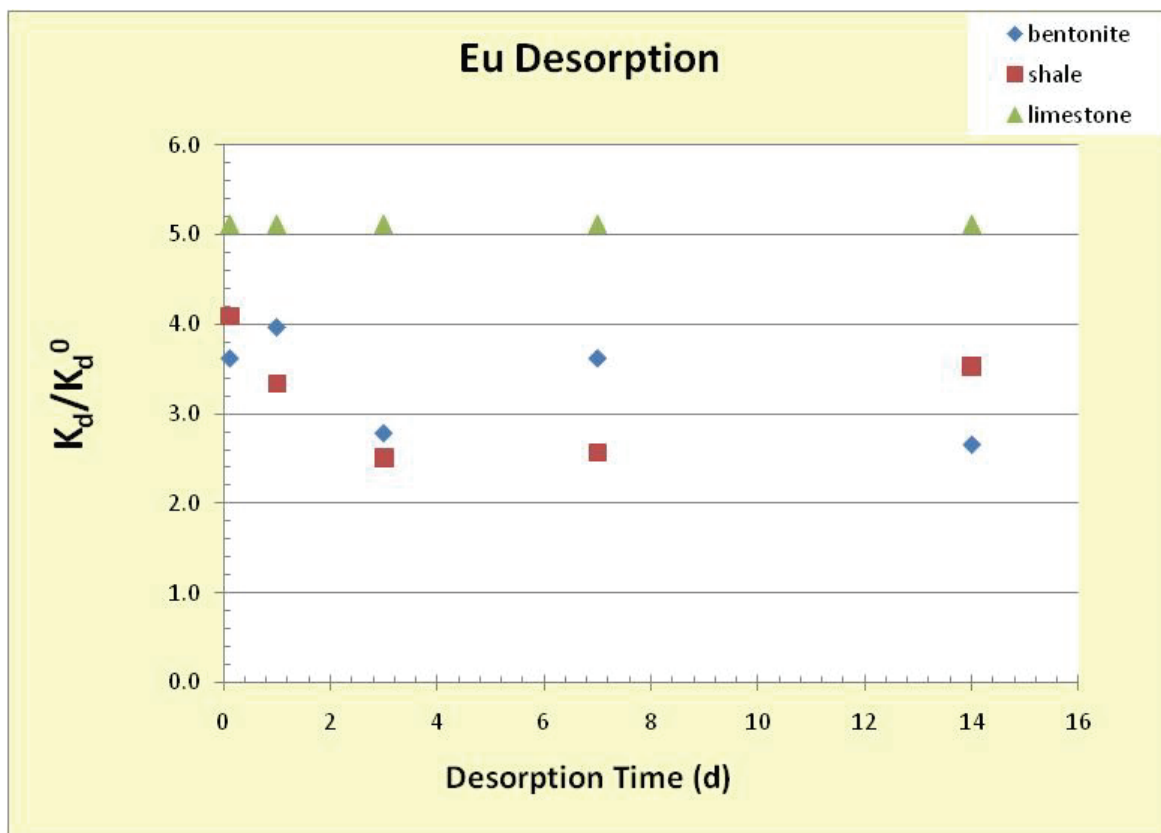


**Figure 27: Europium Desorption Experiment**

*Summary:* Europium sorption on bentonite is affected by Eu complexation with carbonate in solution, which is similar to what was observed with U. Europium sorption on shale and limestone showed significantly less variability with solution composition, with no clear trends with any of the solution parameters. The increased carbonate concentration did not affect sorption on limestone and shale, possibly because Eu was complexing with carbonate sites in both of these rocks or TDS and pH impacted Eu sorption when carbonate concentrations were low. Europium sorption on bentonite and shale appeared to reach equilibrium within 7 to 14 days. However, in several cases sorption on limestone appears to keep increasing over longer periods, possibly exceeding 28 days. Europium sorption displays evidence of irreversibility over a 2 week experimental period. The variation in Eu sorption with pH needs to be investigated using solutions in which only the pH is a variable. These tests need to have a short experimental duration to get around the problem of drifting pH.

In the interests of selecting Eu sorption data for performance assessment, the data from the experiments with conditioned solids were considered to be the most useful. The sorption data from these tests are summarized in Table 29 in the form of average  $K_d$  values determined with reaction times of 7 days. These average values include variability associated with changes in TDS, Ca/Na ratio, carbonate concentration and pH. These average values cover a pH range from 6.0 to 7.5, and ionic strengths of 0.2 to 7.5 (mol/kg). Europium sorption on shale and limestone was similar, and displayed limited variability with solution composition. Sorption on



bentonite was very sensitive to the total carbonate in solutions, and displayed significant variability with solution composition.

**Table 29: Average Eu Sorption  $K_d$  Values ( $\text{cm}^3/\text{g}$ ) for Brine Solutions**

<b>Mineral</b>	<b>Average</b>	<b>Geometric Mean</b>
Bentonite	2200 $\pm$ 3100	750 (7.7)
Shale	170 $\pm$ 50	160 (1.4)
Limestone	180 $\pm$ 100	160 (1.8)

Note: The standard deviation is given as the error for the average, and the geometric standard deviation is in parentheses beside the geometric mean.

## **5. MASS TRANSPORT EXPERIMENT**

The feasibility of performing mass transport experiments in a rock matrix was tested using the High Pressure Radioisotope Migration (HPRM) apparatus (Vilks and Miller, 2007). The HPRM was originally designed for performing radionuclide transport studies in unfractured rock core samples (Drew and Vandergraaf, 1989). More recently it has been used for estimating the permeability of the rock matrix (Vilks, 2007, Vilks and Miller, 2007, Vilks et al., 2003). The objective of this initial test was to use a sample of shale to develop the protocols for using tracers in the HPRM, evaluate the effect of pore fluid composition on permeability, and determine the practicality of using unfractured rock for transport experiments.

### **5.1 METHODS**

The HPRM consists of a core holder assembly, which is placed in a pressure vessel that can be operated with a maximum pressure of about 20 MPa. Core samples, with lengths of 2.0 cm, are placed between two stainless steel cylinders, each containing a centre drilled hole (1.6 mm diameter). The Queenston shale used in this test was a preserved sample taken from borehole DGR1 at the Bruce site. The shale was sub-sampled by drilling a core parallel to the bedding plane. The sample core diameter was 25 mm and the sample thickness was 6 mm. The rock's original moisture content was likely altered during the sub-sampling process. The core sample and stainless steel cylinders were coated with a pliable coating to isolate the circumference of the core from the water used as the pressure medium in the pressure vessel. Once the core and stainless steel cylinders were connected to the lines used to pass sample fluid through the core, the pressure vessel was assembled and partially filled with water. A confining pressure was applied to the pressure vessel, which subjected the core sample to a tri-axial pressure along its length and both ends. Water was then pumped through the core at a constant flow rate and the pressure differential between the inlet and outlet side of the core was measured. Provided that the inlet pressure is not allowed to exceed the confining pressure, water flow is always from the bottom end of the core to the top end, following the interconnected pore

spacings. The flow rate was determined by measuring the mass of water collected at the outlet over a given time interval.

The permeability of the core is given by

$$k = \frac{QL\mu}{A\Delta P} \quad (5)$$

where

- k is the permeability in  $m^2$ ,
- Q is the volumetric flow rate in  $m^3/s$ ,
- L is the length of the core in m,
- $\mu$  is the viscosity of the transport solution in  $N\cdot s/m^2$ ,
- A is the cross sectional area of the core in  $m^2$ , and
- $\Delta P$  is the pressure differential between the inlet and outlet of the core in  $N/m^2$ ;

In addition to sample dimensions, the parameters measured to calculate permeability consist of the volumetric flow rate, Q, which was determined by collecting water for a measured time period. The volume of collected water was determined gravimetrically using a balance that is checked with weights that have their mass traceable to an ASTM Class 1 calibrated weight set. The pressure drop across sample,  $\Delta P$ , was determined by a pressure transducer measuring the pressure of water being applied to one end of the sample. The pressure transducer was calibrated with a deadweight tester on a regular basis.

The confining pressure during the experiment varied from 3.6 to 7.5 MPa, and the pressure drop across the sample varied from 0.6 to 4.5 MPa. The test was started by pumping deionized water into the shale sample and collecting the eluted water in 0.6 mL centrifuge tubes. Permeability was measured as a function of time. The deionized water was replaced with 300 g/L TDS Na-Ca-Cl brine solution to measure changes in permeability and the chloride content of eluted water. Eventually, the injection solution was changed to a brine solution containing Sr and uranine dye.

## 5.2 RESULTS

The average flow rates of water through the rock sample varied from 0.004 to 0.05 mL/day. The variability in estimated permeability ( $m^2$ ) over a 5 month period is illustrated as a function of eluted water mass in Figure 28. The injection was switched to brine at a water mass of 0.51 g (red triangle), and the Sr and uranine labelled brine injection started at 2.81 g (blue triangle). Changing the injection solution from dilute water to brine did not have a significant effect on estimated permeabilities. However, the permeability decreased significantly after the injection of the brine with Sr and uranine. Since Sr is a Group 2 element, not significantly different from Ca, the decrease in permeability is probably caused by uranine. Uranine is an organic dye ( $C_{20}H_{10}NaO_5$ ) that could sorb and lead to plugging of pore spaces.

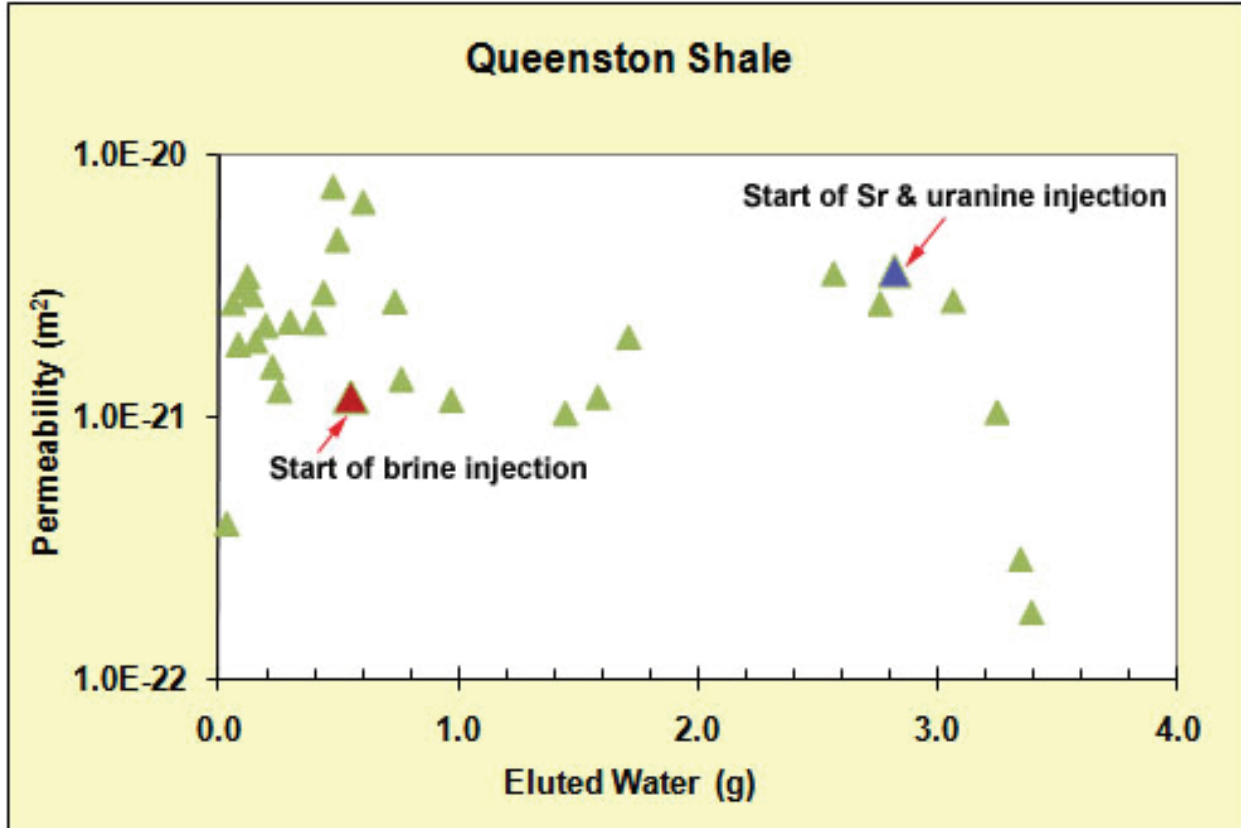


**Figure 28: Estimated Permeability as a Function of Eluted water**

The concentration of Cl<sup>-</sup> in eluted water is shown in Figure 29. The concentration of Cl<sup>-</sup> in the injected brine was 187 g/L. The brine injection started at 0.55 g and the Sr and uranine injection started at 2.81 g. The initial Cl<sup>-</sup> concentration in eluted water was rather high considering that deionized water was being injected. This high Cl<sup>-</sup> concentration probably resulted from the porewater of the shale core sample. The first breakthrough of higher Cl<sup>-</sup> was noted at  $0.27 \pm 0.03$  g after the start of brine injection (0.79 g of eluted water). The sample core volume was 2.945 cm<sup>3</sup>, based a core diameter of 25 mm and a core thickness of 6 mm. The average shale porosity is about 7%, giving the sample a pore volume of 0.21 cm<sup>3</sup>. The mass of brine in this volume is 0.25 g, based on a brine density of 1.213 g/cm<sup>3</sup>. Therefore, the mass of the first breakthrough of Cl<sup>-</sup> provided a good measure of porosity. The eluted Cl<sup>-</sup> concentrations did not get higher than 115 g/L, which is 61% of the Cl<sup>-</sup> concentration in the injected brine. This suggests that anion exclusion might be preventing a fraction of the Cl<sup>-</sup> from migrating through the shale matrix.

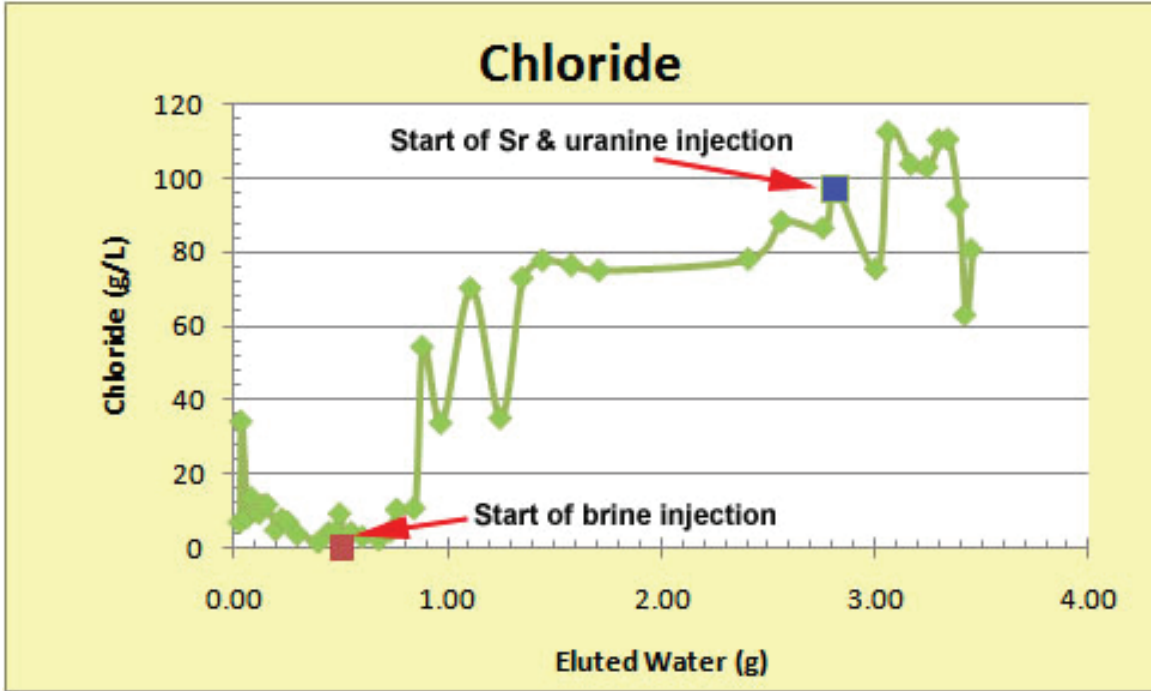


**Figure 29: Chloride Concentration as a Function of Water Mass Eluted from Shale Matrix**

The concentration of uranine injected along with Sr was 19 mg/L. The concentrations of eluted uranine as a function of eluted water mass are illustrated in Figure 30. The initial uranine concentration (0.53 mg/L) represents a background fluorescing compound that was flushed from the core sample. After that the background uranine concentration was about 0.05 mg/L. The first breakthrough of uranine above background occurred at  $0.39 \pm 0.04$  g after the start of the uranine and Sr injection (3.21 g of eluted water). However, the subsequent increase in uranine was very small, reaching only 0.6% of the injected concentration (0.11 mg/L) after 2.6 pore volumes since injection (3.45 g eluted water in Figure 30). This suggests that the time required for eluted uranine concentrations to reach 50% or 100% of the injection concentration would be much longer than available experimental time. However, for illustrative purposes the first arrival of uranine was compared to the first arrival of  $\text{Cl}^-$  (a conservative tracer) to estimate a retardation factor and  $K_d$  value for uranine.

In mass transport experiments that include advection one can compare the velocity of the sorbing tracer with the velocity water, as determined with a non-sorbing tracer. The following equation can be used for describing retardation in rocks with low porosity (Vilks, 2011).

$$R = \frac{v}{v_c} = 1 + \rho * K_d \quad (6)$$

Where

R = retardation factor

v = average linear water velocity (based on  $\text{Cl}^-$ )

$v_c$  = average linear velocity of sorbing contaminant (uranine)

$\rho$  = the bulk mass density of the media through which transport is taking place

Since the eluted pore water masses are inversely proportional to velocities, equation 6 may be rewritten as:

$$R = \frac{mass_{Cl}}{mass_{uranine}} = 1 + \rho * K_d \quad (7)$$

Where

R = retardation factor

mass<sub>Cl</sub> = water mass corresponding to first arrival of Cl

mass<sub>uranine</sub> = water mass corresponding to first arrival of uranine

Since the first arrival of Cl<sup>-</sup> occurred at  $0.27 \pm 0.03$  g, and the first arrival uranine was at  $0.39 \pm 0.04$  g, the retardation factor for uranine was 1.444. Using a bulk mass density of 2.66 for Queenston shale measured by the water immersion technique (Vilks and Miller, 2007), the K<sub>d</sub> value for uranine was calculated to be  $0.167 \pm 0.036$  cm<sup>3</sup>/g. Batch experiments of uranine sorption on dolomite, calcite and quartz in the presence of Dead Sea brine solution found sorption coefficients ranging from 1.5 to 0.09 cm<sup>3</sup>/g (Magal et al., 2008). Although not comparing the same solids, the above calculation demonstrates that reasonable sorption coefficients may be estimated from transport tests.

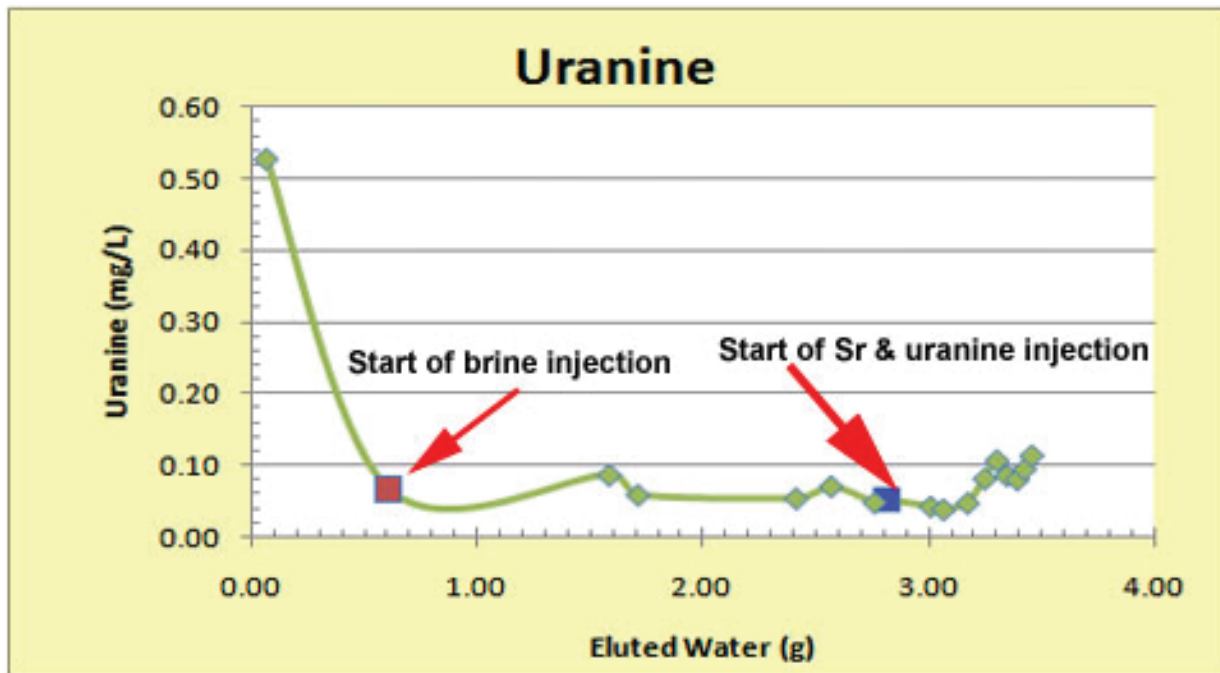


Figure 30: Concentration of Uranine in Water Eluted from Shale Matrix

## 6. DISCUSSION

One of the objectives of the first stage experimental program to explore sorption in brine solutions was to develop experimental protocols for performing batch sorption tests. The initial part of this chapter will discuss the factors that influence sorption measurements and that need to be considered in the formulation of experimental protocols. The actual experimental protocols are summarized in the Appendix of this report. The discussion will then focus on experimental results, discussing the effects of brine composition and sorption reversibility. A summary of preliminary sorption values for Sr(II), Ni(II), Cu(II), Eu(III) and U(VI) will be presented, and implications for radionuclide transport in brine solutions discussed.

### 6.1 DEVELOPMENT OF EXPERIMENTAL PROTOCOLS

The planning and execution of sorption tests requires consideration of a number of experimental factors, such as the solid/liquid ratio, pH, concentration range of sorbing element (sorbate), experimental time, and sample preconditioning. If an element is sorbed in a batch experiment, its concentration in solution will decrease by a few percent to 100 percent. The optimum experimental design will produce a drop in sorbate concentration that is just large enough to determine the amount sorbed with a minimum of error. Considering the uncertainty in the determination of dissolved element concentrations, the percent sorbed should be higher than 5 to 10 percent to obtain a reliable  $K_d$  value. If the reduction in sorbate concentration is large and approaches 100 percent, it will be difficult to establish the equilibrium dissolved concentration responsible for sorption. Not only will detection limits be a problem, but it may not be clear whether some of the sorption that took place was triggered by the initial high sorbate concentration at the start of the experiment. If reverse reactions are slow, the resulting sorption coefficient may not be representative of an equilibrium state.

*Solid/liquid ratio:* One can influence the drop in sorbate concentration by manipulating the solid/solution ratio in the experiment. If an element is sorbed very strongly, one could decrease the solid/liquid ratio to reduce the amount of sorbate removed from solution. Conversely, the solid/liquid ratio could be increased for elements that sorb with very low  $K_d$  values. Considering the results of initial sorption tests, solid/liquid ratios were adjusted for the final sorption tests using conditioned solids in 200 mL volumes. The respective solid/liquid ratios used for Ni sorption on bentonite, shale and limestone were 1.0, 4.0 and 8.0 g/100 mL. The ratios selected for U and Eu sorption on bentonite, shale and limestone were 0.5, 1.0 and 2.5 g/100 mL, respectively. In some cases, such as U sorption on limestone, a higher ratio (such as 8.0) may have improved results by increasing the percent sorbed.

Even when solid/liquid ratios have been adjusted to a range that gives good sorption values, further manipulation of solid/liquid ratios may contribute to variability in  $K_d$  values. In this study Eu  $K_d$  values decreased with increasing solid/liquid ratio for all solids. Eu sorption coefficients determined with a solid/liquid ratio of 2.5 g/100 mL were lower than those determined with a ratio of 0.25 g/100 mL by factors of 2 for bentonite, 3.5 for shale and 3.3 for limestone. Since the percent sorbed values were not high and the dissolved Eu concentrations were not a limit to sorption, it may be that some sorption sites were blocked at higher solid/liquid ratios by particle-particle interactions. Sorption on bentonite may be less affected by the solid/liquid ratio because bentonite has a very large surface area and/or bentonite particles were flocs, with internal sites that were not blocked by interactions with other particles. Changes in

experimental solid/liquid ratio have been reported to affect measured sorption coefficients in some cases. For example, Oscarson and Hume (1998) argued that the lower sorption coefficients for  $\text{Sr}^{2+}$  and  $\text{Cs}^+$  on bentonite at higher solid/liquid ratios were due to particle-particle interactions, which may lead to the blocking of some sorption sites. After presenting their work on Cd sorption on Fe oxyhydroxide and reviewing the literature, McKinley and Jenne (1991) argued that the reported “solids concentration” effect was caused by errors in data interpretation or experimental artefacts. Artefacts could include the release of colloids or complexing organics from the solids that reduce measured sorption by keeping the sorbate in solution, particularly with higher solids concentrations. Higher solids concentrations may promote coagulation that reduces the amount of accessible sorption sites. Changes in solution chemistry caused by varying the solids concentration would be another artefact.

*Element concentration:* The sorbate concentration range used in sorption experiments must strike a balance between the minimum concentration that can be detected with available methods and the maximum concentration that will produce precipitation. Sorption experiments must be performed with sorbate concentrations that are well below solubility limits. Otherwise they become precipitation experiments. Therefore, the solubility and chemical speciation of the sorbate must also be considered in experimental design. Evidence for precipitation in sorption experiments would be an increase in sorption coefficients with increases in sorbate concentration. Estimated  $K_d$  values that contain contributions from precipitation would be too high, and should not be used in performance assessment calculations.

Since the amount of surface or internal sites available for sorption on solids may be limited, increases in sorbate concentration will induce competition for these sites and may decrease the value of the estimated  $K_d$ . The variation of the amount sorbed with sorbate concentration is known as a sorption isotherm. Linear isotherms are described by sorption coefficients, whereas non-linear relations between the amount sorbed and sorbate concentration can be described with a number of different approaches, such as the Langmuir isotherm, Freundlich isotherm, and the Dubinin-Radushkevich isotherm (Vilks, 2009). If the sorbate concentration remains at trace levels, surface sites will likely not be fully occupied and the sorption isotherm will be linear, following Henry’s law.

The concentration of radionuclides released to groundwater would likely be at very low trace levels. If the element concentrations used in sorption experiments are low enough to produce linear isotherms, the resulting  $K_d$  values should accurately describe the sorption behaviour of the radionuclide in groundwater. However, if the experimental element concentration is higher than the radionuclide concentration and sorption is non-linear, the resulting  $K_d$  values will likely be lower than applicable to trace levels. These estimated  $K_d$  values would be conservative for application in performance assessment calculations.

*pH measurement and control:* The pH is an important parameter for sorption reactions. However, the measurement and control of pH in brine solutions poses certain problems that need to be considered. Glass pH electrodes provide a direct measurement of pH, which is defined as the negative logarithm of the hydrogen ion activity,  $[\text{H}^+]$ . In standard pH measurements the electrodes are calibrated with NBS reference buffer solutions with an ionic strength of 0.1 mol/L (Wu et al., 1988). In brine solutions the activity coefficient of the hydrogen ion becomes greater than one, resulting in higher  $[\text{H}^+]$  and lower pH values for a given  $\text{H}^+$  concentration. Ideally, the pH electrode should be able to follow the changes in  $[\text{H}^+]$  caused by increasing ionic strength. However, it is recognized that measurements of pH by glass pH electrodes in concentrated NaCl solutions may give a misleading low indication of pH and introduce errors of up to 0.2 pH units (Hinds et al., 2009). Sources of error include sodium error

and error associated with liquid junction potential. Sodium error occurs when the selectivity of  $H^+$  over  $Na^+$  breaks down as the  $[Na^+]$  becomes 10 orders of magnitude higher  $[H^+]$ , when the pH is greater than 10. Sodium error is not a factor in neutral pH ranges. Changes in the liquid junction potential caused by differences in the ionic diffusivity between the reference electrode and the sample solution are more likely to affect pH measurements in the pH ranges of interest for sorption studies.

Proposed solutions to improve pH measurements in brine solutions include the use of specialist buffers with ionic strengths that match those in the brines solutions being studied, and acid-base titrations at high and low pH in brine solutions to calibrate electrodes (Wiesner et al., 2006; Baumann, 1972). The challenge with these approaches is that they require activity coefficients for the  $H^+$  ion and ionic components of the pH buffers at high ionic strength. Calculated activity coefficients are model dependent. Activity coefficients estimated with Pitzer equations differ from those predicted by SIT (Specific Ion Interaction) theory. Therefore, electrodes calibrated with specialist buffers or acid titrations cannot be directly traced to the IUPAC (International Union of Pure and Applied Chemistry, Research Triangle Park, North Carolina) definition of pH, without making assumptions regarding activity coefficients. Consequently, in this study pH electrodes were only calibrated with NBS reference buffer solutions with an ionic strength of 0.1 mol/L, and no attempt was made to use buffers with a higher ionic strength.

Many sorption studies have been performed over a wide pH range in order to define the sorption edge, which marks the pH interval where there is a dramatic increase in sorption as a result of surface charge reversal or deprotonation of surface complexation sites. The challenge with performing sorption experiments over an extended time period at a controlled pH value is that the bentonite, shale and limestone strongly buffer the pH of experimental solution to values that are determined by brine composition and reactions with carbonate and silicate surfaces. The additions of acid or base to counter this buffering and to control the pH, will change the sorbing surfaces with time. The use of pH buffers could control pH, but might also influence the sorption process and would have to be considered in any efforts to model sorption by surface complexation. Another option is to use a short experimental time (one to several hours as opposed to days and weeks) to avoid significant pH drift.

*Sorption time:* When designing sorption tests one needs to decide what is an appropriate experimental time. In this study the  $K_d$  values of Ni, U and Eu displayed variations with time that are typical of many sorption reactions (Vilks, 2009). There was an initial sorption jump defined by the shortest reaction time (1 hour in this study), followed by a period of relatively rapid sorption increase lasting several days. This was usually followed by a slow upward drift in pH that in some cases reached a steady state after 1 to 2 weeks.

Most studies of metal sorption on soil materials revealed that two or more sorption rates are controlling the metal uptake, suggesting that more than one mechanism is responsible for sorption (Vilks, 2009). Some studies, which have used fast measuring techniques, have reported instantaneous sorption reactions. These very fast sorption reactions may have similar rates to acid-base or complex formation reactions in solution. They have been also attributed to ion exchange and are probably limited by film or particle diffusion. Some of the slow reactions are believed to result from surface precipitation, fixation reactions or even structural penetration. Other explanations for slow long-term sorption reactions could be changes in mineral surfaces caused by alteration by the experimental solutions, or perhaps microbial effects. Desorption times ranged from minutes to over a hundred days.



The half lives for various sorption mechanisms reported in the literature vary from instantaneous to many days. The reported rates will of course be a function of the sorbate and sorbent used in the study. However, experimental conditions will also influence the observed sorption kinetics because factors such as ionic medium and pH can determine which mechanism(s) will control the overall sorption rate. The method of measuring sorption will also influence the observed kinetics. If samples have to be separated by filtration or centrifugation, the very fast mechanisms cannot be followed. Also, errors introduced by the separation process may mask subtle changes produced by very slow reactions. The use of specific ion electrodes or conductivity measurements is essential to follow very fast kinetics. Copper sorption can be followed with electrodes, but not in solutions with high  $\text{Cl}^-$  concentrations used in this study.

Given that sorption processes are likely controlled by several rates, corresponding to different processes, one must consider several factors in choosing an appropriate experimental time frame. Is a steady-state in sorption values achieved and how close to the steady-state value can we get with a sorption time that is practical to achieve experimentally? Is the stability of the solid surface towards chemical alteration likely to be a problem in long-term sorption tests? Would the experimental time frame be appropriate for the sorption mechanisms of interest? The other important consideration is whether or not the measured sorption values are conservative for application in performance assessment. It would be better to use the lower sorption values derived from short-term tests rather than use higher values from longer term tests where processes contributing to sorption are poorly understood. In this study the reference sorption time for defining  $K_d$  values was selected as 7 days to ensure that processes associated with surface complexation are complete and to avoid the risk of reporting high values that might have been caused by surface precipitation, structural penetration, or a surface weather process. These values are considered to be conservative since they are lower than values observed over extended time periods.

*Sample preconditioning:* Since the crushed rock has freshly exposed surfaces with broken bonds, it is sometimes deemed necessary to condition the solid material by exposing it to the experimental ionic medium before starting sorption tests (Ticknor et al., 1996). In this study it was assumed that a 1 week contact would be sufficient to condition these sites and make the rock samples more representative of in-situ conditions. A comparison of Ni  $K_d$  values for bentonite, shale and limestone in 10 and 300 g/L brine solutions indicated sorption on conditioned solids was reduced by factors of 2 to 7. However, U sorption on bentonite in 300 g/L brine was not significantly different for conditioned solids. Comparisons for U sorption on the other solids, and for Eu sorption were not possible due to significant differences in other experimental factors such as solid/liquid ratios and sorbate concentrations. In summary, the conditioning of crushed solids with experimental solutions affects sorption results for some elements. Therefore, preconditioning has been adopted as a standard procedure for future experiments.

## 6.2 SORPTION RESULTS

*Sorption and brine composition:* Strontium was not observed to sorb on bentonite or sedimentary rocks in the Na-Ca-Cl brine solution because it could not compete with the dissolved  $\text{Ca}^{2+}$  concentration, which exceeded that of  $\text{Sr}^{2+}$  by 3 to 4 orders of magnitude. One could argue that the solid/liquid ratio should have been increased in an attempt to determine whether a small amount of  $\text{Sr}^{2+}$  actually does sorb. The problem with that is that bentonite and sedimentary rocks contain  $\text{Sr}^{2+}$  as part of their natural composition. Leaching experiments with

deionized water showed that this  $\text{Sr}^{2+}$  is 58% leachable from bentonite, 31% from shale and 10% from limestone (Table 4). When these solids were contacted with 300 g/L brine during the sorption tests the  $\text{Sr}^{2+}$  concentration of the brine actually increased due to the release of  $\text{Sr}^{2+}$  from the solids. Bentonite released about 180 to 200 mg/kg (ppm)  $\text{Sr}^{2+}$  by a cation exchange reaction, probably with  $\text{Ca}^{2+}$ , and to a lesser extent  $\text{Na}^+$ , in the brine. The amounts of  $\text{Sr}^{2+}$  leached from shale and limestone were 0 to 60 mg/kg and 0 to 20 mg/kg, respectively. Although limestone has the highest  $\text{Sr}^{2+}$  concentration, most of this  $\text{Sr}^{2+}$  is likely trapped within carbonate minerals and is not exchangeable. These results indicate that  $\text{Sr}^{2+}$  sorbs mainly by nonspecific cation exchange, and is not able to compete with the high concentration of  $\text{Ca}^{2+}$  in the brine. Consequently, group 1 and 2 elements are not expected to be sorbed by sedimentary rocks in concentrated brine solutions and without more data it should be assumed that elements, such as  $\text{Ra}^{2+}$ , have a  $K_d$  of 0 in brine solutions.

The sorption of Ni, Cu, Eu and U was affected by solution composition. It should be remembered that in this study pH and salt concentration were not independent variables because the solids buffered the pH to values that depended upon the salt concentration. Therefore, the observations in the following discussions regarding the effects of pH and solution composition are still speculative and need to be confirmed by sorption experiments where pH effects are isolated from the effects of solution composition (salt and carbonate concentration). The effect of pH needs to be addressed by performing sorption tests over a wide pH range for a given brine composition.

The presence of Ca in Na-Ca-Cl brines was shown to reduce Ni sorption by a factor 2 to 7 compared to sorption in Na-Cl brines. Ca likely has a similar effect on Cu. Nevertheless, pH probably had a more important effect than salt concentration on the variability of Ni and Cu sorption. This conclusion is based on observed variations with pH in this study and by the argument that the mass action of salt had probably already suppressed non-specific coulombic attraction in the solution with the lowest TDS. If further increases in salt concentration had no further effect on non-specific sorption, it follows that Ca must compete with Ni for surface complexation sites.

The sorption of metals is very pH dependent (Figure 31), often with sharp increases in sorption between pH 4 and 8. This phenomenon was described for transition metal sorption on oxides of Si, Al, Fe, and Mn by Kurbatov et al. (1951), Dugger et al. (1964), Grimme (1968), James and Healy (1972), Schindler et al. (1976), and Hohl and Stumm (1976). A similar sorption relationship with pH has also been described for clays by Hodgson (1960), O'Connor and Kester (1975), Payne and Pickering (1975), and Farrah and Pickering (1976a, 1976b, 1979). This sharp increase in sorption for a given element over a narrow pH range has been called the sorption edge. At very high pH sorption may decrease again because of the formation of soluble hydroxyl species. The effect of pH on the sorption of a given metal depends upon which mineral is controlling the sorption. For example, sorption on kaolinite and illite is more affected by pH than sorption on montmorillonite. The pH may affect sorption by (1) the effect of  $\text{H}^+$  as a counter ion in non-specific adsorption, (2) the dependence of some surface charges on pH, (3) the dissolution of Al at low pH, and (4) the effect of  $\text{H}^+$  on the complexing capability of surface sites and the precipitation of hydroxides. In brine solutions with mid-pH values, only the latter phenomenon is likely to be important. The sorption edge for different metals occurs at different pH values, which would not be the case if the sorption jump was caused by a change in the surface charge. The cations with the strongest hydrolysis constants have their sorption jumps at lower pH values, suggesting the formation of metal oxygen bonds. These sorption jumps cannot be explained as simple hydroxide precipitation since metal solubility was not exceeded in the bulk solution. The presence of complexing ligands will complicate sorption reactions,

particularly their relationship to pH (Farrah and Pickering, 1977). Ligands can reduce sorption by keeping a metal in solution or they may enhance adsorption if the ligand has an affinity for the surface.

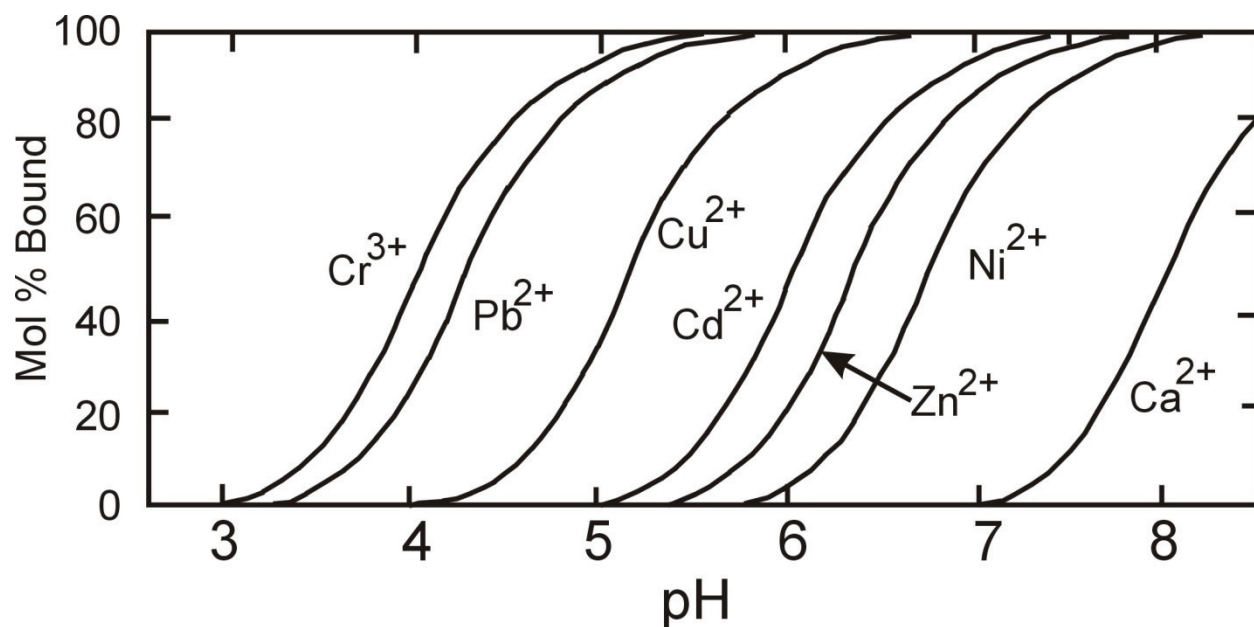


**Figure 31: The pH Dependence of Metal Sorption on Fe Oxide (After Stumm, 1992)**

The sorption edge for Ni on Fe oxide (Figure 31) corresponds to the pH range observed in the experiments with sedimentary rocks in brine. Therefore, it was not surprising to observe an increase in Ni sorption over this pH range. However, based on Figure 31 one could have expected the Cu sorption edge to have reached its maximum sorption values by pH 6. Apparently this was not the case as the sorption edge for Cu on sedimentary rocks in brine solution occurred in a similar pH range as for Ni.

The sorption of U and Eu appeared to be independent of pH (within the experimental pH range), except when sorption was affected by complexation with carbonate in solution. The reported sorption of U(VI) on montmorillonite and illite reached a maximum in the pH range 6 to 7 (Bradbury and Baeyens, 2005 and 2009b). However, Eu sorption on montmorillonite and illite in this pH range should increase with pH (Bradbury and Baeyens, 2005 and 2009a). The sorption of Eu and U was not affected by salt concentration, confirming that sorption is by surface complexation. The sorption test using Na-Cl brine failed to demonstrate that U sorption was not affected by Ca, because the higher concentration of carbonate in the Na-Cl brine reduced U sorption.

*Reversibility:* Based on a comparison of  $K_d$  values before and after desorption, Ni sorption was the least reversible on shale, followed by limestone and bentonite. The  $K_d$  values decreased during the first 3 days of desorption, after which the  $K_d$  values started to increase indicating that desorption was complete. The steady-state respective Ni  $K_d/K_d^0$  values for shale, limestone and bentonite were 50, 30 and 5. Europium desorption  $K_d$  values remained constant during the two week period, suggesting irreversible sorption for long time periods. There is a weak indication

that Eu sorbed on bentonite may eventually return to equilibrium, but Eu sorbed to shale and limestone appear likely to remain fixed for years. The respective  $K_d/K_d^0$  values for Eu after two weeks for limestone, shale and bentonite were 5, 4, and 3. The trend in U  $K_d/K_d^0$  values with desorption time indicated that U sorption was reversible. Exponential extrapolations suggest that the times to return to equilibrium were 12 days for bentonite, 20 days for shale and 30 days for limestone. At 7 days the respective  $K_d/K_d^0$  values for limestone, shale and bentonite were 71, 9 and 4. In summary, the reversibility of sorption reactions depends very much on the sorbing element. In this study the only element (U) whose sorption was reversible had a solution chemistry dominated by negatively charged carbonate species. The other elements were dominated by a few cationic species.

The question of reversibility should be considered in the planning of batch sorption tests. If sorption is not reversible or is slow to reach equilibrium, one should avoid very large decreases in sorbate concentrations because the amount of sorbed element could reflect a higher sorbate concentration than was determined as the equilibrium value at the end of the sorption test. This would lead to high, nonconservative  $K_d$  values. When  $K_d$  values are used to estimate the effects of sorption in mass transport calculations it is assumed that the  $K_d$  values represent sorption process that are reversible over the time scale of the mass transport calculations. If sorption is not reversible the actual radionuclide transport will be significantly reduced compared to the results of transport simulations. The results of this study suggest that mass transport experiments with Ni or Eu, that last several weeks, could be affected by irreversible sorption. The transport of U(VI) is much less likely to be affected by irreversible sorption. Irreversibility in the lab does not necessarily mean that sorption is irreversible over geologic time scales. Given that sorption is probably reversible over very long time periods and that the assumption of reversibility is conservative, the continued use of  $K_d$  values in long time scale performance assessment calculations is justified.

*Mass transport:* The mass transport experiment with shale, using the HPRM, demonstrated that it is possible to observe mass transport through the rock matrix. However, the experimental time frame is prohibitively long and not practical for any more than one or two samples. The use of cores with a fracture, or columns of crushed rock would be more practical because it would be possible to transport a pore volume of solution through the system in a matter of hours or days.

*Summary of sorption values relevant to sedimentary rocks and brine solutions:* The sorption coefficients of the elements included in this study are summarized in Table 30 in terms of the total range in values, along with the geometric mean and geometric standard deviation. Since the reference sorption time was 7 days, one must keep in mind that  $K_d$  values could be higher if longer sorption times are considered. The variability in the  $K_d$  values in Table 30 due to the different experimental solution compositions which cover a pH range from 6.0 to 7.5, and ionic strengths of 0.2 to 7.5 (mol/kg). The total carbonate concentration ranged from  $5 \times 10^{-5}$  to  $8 \times 10^{-3}$  mol/L. Since the experimental solutions covered the range of brine compositions (in terms of TDS, pH and carbonate concentrations) that could be expected in sedimentary rock, the observed variability in  $K_d$  values is probably a good indicator of variability that is likely to be observed under in-situ conditions.

**Table 30: Summary of Element Sorption Coefficients (cm<sup>3</sup>/g)**

Element	Bentonite		Shale		Limestone	
	Range	Geomean	Range	Geomean	Range	Geomean
Sr(II)	0	0	0	0	0	0
Ni(II)	22 - 82	42 (2)	6 - 47	16 (3)	0.4 - 8.0	2.2 (4)
Cu(II)	6.5 - 256	22 (4)	0- 489	8 (23)	0.2 - 123	10 (12)
Eu(III)	97 - 5700	750 (8)	108 - 215	160 (1)	93 - 293	160 (2)
U(VI)	14 - 565	130 (7)	1.7 - 51	10 (6)	2 - 17	6 (3)

Note: The geometric standard deviation is in parenthesis beside the geometric mean.

The sorption values in Table 30 demonstrate that a number of elements, including divalent metals, trivalent rare earth elements and hexavalent uranium, will sorb on sedimentary rocks in the presence of concentrated Na-Ca-Cl brine solutions despite the mass action effect of the salt. If the geometric mean is used as a reference, sorption coefficients on bentonite were always higher than on shale or limestone. This is expected given that the surface area of bentonite is a factor 2.2 to 8.6 higher than the surface areas of shale and limestone. One would anticipate that sorption on limestone would be very low due to the very low clay content. However, Cu(II) sorbed more strongly on limestone, while the sorption of the other elements on limestone was only slightly lower than on shale. This indicates that calcite, the main component of limestone, was able to sorb Ni, Cu, Eu and U, by complexation to surface carbonate sites or by incorporating these elements into the calcite structure. In summary, sorption onto bentonite, shale and limestone will be an effective retardation mechanism for the transport of a number of radionuclides from a deep geologic repository hosted in sedimentary rocks containing brine solutions.

*Moving Forward:* Since sorption is influenced by solution parameters such as pH, Eh, and carbonate concentration, surface complexation modelling by PHREEQC is required to account for these parameters and to extrapolate measured sorption data to other solution compositions. For modelling purposes there is a need to have sorption data over a pH range from 5-8 to better define surface complexation reactions. These tests need to be short term to avoid altering rock surfaces and drastic pH shifts between the start and finish of the experiments.

Furthermore, our understanding of sorption processes in brine solutions is not complete with respect to kinetics. While the sorption of some elements such as U and Eu appears to reach a plateau after 1 to 2 weeks, the sorption of other elements, such as Ni, continues to change for periods that may exceed 4 weeks. Therefore, it would be useful to perform long-term tests to study the effect of sorption time over extended time periods of several months. In addition, more detailed desorption experiments should be performed to focus on the effects of sorption time on sorption reversibility, which is important for understanding the effect of sorption on mass transport.

Although the high brine concentrations may not be favourable to microbial growth, it remains to be demonstrated that microbes do not affect sorption results, particularly over long time periods. Microbes could influence the pH and redox of the experimental system. The redox change could go unnoticed and might influence the sorption of redox sensitive elements. Microbes

could release organic complexes that could alter the aqueous speciation of elements being studied. Microbial cells could sorb the element being studied. If the cells stay in suspension the apparent sorption will be reduced, but if the cells form a biofilm on mineral surfaces sorption would be increased. If microbial cells are able to metabolize metals on solid surfaces, there is a potential for breaking down solid surfaces and releasing adsorbed elements with time. The actual impact of microbial growth on sorption experiments with brine solutions is not known. Therefore, a number of control sorption tests should be repeated under sterile conditions, taking care to ensure that the sterilization procedure does not alter the geologic material in any way. The results of the control tests should be compared to the normal tests to confirm whether or not microbes have had any affect.

## 7. CONCLUSIONS

Protocols for batch sorption tests to be performed with Na-Ca-Cl brine solutions have been developed and are summarized in Appendix A. These include guidelines for experimental configurations, solid/liquid ratios, phase separation methods and sorption time scales. Analytical capabilities were defined along with reasonable sorbate concentration ranges. The sorption of Sr(II), Ni(II), Cu(II), Eu(III) and U(VI) was characterized on bentonite, shale and limestone in Na-Ca-Cl brine solutions with TDS values as high as 300 g/L. Preliminary recommendations for sorption coefficients applicable to sedimentary rocks were suggested. The results demonstrate that radionuclides will sorb in the presence of brine solutions, and that although bentonite has the highest sorption capacities, both shale and limestone are likely to sorb significant amounts of radionuclides.

Strontium sorption was not observed in brine solutions, indicating that sorption coefficients for group 1 and group 2 elements, such as radium, should be assigned values of 0 for sedimentary rocks that are in contact with brine solutions. Transition metals, such as Ni(II) and Cu(II), and the trivalent Eu(III) and hexavalent U(VI) sorb by surface complexation mechanisms to bentonite, shale and limestone. The sorption of Ni(II) and Cu(II) increases with pH in the pH range 6.0 to 7.5. The relatively high concentrations of Ca(II) compete with Ni(II) for sorption sites. The sorption properties of Eu(III) and U(VI) appeared not affected by pH in the pH range of 6.0 to 7.5. The formation of complexes with carbonate reduced the sorption of both of these elements and in the case of Eu(III) likely masked its expected increase in sorption with higher pH. It should be noted that in Na-Ca-Cl brines carbonate concentrations will be at a minimum due to calcite precipitation. As a result, U(VI) and Eu(III) sorption will be higher in Na-Ca-Cl brines despite any competition with Ca(II).

Although Ni(II) sorption was 70 to 90 percent complete after 1 week, Ni(II) continued to sorb at a slow rate and probably did not reach steady-state until after 4 weeks. The sorption of Eu(III) and U(VI) appeared to reach a steady-state after 1 to 2 weeks, although Eu(III) sorption on limestone may have continued for longer than 4 weeks in some cases. Although the sorption of U(VI) appeared to be reversible over a several week period, the sorption of Ni(II) and Eu(III) was irreversible within a two week period. The issue of irreversible sorption has a greater impact on experimental design and the interpretation of laboratory transport experiments, than on performance assessment calculations considering geologic time scales.

## **ACKNOWLEDGEMENTS**

Randy Herman and Chantelle Kryschuk (Analytical Science Branch, Whiteshell Laboratories) performed ICP analyses of Sr, Cu and Ni. Peter Hayward was contracted to perform thermal analyses of bentonite, shale and limestone samples, as well as tests to determine the leachability of selected elements that could affect sorption measurements. Tammy Yang, Sarah Hirschorn, Monique Hobbs and Jennifer McKelvie of NWMO provided fruitful discussion and review.

## REFERENCES

- Barone, F.S., R.K. Rowe and R.M. Quigley. 1990. Laboratory determination of chloride diffusion coefficients in an intact shale. *Can. Geotech.*, 27, 177-184.
- Baumann, E. 1973. Determination of pH in concentrated salt solutions. *Analytica Chimica Acta*, 64, 284-288.
- Benbow, S., R. Metcalfe and J. Wilson. 2008. Pitzer databases for use in thermodynamic modelling. Nuclear Waste Management Organization Technical Memorandum (QRS-3021A-TM1) Version: 1.0. Toronto, Canada.
- Bradbury, M.H., B. Baeyens and T. Thoenen. 2010. Sorption data bases for generic Swiss Argillaceous Rock Systems. Nagra Technical Report 09-03, Switzerland.
- Bradbury, M.H. and B. Baeyens. 2010. Comparison of the reference Opalinus clay and MX-80 bentonite sorption data bases used in the Entsorgungsnachweis with sorption data bases predicted from sorption measurements on illite and montmorillonite. Nagra Technical Report 09-07, Switzerland.
- Bradbury, M.H. and B. Baeyens. 2009a. Sorption modelling on illite Part I: Titration measurements and the sorption of Ni, Co, Eu and Sn. *Geochimica et Cosmochimica Acta*, 73, 990-1003.
- Bradbury, M.H. and B. Baeyens. 2009b. Sorption modelling on illite Part II: Actinide sorption and linear free energy relationships. *Geochimica et Cosmochimica Acta*, 73, 1004-1013.
- Bradbury, M.H. and B. Baeyens. 2005. Modelling the sorption of Mn(II), Co(II), Ni(II), Zn(II), Cd(II), Eu(III), Am(III), Sn(IV), Th(IV), Np(V) and U(VI) on montmorillonite: Linear free energy relationships and estimates of surface binding constants for some selected heavy metals and actinides. *Geochimica et Cosmochimica Acta*, 69, 875-892.
- Bradbury, M.H. and B. Baeyens. 2003. Near-Field Sorption Data Bases for Compacted MX-80 Bentonite for Performance Assessment of a High-Level Radioactive Waste Repository in Opalinus Clay Host Rock. NAGRA Technical Report 02-18.
- Brunauer, S., P.H. Emmett and E. Teller. 1938. *Journal American Chemical Society*, 60, 309-319.
- Davis, J.A., M. Ochs, M. Olin, T.E. Payne and C.J. Tweed. 2005. NEA Sorption Project Phase II. Interpretation and prediction of radionuclide sorption onto substrates relevant for radioactive waste disposal using thermodynamic sorption models. OECD, NEA No. 5992.
- Drew, D.J. and T.T. Vandergraaf. 1989. Construction and operation of a high-pressure radionuclide migration apparatus. Atomic Energy of Canada Limited Technical Record, TR-476.
- Dugger, D.L., J.H. Stanton, B.N. Irby, B.L. McConnell, W.W. Cummings and R.W. Mautman. 1964. The exchange of twenty metal ions with the weakly acidic silanol group of silica gel. *Journal of Physical Chemistry*, 68, 757-760.



- Earnest, C.M. 1991. Thermal analyses of selected illite and smectite clay minerals. PartII. Smectite clay minerals. In W. Smykatz-Kloss and S.St.J. Warne (eds.), Thermal Analysis in the Geoscience, Springer-Verlag.
- Elizalde, M.P. and L. Aparicio. 1995. Current theories in the calculation of activity coefficients – II Specific interaction theories applied to some equilibria studies in solution chemistry. *Talanta*, 42, 395-400.
- Farrah, H. and W.F. Pickering. 1979. pH effects in the adsorption of heavy metal ions by clays. *Chemical Geology*, 25, 317-326.
- Farrah, H. and W.F. Pickering. 1977. Influence of clay-solute interactions on aqueous heavy metal ion levels. *Water, Air and Soil Pollution*, 8, 189-197.
- Farrah, H. and W.F. Pickering. 1976a. Sorption of copper species by clays. I Kaolinite. *Australian Journal of Chemistry*, 29, 1167-1176.
- Farrah, H. and W.F. Pickering. 1976b. Sorption of lead and cadmium species by clay minerals. *Australian Journal of Chemistry*, 30, 1417-1422.
- Grimme, R.E. 1968. *Clay Mineralogy*. 2nd ed., McGraw-Hill.
- Gu, X., L. Evans, and S.J. Barabash. 2010. Modeling the adsorption of Cd (II), Cu(II), Ni(II), Pb(II) and Zn(II) onto montmorillonite. *Geochimica et Cosmochimica Acta*, 74, 5718-5728.
- Hinds, G., P. Cooling, A. Wain, S. Zhou and A. Turnbull. 2009. Technical Note: Measurement of pH in concentrated brines. *Corrosion*, 65, 635-638.
- Hodgson, J.F. 1960. Cobalt reactions with montmorillonite. *Soil Science Society Proceedings*, 29, 165-168.
- Hohl, H. and W. Stumm. 1976. Interaction of Ph(II) with hydrous Al<sub>2</sub>O<sub>3</sub>. *Journal of Colloid and Interface Science*, 55, 281-288.
- James, R.O. and T.W. Healy. 1972. Adsorption of hydrolyzable metal ions to the oxide-water interface. *Journal of Colloid and Interface Science*, 40, 65-81.
- Johnson, D.A. and T.M. Florence. 1971. Spectrophotometric determination of uranium(VI) with 2-(5-bromo-2-pyridylazo)-5-diethylaminophenol. *Analitica Chimica Acta*, 53, 73-79.
- Kurbatov, M.H., G.B. Wood and J.D. Kurbatov. 1951. Isothermal adsorption of cobalt from dilute solutions. *Journal of Physical Chemistry*, 55, 1170-1182.
- Lajudie, A., J. Raynal, J-C. Petit and P. Toulhoat. 1995, Clay-based materials for engineered barriers: A review. In *Materials Research Society Symposium Proceedings*, V 353.
- Liu, J. and I. Neretnieks. 2006 Physical and chemical stability of the bentonite buffer, SKB Report R-06-103.

- Magal, E., N. Weisbrod, A. Yakirevich and Y. Yechieli. 2008. The use of fluorescent dyes as tracers in highly saline groundwater. *Journal of Hydrology*, 358, 124-133.
- Marczenko, Z. and M. Balcerzak. 2000. Separation, preconcentration and spectrophotometry in inorganic analysis. *Analytical Spectroscopy Library – 10*, Elsevier.
- McKinley, J. P. and E. A. Jenne. 1991. Experimental Investigation and Review of the “Solids Concentration” Effect in Adsorption Studies. *Environmental Science and Technology*, 25, 2082-2087.
- Morton, J.D., J.D. Semrau and K.F. Hayes. 2000. Structure and reversibility of copper adsorbed by montmorillonite clay. In *Chemical Speciation and Reactivity in Water Chemistry and Water Technology; A symposium in Honor of James J. Morgan.*, American Chemical Society, Washington, D.C., p 650-652.
- NWMO. 2011. OPG’s Deep Geologic Repository for Low & Intermediate Level Waste. Geosynthesis. Nuclear Waste Management Organization, NWMO DGR-TR-2011-11 (Available at [www.nwmo.ca](http://www.nwmo.ca)).
- NWMO. 2005. Choosing a way forward. The future management of Canada’s used nuclear fuel. Nuclear Waste Management Organization (Available at [www.nwmo.ca](http://www.nwmo.ca)).
- Ochs, M., J.A. Davis, M. Olin, T.E. Payne, C.J. Tweed, M. Askarieh and S. Altmann. 2006. Use of thermodynamic sorption models to derive radionuclide  $K_d$  values for performance assessment: selected results and recommendations of the NEA sorption project. *Radiochimica Acta*, 94, 779-785.
- O'Connor, T.P. and D.R Kester. 1975. Adsorption of copper and cobalt from fresh and marine systems. *Geochimica et Cosmochimica Acta*, 39, 1531-1543.
- Oscarson, D. W. and H. B. Hume. 1998. Effect of solid: Liquid ratio on the sorption of  $Sr^{2+}$  and  $Cs^+$  on bentonite. In *Adsorption of Metals by Geomedia. Variables, Mechanisms, and Model Applications*, E. A. Jenne (ed.), p. 277-289, Academic Press, San Diego, California.
- Parkhurst, D.L. and C.A.J. Appelo. 1999. User’s guide to PHREEQC (Version2)-A computer program for speciation, batch-reaction, one-dimensional transport, and inverse geochemical calculations: U.S. Geological Survey Water-Resources Investigations Report 99-4259, 310 p.
- Payne, K. and W.F. Pickering. 1975. Influence of clay-solute interactions on aqueous copper ion levels. *Water, Air, and Soil Pollution*, 5, 63-69.
- Rüegger, B. and K.V. Ticknor. 1992. The NEA sorption database (SDB). In *Radionuclide Sorption from the Safety Evaluation Perspective. Proceedings of an NEA Workshop*, Interlaken, Switzerland, 1991, 57-78.
- Schindler, P.W., B. Fuerst, P.V. Wolf and R. Dick. 1976. Ligand properties of surface silanol groups. (1) Surface complex formation with Fe(III), Cu(II), Cd(II), and Pb(II). *Journal of Colloid and Interface Science*, 55, 469-475.

- Stumm, W. 1992. *Chemistry of the Solid-Water Interface*. John Wiley & Sons, Inc., New York, Chichester, Brisbane, Toronto, Singapore.
- Stumm, W. and J.J. Morgan. 1981. *Aquatic Chemistry An Introduction Emphasizing Chemical Equilibria in Natural Waters*. John Wiley & Sons.
- Ticknor, K.V., T.T. Vandergraaf, J. McMurry, L. Boisvenue, and D.L. Wilkin. 1996. Parametric studies of factors affecting Se and Sn sorption. Atomic Energy of Canada Ltd. Technical Record, TR-723.
- USEPA (United States Environmental Protection Agency). 1998. Technical support document for Section 194.14: Assessment of Kds used in the CCA. DOCKET NO: A-93-02 V-B-4.
- Vilks, P. 2011. Sorption of selected radionuclides on sedimentary rocks in saline conditions – literature review. Nuclear Waste Management Organization Technical Report NWMO TR-2011-12 (in progress).
- Vilks, P. 2009. Sorption in highly saline solutions – state of the science review. Nuclear Waste Management Organization Technical Report NWMO TR-2009-18, (Available at [www.nwmo.ca](http://www.nwmo.ca)).
- Vilks, P., and N.H. Miller. 2007. Evaluation of experimental protocol for characterizing diffusion in sedimentary rocks. Nuclear Waste Management Organization Technical Report NWMO TR-2007-11 (Available at [www.nwmo.ca](http://www.nwmo.ca)).
- Vilks, P. 2007. Forsmark site investigation. Rock matrix permeability measurements on core samples from borehole KFM01D, SKB Report P-07-162, ISSN 1651-4416.
- Vilks, P., N.H. Miller and F.W. Stanchell. 2004. Phase II in-situ diffusion experiment. Ontario Power Generation Report 06819-REP-01200-10128-R00.
- Warnecke, E., A. Hollmann, G. Tittel and P. Brennecke. 1994. Gorleben radionuclide migration experiments: more than 10 years of experience. *Radiochimica Acta*, 66/67, 821-827.
- Wiesner, A.D., L.E. Katz and C.-C. Chen. 2006. The impact of ionic strength and background electrolyte on pH measurements in metal ion adsorption experiments. *Journal of Colloid and Interface Science*, 301, 329-332.
- Wu, Y.C., W.F. Koch, and R.A. Durst. 1988. Standardization of pH Measurements. NBS Special Publication 260-53, U.S. Department of Commerce / National Bureau of Standards, Gaithersburg, MD, 20899.
- Zazzi, A. 2009. Chlorite: Geochemical Properties, Dissolution kinetics and Ni(II) sorption. Doctoral Thesis in Chemistry, Royal Institute of Technology, Stockholm, Sweden.



**APPENDIX A: PROTOCOLS USED IN SORPTION EXPERIMENTS**

**CONTENTS**

	<b><u>Page</u></b>
A.1 SORPTION TEST – SMALL VOLUME .....	89
A.2 SORPTION TEST – LARGE VOLUME .....	92
A.3 DESORPTION TEST .....	95
A.4 NICKEL ANALYSIS – BROMO-PADAP COLORIMETRIC METHOD .....	97
A.5 URANIUM ANALYSIS – BROMO-PADAP COLORIMETRIC METHOD .....	99
A.6 EUROPIUM ANALYSIS – FLUORESCENCE .....	101



## A.1 SORPTION TEST – SMALL VOLUME

### Introduction

This protocol describes the general method for determining a single sorption measurement in the form of a sorption coefficient ( $K_d$ ). The main applications for this method include the study of the effect of pH on sorption (current work), and the evaluation of the effects of salt concentration, solid/liquid ratio, sorption time, and sorbent concentration on sorption (previous work). With this protocol a solution containing a known concentration of sorbate is contacted with a sorbing solid for a given time period. At the completion of the sorption test, the solution is separated from the solid and analyzed to determine the decrease in sorbate concentration. This decrease in sorbate concentration is used to calculate the amount of sorbate that has sorbed to the solid and to determine a  $K_d$  value. The solid and solution are not used for further experiments.

### Definitions

*Sorbent*: the rock or mineral whose sorption properties are being studied

*Sorbate*: the element whose sorption properties are being studied

*Ionic medium*: the solution in which sorption is being studied. For example, the 300 g/L Na-Ca-Cl brine.

*Blank test*: the sorption test without a sorbent that is used to account for sorbate losses to vessel walls, and to precipitation in case predicted solubility limits were not accurate.

*Reaction vessel*: the container used to hold the sorbent and reaction solution.

### Materials

- Powdered rock sample (such as bentonite, shale, limestone) that has been sized to between 100 and 200  $\mu\text{m}$  by dry sieving.
- Brine solution prepared from reagent grade  $\text{CaCl}_2$  and  $\text{NaCl}$ , and deionized water.
- The *reaction vessels* are polycarbonate, 30 mL volume, Oak Ridge style centrifuge tubes.
- Reagent grade or better sorbate salts (such as  $\text{SrCl}_2 \cdot 6\text{H}_2\text{O}$ ,  $\text{CuCl}_2 \cdot 2\text{H}_2\text{O}$ ,  $\text{NiCl}_2 \cdot 6\text{H}_2\text{O}$ ,  $\text{N}_2\text{O}_8\text{U} \cdot 6\text{H}_2\text{O}$ ,  $\text{EuCl}_3 \cdot 6\text{H}_2\text{O}$ ,  $\text{ZrOCl}_2 \cdot 8\text{H}_2\text{O}$ ,  $\text{SeO}_2$ , and  $\text{PbO}_2$ ).

### Method

1. Weigh out the mass (for example, 0.1 to 1.0 g) of *sorbent* into the *reaction vessel*.
2. Add the specified volume (for example, 10 to 20 mL) of ionic medium to the reaction vessel. This could involve one of two possibilities:
  - If the solids are not preconditioned the *ionic medium* would contain a known concentration of *sorbate*. This initiates the sorption test.
  - If the solids are to be preconditioned, the *ionic medium* will not contain *sorbate*. After allowing the solids to be conditioned in the *ionic medium* for a week or longer, remove a one half portion of the *ionic medium*. Replace with an equal volume of *ionic medium* containing a known concentration of *sorbate*. This initiates the sorption tests. (Sorption data from tests with conditioned solids are considered to be more useful since artefacts from the rock crushing have been reduced.)
3. Initiate *blank tests* close to the start of sorption tests. Add the specified volume of ionic medium, containing *sorbate* (in similar concentrations used in the sorption tests) to *reaction vessels* that do not contain any *sorbents*. The pH of the blank tests should match that of the sorption tests, or should include a range of pH values that would

bracket the anticipated pH values of the sorption tests. Apply the same steps to the *blank tests* as would be applied to the sorption tests.

4. Measure the pH of the test solutions at the beginning of the experiment. (The pH is determined without stirring, generally when the solids have settled to the bottom of the *reaction vessel*.)
5. During the sorption period shake the *reaction vessels* at least once a day.
6. At the completion of the specified reaction period (hours, days, or weeks) determine the solution pH.
7. Separate the solution from the solid by centrifuging (15 minutes at 20000 rpm) to ensure that colloidal particles are not entrained in the solution.
8. Decant the centrifuged supernatant and acidify to pH 2 to ensure that elements remain in solution.
9. Analyze the acidified samples or submit to Analytical Science for analyses.

## Notes

**Optimum Percent Sorbed Values.** Experimental parameters may be manipulated to achieve an optimal level of sorption, which can be expressed as the percent of the total element that is sorbed. The target is to have 40 to 60 percent of the total element sorbed to ensure optimum accuracy in measuring the amount sorbed and the amount left in solution. If the amount of sorption approaches 100 percent the uncertainty in the measured sorption coefficient will be high due to uncertainty in the dissolved element concentration and the risk of non-equilibrium.

**Solid/Liquid Ratio.** The solid/liquid ratio can be manipulated to control how much of the sorbate is removed from solution. Obviously with more solid, larger amounts of sorbate are removed from solution. Ideal solid/liquid ratios depend upon the element and the mineral being studied. For example, solid/liquid ratios have been varied from 0.5 to 9 g/100 mL.

## Calculations

Sorption results are expressed as sorption coefficients ( $K_d$ ), which are calculated as follows:

$$K_d = \frac{S}{C} = \frac{(C_0 - C) \times \text{vol}}{C \times m} \times 1000 \quad (\text{cm}^3/\text{g})$$

Where:  $C_0$  = initial concentration of sorbate (mol/L) determined from blank tests.

$C$  = equilibrium concentration of sorbate measured in solution (mol/L)

$S$  = concentration of sorbate on the solid (mol/g)

Vol = total volume of solution that was in the *reaction vessel* (L)

$m$  = mass of sorbing solid (*sorbent*) in the system (g)

Conversion factor: 1000  $\text{cm}^3/\text{L}$

The percent sorbed is defined as:

$$\text{percent sorbed} = \frac{\text{mass sorbate removed from solution} \times 100\%}{\text{total sorbate available for sorption}}$$

## Quality Assurance

Analytical balances and pipettes are calibrated on a regular basis using documented protocols. The reproducibility of sorption measurements may be established with replicate tests that would



account for the effects of rock heterogeneity and variability associated with sorbate analyses, rock mass determination and the dispensing of solution volumes.

## A.2 SORPTION TEST – LARGE VOLUME

### Introduction

This protocol describes the general method for determining multiple sorption measurements from a single large volume *reaction vessel*. The advantage of using larger quantities of solids and solution is that the effect of sample variability has been reduced and sorption can be monitored as a function of time using the same solid sample. The main applications for this method include the study of the effects of salt concentration, solid/liquid ratio, sorption time, and reversibility. With this protocol a solution containing a known concentration of sorbate is contacted with a sorbing solid. At designated time interval the reaction vessel is sampled in such a way as to not change the solid/liquid ratio for the experiment. The solution is separated from the solid in each sample and analyzed to determine the decrease in sorbate concentration. This decrease in sorbate concentration is used to calculate the amount of sorbate that has sorbed to the solid and to determine a  $K_d$  value.

### Definitions

*Sorbent*: the rock or mineral whose sorption properties are being studied

*Sorbate*: the element whose sorption properties are being studied

*Ionic medium*: the solution in which sorption is being studied. For example, the 300 g/L Na-Ca-Cl brine.

*Blank test*: the sorption test without a sorbent that is used to account for sorbate losses to vessel walls and to precipitation in case predicted solubility limits were not accurate.

*Reaction vessel*: the container used hold the sorbent and reaction solution.

*Sample*: The portion of liquid with suspended solids removed from the reaction vessel determine sorption at a specified time.

### Materials

- Powdered rock sample (such as bentonite, shale, limestone) that has been sized to between 100 and 200  $\mu\text{m}$  by dry sieving.
- Brine solution prepared from reagent grade  $\text{CaCl}_2$  and  $\text{NaCl}$ , and deionized water.
- The *reaction vessels* are 250 mL Nalgene (polypropylene) wide mouth bottles.
- Reagent grade or better sorbate salts (such as  $\text{SrCl}_2 \cdot 6\text{H}_2\text{O}$ ,  $\text{CuCl}_2 \cdot 2\text{H}_2\text{O}$ ,  $\text{NiCl}_2 \cdot 6\text{H}_2\text{O}$ ,  $\text{N}_2\text{O}_8\text{U} \cdot 6\text{H}_2\text{O}$ ,  $\text{EuCl}_3 \cdot 6\text{H}_2\text{O}$ ,  $\text{ZrOCl}_2 \cdot 8\text{H}_2\text{O}$ ,  $\text{SeO}_2$ , and  $\text{PbO}_2$ ).

### Method

1. Weigh out the mass (for example, 1 to 16 g) of *sorbent* into the *reaction vessel*.
2. Add the specified volume (for example, 200 mL) of ionic medium to the reaction vessel. This could involve one of two possibilities:
  - If the solids are not preconditioned the *ionic medium* would contain a known concentration of *sorbate*. This initiates the sorption test.
  - If the solids are to be preconditioned, the *ionic medium* will not contain *sorbate*. After allowing the solids to be conditioned in the *ionic medium* for a week or longer, remove one half portion of the *ionic medium* in volume. Replace with an equal volume of *ionic medium* containing a known concentration of *sorbate*. This initiates the sorption tests. (Sorption data from tests with conditioned solids are considered to be more useful since artefacts from the rock crushing have been reduced.)
3. Initiate *blank tests* close to the start of sorption tests. Add the specified volume (same as in step 2) of ionic medium, containing *sorbate* (in similar concentrations used in the

sorption tests) to *reaction vessels* that do not contain any *sorbents*. The pH of the blank tests should match that of the sorption tests, or should include a range of pH values that would bracket the anticipated pH values of the sorption tests. Apply the same steps to the *blank tests* as would be applied to the sorption tests. The blank tests are sampled immediately after initiating sorption test to confirm initial sorbate concentrations.

4. Measure the pH of the test solutions at the beginning of the experiment and immediately before each sampling session. (The pH is determined without stirring, generally when the solids have settled to the bottom of the *reaction vessel*.)
5. During the sorption period shake the *reaction vessels* at least once a day.
6. At each designated time interval (hours, days, or weeks) ensure that the solids are evenly dispersed in suspension and remove 10 mL of fluid with entrained solids.
7. Centrifuge each *sample* (15 minutes at 20000 rpm) to ensure complete separation of fluid from solids.
8. Decant the centrifuged supernatant and acidify to pH 2 to ensure that elements remain in solution.
9. Analyze the acidified samples or submit to Analytical Science for analyses.

## Notes

**Optimum Percent Sorbed Values.** Experimental parameters may be manipulated to achieve an optimal level of sorption, which can be expressed as the percent of the total element that is sorbed. The target is to have 40 to 60 percent of the total element sorbed to ensure optimum accuracy in measuring the amount sorbed and the amount left in solution. If the amount of sorption approaches 100 percent the uncertainty in the measured sorption coefficient will be high due to uncertainty in the dissolved element concentration and the risk of non-equilibrium.

**Solid/Liquid Ratio.** The solid/liquid ratio can be manipulated to control how much of the sorbate is removed from solution. Obviously with more solid, larger amounts of sorbate are removed from solution. Ideal solid/liquid ratios depend upon the element and the mineral being studied. For example, solid/liquid ratios have been varied from 0.5 to 9 g/100 mL.

## Calculations

Sorption results are expressed as sorption coefficients ( $K_d$ ), which are calculated as follows:

$$K_d = \frac{S}{C} = \frac{(C_0 - C) \times \text{vol}}{C \times m} \times 1000 \quad (\text{cm}^3/\text{g})$$

Where:  $C_0$  = initial concentration of sorbate (mol/L) determined from blank tests.

$C$  = equilibrium concentration of sorbate measured in solution (mol/L)

$S$  = concentration of sorbate on the solid (mol/g)

Vol = total volume of solution that was in the *reaction vessel* (L)

$m$  = mass of sorbing solid (*sorbent*) in the system (g)

Conversion factor: 1000  $\text{cm}^3/\text{L}$

The percent sorbed is defined as:

$$\text{percent sorbed} = \frac{\text{mass sorbate removed from solution} \times 100\%}{\text{total sorbate available for sorption}}$$

**Quality Assurance**

Analytical balances and pipettes are calibrated on a regular basis using documented protocols. The reproducibility of sorption measurements may be established with replicate samples taken at a specified time. This would account for the effects of variability associated with sorbate analyses, and the reproducibility the sampling procedure.

### A.3 DESORPTION TEST

#### Introduction.

This protocol describes method used to test the reversibility of a sorbate's sorption by diluting the dissolved sorbate concentration and observing the response of sorption coefficient values. If the sorption process is completely reversible, over a relatively short time period enough sorbate will be desorbed to return the system to equilibrium and the observed sorption coefficients will be very similar to values before the desorption test. If the process is not reversible within the experimental time span the observed sorption coefficient values will be higher because insufficient sorbate would have desorbed to return the system to equilibrium. The effect of sorption time on reversibility is tested by performing desorption studies on experimental systems that have reacted for periods of 1 day to 1 month.

#### Definitions

*Sorbent*: the rock or mineral whose sorption properties are being studied

*Sorbate*: the element whose sorption properties are being studied

*Ionic medium*: the solution in which sorption is being studied. For example, the 300 g/L Na-Ca-Cl brine.

*Blank test*: the sorption test without a sorbent that is used to account for sorbate losses to vessel walls and to precipitation in case predicted solubility limits were not accurate.

*Reaction vessel*: the container used hold the sorbent and reaction solution.

*Sample*: The portion of liquid with suspended solids removed from the reaction vessel determine sorption at a specified time.

#### Method

1. Perform a set sorption tests as described by Protocol SSP-02 (Sorption Test – Large Volume), using an experimental volume of 100 mL. The durations of these tests will be 1 day, 1 week and 1 month.
2. At the end of the selected sorption period remove 80 mL ( $vol_{rem}$ ) of solution from the reaction vessel. During the removal ensure that the solids remain undisturbed on the bottom of the reaction vessel. Keep 10 mL of this solution as an acidified sample to determine the concentration of sorbate in solution ( $C_{rem}$ ). This is used to determine the  $K_d$  value before desorption and to calculate the total sorbate concentration in the system after dilution ( $C_0$ ). Measure the pH of the remaining 70 mL that was not acidified.
3. Add 80 mL of sorbate-free ionic medium to the reaction vessel to initiate the desorption process by diluting the sorbate concentration.
4. Sample the reaction vessel at time periods of 1 h, 1 day, 1 week and 2 weeks after desorption was initiated.

#### Calculations

The sorption coefficients ( $K_d$ ) determined before desorption are calculated as follows:

$$K_d = \frac{S}{C} = \frac{(C_0 - C) \times vol}{C \times m} \times 1000 \quad (\text{cm}^3/\text{g})$$

Where:  $C_0$  = initial concentration of sorbate (mol/L) determined from blank tests.

$C$  = equilibrium concentration of sorbate measured in solution (mol/L)

$S$  = concentration of sorbate on the solid (mol/g)

$Vol$  = total volume of solution that was in the *reaction vessel* (L)

$m$  = mass of sorbing solid (*sorbent*) in the system (g)  
Conversion factor: 1000 cm<sup>3</sup>/L

The calculation of sorption coefficients for the desorption phase must account for the removal of dissolved sorbate when 80 mL of solution were replaced with 80 mL of sorbate-free ionic medium. This is done by adjusting the quantity,  $C_0$ , to account for this loss. The modified total concentration of sorbate in the system,  $^*C_0$ , is calculated as follows:

$$^*C_0 = \frac{C_0 \times vol - C_{rem} \times vol_{rem}}{vol}$$

Where:  $vol_{rem}$  = volume of solution removed to initiate desorption.

$C_{rem}$  = concentration of sorbate measured in solution before desorption (mol/L).

The quantity  $^*C_0$  is then used to replace  $C_0$  in the calculation of sorption coefficients. If the percent sorbed value is high before the desorption experiment, the  $^*C_0$  value will be similar to the original  $C_0$  value. Conversely, if the percent sorbed is low the  $^*C_0$  value will be significantly lower than  $C_0$ .

## A.4 NICKEL ANALYSIS – BROMO-PADAP COLORIMETRIC METHOD

### Introduction

This protocol describes the colorimetric method for determining Ni concentrations in brine solutions. The method is based on procedures described by Marczenko Z. and M. Balcerzak (2000), and was optimized for use with brine solutions. The amount of Nickel in solution is determined by the measured absorbance of a Bromo-PADAP complex at a wavelength of 558 nm.

The sample volume used in the procedure should contain between 1 and 10 µg of nickel. The complex formed is stable for approximately 2 hours, though unstable for longer than 12 hours. The molar absorptivity is  $1.01 \times 10^5 \text{ L mol}^{-1} \text{ cm}^{-1}$ . Known interferences include: Ca(II), Cd(II), Zn(II), Mn(II), Co(II), Cu(II), Pb(II), Hg(II), Ag(I), Fe(III), Al(III) and Zr(IV).

### Equipment and Reagents

- 1) Genova Spectrophotometer
- 2) Buffering Solution:  
Weigh 149 g of triethanolamine and dilute to 800 mL with distilled deionised water (DIW). Lower the pH of the solution to 7.85 with concentrated hydrochloric acid. Let solution rest for one full day, and then adjust the pH again to 7.85. Dilute to 1 L with DIW.
- 3) Bromo-PADAP is short for 2-(5-Bromo-2-pyridylazo)-5-diethylaminophenol (Aldrich). Dissolve 0.1 g of Bromo-PADAP in 100 mL of ethanol.
- 4) Ethanol

### Method

1. Prepare a set of nickel standards which contain between 1 µg and 10 µg of nickel per aliquot, as well as a blank solution containing the brine composition used in experiments.
2. Transfer an aliquot (for example 0.5 to 5 mL) of sample into a 25 mL volumetric flask
3. Add approximately 5 mL DIW.
4. Add 2 mL of the buffer solution. Mix.
5. Add 10 mL of ethanol. Mix.
6. Add 0.5 mL of Bromo-PADAP. Mix.
7. Dilute to 25 mL with DIW. mix
8. Allow to stand for a minimum of 1 hour
9. Measure the absorbance at 558 nm using DIW as a reference.
10. Determine the nickel concentration from a calibration curve of nickel versus absorbance.

### Quality Assurance

Analytical balances and pipettes are calibrated on a regular basis using documented protocols. The accuracy of the method is estimated from the calibration curve, which includes a blank made up from the experimental brine solution.

**References**

- 1) Marczenko, Z. and M. Balcerzak. 2000. Separation, preconcentration and spectrophotometry in inorganic analysis. Analytical Spectroscopy Library – 10, Elsevier.



## A.5 URANIUM ANALYSIS – BROMO-PADAP COLORIMETRIC METHOD

### Introduction

This protocol describes the colorimetric method for determining uranium in aqueous solutions that was based on that of Johnson and Florence (1971). Uranium is determined colorimetrically as its bromo-PADAP complex at pH 7.6. The complex is stable for 24 h, and absorbance is measured at the 578 nm wavelength.

The sample volume used in the procedure should contain between 2 and 100 µg of uranium. The molar absorptivity is  $7.1 \times 10^4 \text{ L mol}^{-1} \text{ cm}^{-1}$ . Known interferences include As(V), Co(II), Cr(III), Cr(VI), Cu(II), Ni(II), V(V), V(IV), Zr(IV), Th, Fe(III), Pu(IV) and Pu(III).

### Equipment and Reagents

1. Genova Spectrophotometer
2. Complexing solution:  
Suspend 25 g of (1,2-cyclohexylenedinitrilo)tetraacetic acid (CyDTA), purchased from Fluka as IDRANAL@ IV, 5 g of sodium fluoride (Aldrich), and 65 g of sulphosalicylic acid (Sigma-Aldrich) in 800 mL of water. Neutralize to pH 7.85 with 40 w/v sodium hydroxide. Dilute to 1 L with distilled deionised water (DIW).
3. Sodium Hydroxide, 40 w/v: dissolve 40 g of sodium hydroxide pellets in 100 mL of DIW.
4. Buffering Solution:  
Dissolve 149 g of triethanolamine (Mallinckrodt) and in 800 mL of DIW. Lower the pH of the solution to 7.85 with concentrated hydrochloric acid. Let solution stand for one full day, and then adjust the pH again to 7.85. Dilute to 1 L with DIW.
5. Bromo-PADAP is short for 2-(5-Bromo-2-pyridylazo)-5-diethylaminophenol (Aldrich). Dissolve 0.1 g of Bromo-PADAP in 100 mL of ethanol.
6. Ethanol

### Method

1. Prepare a set of uranium standards which contain between 2 µg and 100 µg of uranium per aliquot, as well as blank solutions containing the brine composition used in experiments.
2. Transfer an aliquot (for example 0.5 to 5 mL) of sample, containing 2 to 100 µg of uranium to a 25 mL volumetric flask.
3. Add 2 mL of complexing solution. Mix.
4. Add 2 mL of buffer solution. Mix.
5. Add 10 mL of ethanol. Mix.
6. Dilute to ~ 20 mL with DIW.
7. Adjust the pH, if necessary, to  $7.6 \pm 0.5$  with concentrated HCl or 40 w/v NaOH.
8. Add 0.5 mL of bromo-PADAP. Mix.
9. Dilute to 25 mL with DIW.
10. Allow to stand for 40 minutes.
11. Measure the absorbance in a 1 cm cell at 578 nm, within 24 h.

12. Determine the uranium concentration from a calibration curve of uranium versus absorbance.

### **Quality Assurance**

Analytical balances and pipettes are calibrated on a regular basis using documented protocols. The accuracy of the method is estimated from the calibration curve, which includes a blank made up from the experimental brine solution.

### **References**

- 1) Johnson, D.A. and T.M. Florence. 1971. Spectrophotometric determination of uranium(VI) with 2-(5-bromo-2-pyridylazo)-5-diethylaminophenol. *Analitica Chimica Acta*, 53, 73-79.

## A.6 EUROPIUM ANALYSIS – FLUORESCENCE

### Introduction

This protocol describes the general method for determining europium in aqueous solutions using its fluorescence properties. Europium was determined with acidified samples using time resolved fluorescence (phosphorescence) by a method developed by AECL at Whiteshell. The excitation wavelength for Europium was 340 nm and the emission wavelength for detection of Europium was 595 nm. The Europium detection limit was  $1 \times 10^{-6}$  mol/L. A calibration curve is prepared for each matrix solution to eliminate any effects for salt concentration on measured fluorescence.

### Equipment and Reagents

1. Varion Cary Eclipse fluorescence spectrophotometer.

### Method

- 1) Prepare a set of europium standards for each brine composition with europium concentrations between  $1 \times 10^{-5}$  and  $2 \times 10^{-4}$  mol/L. The set includes a blank brine solution with no europium. The standards should be acidified (pH 2) to match the sample pH.
- 2) Allow the fluorescence spectrophotometer to warm up for a minimum of 1 hour before use.
- 3) Set up the analysis method to have the following parameters:
  - a. Excitation wavelength (nm) - 340
  - b. Emission wavelength (nm) - 595
  - c. Data mode – Phosphorescence
  - d. Total decay time (s) – 0.005
  - e. Number of flashes – 1
  - f. Delay time (ms) – 0.100
  - g. Gate time (ms) – 1.00
  - h. Excitation slit (nm) – 20
  - i. Emission slit (nm) – 20
  - j. Average time (s) – 0.500
  - k. PMT voltage (V) – high
  - l. Standard and sample replicates – 5
- 4) Zero the fluorescence spectrophotometer against distilled deionised water (DIW) multiple times. Average these numbers and zero again to the average.
- 5) Calibrate the instrument by analyzing the standards and blank. The standard results are saved for future comparisons. Select the type of calibration curve (linear or quadratic) that will be used to calculate concentration from fluorescence measurements.
- 6) Open the setup for running samples and enter the sample names.
- 7) Initiate sample analysis by running a distilled water sample. It should be close to 0, if not, re-zero, and rerun.
- 8) Run the samples.
- 9) When finished, save the file as both a BATCH file and a RTF file into the designated file folder.

### Quality Assurance

Analytical balances and pipettes are calibrated on a regular basis using documented protocols. The error of the measurement is determined by the standard deviation of 5 replicate measurements.